

Growth and Survival Pathways in Normal and Malignant B-Lymphocytes

Author: Maria Gumina

Persistent link: <http://hdl.handle.net/2345/1400>

This work is posted on [eScholarship@BC](#),
Boston College University Libraries.

Boston College Electronic Thesis or Dissertation, 2009

Copyright is held by the author, with all rights reserved, unless otherwise noted.

Boston College

The Graduate School of Arts and Sciences

Department of Biology

GROWTH AND SURVIVAL PATHWAYS
IN NORMAL AND MALIGNANT B-LYMPHOCYTES

a dissertation

by

MARIA ROSE GUMINA

submitted in partial fulfillment of the requirements

for the degree of

Doctor of Philosophy

August 2009

© Copyright by MARIA ROSE GUMINA

2009

ABSTRACT

GROWTH AND SURVIVAL PATHWAYS IN NORMAL AND MALIGNANT B-LYMPHOCYTES

Author: Maria R. Gumina

Advisor: Thomas C. Chiles, Ph.D.

Normal B lymphocytes require extrinsic factors to grow and proliferate. Surface receptors (*e.g.*, B-cell antigen receptor, BCR) function, in part, to link growth factors to signal transduction/metabolic pathways and the cell cycle machinery. Accumulating evidence indicates that signal transduction-dependent changes in both glucose energy metabolism and *de novo* transcription of the D-type cyclin-cdk4/6 pathway are necessary for quiescent B-lymphocytes to enter G₁-phase of the cell cycle and grow. B cell growth represents a critical checkpoint for subsequent proliferation and clonal expansion of antigen-specific lymphocytes. On the former, we have shown earlier that acquisition of extracellular glucose and metabolism via the glycolytic pathway is required for conventional splenic B-2 lymphocytes to grow (*i.e.*, increase cell size and mass) in response to antigen challenge; however, the metabolic fate and biological significance of glucose-derived carbons are unknown. Here, we show that in response to BCR ligation, glucose carbon flow is directed into a *de novo* lipogenic pathway that is regulated, in part, via phosphoinositide-3 kinase (PI-3K)-dependent activation of ATP citrate lyase (ACL),

a key rate-limiting enzyme in *de novo* lipogenesis. Inhibition of ACL results in a loss of B-cell growth and cell viability. Regarding the latter point, the B-1a lymphocyte subset expresses cyclins D2 and D3 that are transiently expressed in a non-overlapping manner, notably cyclin D3 expression immediately precedes the G₁/S phase transition, suggesting distinct functions for these D-type cyclins in B-1a lymphocyte G₀-to-S phase progression. We show herein that murine B-1a cells deficient in cyclin D3 proliferate normally in response to extracellular stimuli, in part, due to a compensatory sustained up-regulation of cyclin D2. In keeping with this, human diffuse large B-cell lymphoma (DLBCL) represents a malignant clonal expansion of B cells characterized by several subsets, including germinal center (GC) and activated B-cell (ABC) types. Here, we show that the GC-type LY18 human DLBCL exhibits constitutive expression of cyclin D3, but not cyclins D1 and D2. Targeting of cyclin D3-holoenzyme complexes with cell permeable chemical- and peptide-based cdk4 inhibitors results in G₁-phase arrest and apoptosis via a pathway that involves inhibition of pRb phosphorylation. By contrast, endogenous knock down of cyclin D3 with siRNA did not induce growth arrest or apoptosis, in part, due to redundancy with cyclin E.

This dissertation is dedicated to
Anthony John Mastrangelo
for his unwavering love, support, and encouragement.

ACKNOWLEDGEMENTS

First, I would like to thank my advisor, Dr. Thomas Chiles. I wish I could articulate how grateful I am for his patience and guidance over the years. Tom provided an excellent lab environment and challenged me everyday to be a better scientist and person. He is an excellent mentor and a brilliant scientist.

I owe many thanks to Fay Dufort and Dr. Derek Blair for their knowledge, friendship, and support. Also, a sincere thank you to the talented colleagues within the Biology and Chemistry departments, past and present, to which I have had the pleasure to work alongside.

I must also thank my family and friends that have provided me with support over my graduate career, specifically, all of my siblings (Paul, Rachel, Katrina, Joseph, and Angela) and my parents, Paul and Mary. Without the love and support of my parents I would not be here today-I am forever grateful for all that they have done for me. Also, a very special thank you to Brownyn and Anthony Mastrangelo for pushing me to work harder when I did not think I had the strength.

Finally, I must thank Anthony John. I will always be grateful for his support, strength, and encouragement. His confidence in me has been more than I could have ever asked for.

TABLE OF CONTENTS

Dedication	i
Acknowledgements	ii
Table of Contents	iii
List of Figures	v
List of Abbreviations	ix
Introduction	1
I. <i>The Immune System</i>	1
II. <i>B Lymphocytes</i>	2
III. <i>Bioenergetics and Immune Function</i>	6
IV. <i>Cyclin D/cdk4/pRb Pathway in B Lymphocytes</i>	11
V. <i>Cyclin Dependent Kinase Inhibitors (cdki)</i>	18
VI. <i>B-1 Lymphocytes</i>	22
VII. <i>Cyclin D/cdk4/pRb Pathway in B Cell Lymphoma</i>	25
VIII. <i>Non-Hodgkin's Lymphoma</i>	27
IX. <i>Summary/Aims of Study</i>	30
Materials and Methods	33
<i>Reagents and Antibodies</i>	33
<i>Preparation of Murine B-1a and B-2 Lymphocytes and Cell Culture</i>	34
<i>TAT Peptides</i>	36
<i>Flow Cytometry</i>	36
<i>Proliferation Assay</i>	37
<i>Western Blotting</i>	37
<i>Fluorescence Microscopy</i>	38
<i>Nucleofection</i>	39
<i>Lipid Isolation, Purification, and Quantification</i>	39
<i>High-Performance Thin-Layer Chromatography</i>	40
<i>ATP Citrate Lyase (ACL) Enzyme Activity</i>	41

Chapter 1: The role of cyclin D3 in the proliferation of primary peritoneal B-1 cells	43
Results	44
Figures and Legends	52
Chapter 2: Cyclin D3-cdk4/6 complexes are dispensable in the growth and survival of the human Diffuse Large B-cell Lymphoma, OCI-LY18; evidence for redundancy by cyclin E	72
Results	73
Figures and Legends	97
Chapter 3: Function and regulation of ATP citrate lyase (ACL) in B-lymphocyte growth	165
Results	166
Figures and Legends	172
Discussion	184
I. <i>Chapter 1</i>	184
II. <i>Chapter 2</i>	192
III. <i>Chapter 3</i>	203
References	207

LIST OF FIGURES

1.	TAT-p16 wild-type peptide blocks formation of cyclin D3-cdk4 complexes in B-1a cells.	52
2.	TAT-p16 wild-type peptide inhibits DNA synthesis in B-1a cells in response to PMA, LPS, or CD40L.	54
3.	TAT-p16 wild-type peptide inhibits pRb ^{Ser807/811} phosphorylation in B-1a cells in response to PMA.	56
4.	D-type cyclin expression in B-1a cells in wild-type and cyclin D3-deficient mice.	58
5.	Initial characterization of B-1a cell lymphoid compartments in wild-type and cyclin D3-deficient mice.	60
6.	DNA synthesis in B-1a cells in cyclin D3-deficient mice.	62
7.	Expression of cyclin D2 is elevated in PMA stimulated cyclin D3-deficient B-1a cells.	64
8.	Cyclin D2 compensates for the loss of cyclin D3 in PMA stimulated cyclin D3-deficient B-1a cells.	66
9.	TAT-p16 wild-type peptide inhibits DNA synthesis in PMA stimulated cyclin D3-deficient B-1a cells.	68
10.	Cycloheximide decreases endogenous cyclin D2 and cyclin D3 in PMA treated B-1a.	70
11.	Protein expression profiles of relevant G ₁ proteins reveals LY18 cells uniquely express cyclin D3.	97
12.	Cyclin dependent kinase 4 (cdk4) forms complexes with cyclin D3 in LY18 cells.	99
13.	TAT-p16 wild-type peptide causes an increase in hypodiploid DNA resulting in apoptosis in LY18 cells.	101
14.	TAT-p16 wild-type peptide inhibits pRb ^{Ser807/811} phosphorylation	103

	in LY18 cells.	
15.	Treatment of LY18 cells with the cyclin dependent kinase 4 inhibitor (cdk4i) causes a decrease in viable cells.	105
16.	Cyclin dependent kinase 4 inhibitor (cdk4i) blocks cell cycle progression in LY18 cells.	107
17.	Cyclin dependent kinase 4 inhibitor (cdk4i) inhibits DNA synthesis in LY18 cells.	109
18.	Cdk4 and cyclin D3 protein expression decreases over time in cyclin dependent kinase 4 inhibitor (cdk4i) treated LY18 cells.	111
19.	Cyclin dependent kinase 4 inhibitor (cdk4i) inhibits constitutive pRb ^{Ser807/811} and pRb ^{Thr821} phosphorylation in LY18 cells.	113
20.	Cyclin dependent kinase 4 inhibitor (cdk4i) inhibits cdk2 ^{Thr160} phosphorylation, but does not affect total cdk2 levels in LY18 cells.	115
21.	LY18 cells treated with cyclin dependent kinase 4 inhibitor (cdk4i) results in a time-dependent increase in endogenous p27 protein expression.	117
22.	TAT-p27 fusion proteins do not measurably alter LY18 cell viability.	119
23.	Incubation of LY18 cells with TAT-p27 fusion proteins does not measurably alter the percentage of cells in G ₁ -phase or S+G ₂ /M-phase of the cell cycle.	121
24.	siRNA-mediated knockdown of endogenous p27 has no measurable effect on the viability of cyclin dependent kinase 4 inhibitor (cdk4i) treated LY18 cells.	123
25.	siRNA-mediated knockdown of endogenous p27 has no measurable effect on G ₁ -phase or S+G ₂ /M-phase of the cell cycle, in cyclin dependent kinase 4 inhibitor (cdk4i) treated LY18 cells.	125
26.	siRNA-mediated knockdown of endogenous cyclin D3 has no measurable effect on LY18 cell viability.	127
27.	siRNA-mediated knock down of endogenous cyclin D3 does not measurably alter the cell cycle in LY18 cells.	129

28.	siRNA-mediated knock down of endogenous cyclin D3 does not measurably affect DNA synthesis in LY18 cells.	131
29.	siRNA-mediated knockdown of both cyclin D3 and cyclin E and of cdk4, cdk6, and cdk2 reduces constitutive pRb ^{Ser807/811} and pRb ^{Thr821} phosphorylation in LY18 cells.	133
30.	siRNA-mediated knock down of endogenous cdk4 has no measurable effect on LY18 cell viability.	137
31.	Knockdown of endogenous cdk6 following incubation of LY18 cells with cdk6 siRNA has no measurable effect on the viability.	139
32.	siRNA-mediated knock down of endogenous cdk4 does not measurably alter the cell cycle in LY18 cells.	141
33.	Knockdown of endogenous cdk6 following incubation of LY18 cells with cdk6 siRNA does not measurably alter the cell cycle.	143
34.	Knockdown of endogenous cdk2 following incubation with cdk2 siRNA has no measurable effect on LY18 cell viability.	145
35.	siRNA-mediated knockdown of endogenous cyclin E has no measurable effect on LY18 cell viability.	147
36.	siRNA-mediated knockdown of endogenous cyclin E has no measurable effect on the cell cycle in LY18 cells.	149
37.	Knockdown of endogenous cdk2 following incubation of LY18 cells with cdk2 siRNA does not measurably alter the cell cycle.	151
38.	siRNA-mediated knockdown of endogenous cdk4 and cdk6 has no detectable effect on LY18 cell viability.	153
39.	siRNA-mediated knockdown of endogenous cdk4 and cdk6 results in an increase in the percentage of LY18 cells in G ₁ -phase of cell cycle and a decrease in the percentage of LY18 cells in S+G ₂ /M-phase of the cell cycle.	155
40.	siRNA-mediated knockdown of endogenous cdk6 and cdk2 has no detectable effect on LY18 cell viability, however, it results in an increase in the percentage of LY18 cells in G ₁ -phase of cell cycle and a decrease in the percentage of LY18 cells in S+G ₂ /M-phase of the cell cycle.	157

41.	siRNA-mediated knockdown of endogenous cdk4, cdk6, and cdk2 has no measurable effect on LY18 cell viability, however, it results in an increase in the percentage of LY18 cells in G ₁ -phase of cell cycle and a decrease in the percentage of cells in S+G ₂ /M-phase of the cell cycle.	159
42.	siRNA-mediated knockdown of endogenous cyclin D3 and cyclin E has no measurable effect on the viability in LY18 cells.	161
43.	siRNA-mediated knockdown of endogenous cyclin D3 and cyclin E results in an increase in the percentage of LY18 cells in G ₁ -phase of the cell cycle and inhibits DNA synthesis.	163
44.	Glucose-derived carbon is incorporated into <i>de novo</i> lipid synthetic pathways in splenic B cells stimulated via the BCR.	172
45.	Phosphorylation of ATP citrate lyase (ACL) on Ser ⁴⁵⁴ and ACL enzyme activity increases in splenic B-lymphocytes stimulated through the BCR.	174
46.	ATP citrate lyase (ACL) phosphorylation on Ser ⁴⁵⁴ and ACL enzyme activity increases in IL-4-stimulated splenic B-lymphocytes.	176
47.	Increased phospho-ATP citrate lyase (ACL) ^{Ser454} and ACL enzyme activity in response to BCR cross-linking is impaired in PI-3K-deficient B-lymphocytes.	178
48.	Phosphorylation of ATP citrate lyase (ACL) on Ser ⁴⁵⁴ and ACL enzyme activity in IL-4 stimulated B-lymphocytes requires PI-3K activity.	180
49.	Treatment of splenic B-lymphocytes stimulated via the BCR with hydroxycitrate (HC) causes a decrease in viable cells.	182

LIST OF ABBREVIATIONS

Ab	Antibody
ACL	ATP citrate lyase
Ag	Antigen
anti-IgM	F(ab') ₂ fragments of goat anti-mouse immunoglobulin M
AML-1	Acute myeloid leukemia 1
BCR	B cell receptor
CDK	Cyclin-dependent kinase
Cdk4i	Cyclin-dependent kinase 4 inhibitor
CAK	Cdk-activating kinase
DLBCL	Diffuse large B cell lymphoma
ERK3	Extracellular-signal regulated kinase 3
FCS	Fetal calf serum
FITC	Fluorescein isothiocyanate
GC	Germinal center
HC	Hydroxycitrate
HSC	Hematopoietic stem cells
Ig	Immunoglobulin
INK4	Inhibitors of CDK4
LPS	Lipopolysaccharide
LY	LY294002
MHC	Major Histocompatibility Complex
NHL	Non-Hodgkin's Lymphoma
NF-κB	Nuclear factor kappa light chain enhancer of activated B cells
OCI-LY18	Ontario Cancer Institute-LY18
PI	Propidium iodide
PI-3K	Phosphoinositide 3-kinase
PMA	Phorbol 12-myristate 13-acetate

pRb	Retinoblastoma tumor suppressor protein
TAT	Trans-activator of transcription
TBS-T	Tris-buffered saline/Tween-20
WT	Wortmannin

INTRODUCTION

I. The Immune System

The immune system is a complex defense mechanism within an organism that identifies and protects against invading pathogens (*i.e.*, viruses, bacteria, parasites). The different immune cells and mediators collaborate in a dynamic network to detect foreign pathogens, synchronize an attack, and finally kill and remove the pathogen and damaged cells.

The immune system is divided into two branches, innate and adaptive, each being functionally distinct but highly interactive. Innate immunity is the first line of defense a host has against infection and it is non-specific in nature. Effector cells rapidly respond to common surface molecules on the invading pathogen in a similar manner regardless of the pathogen and therefore, do not illicit long lasting immunity. Activation of the innate immune response often primes the system for the complex adaptive immune response. Adaptive immunity is a specialized and stronger response that offers long lasting immunity. The adaptive branch is divided into humoral immunity orchestrated by B-lymphocytes (B cells), and cell mediated immunity with T-lymphocytes (T cells). B and T cells recognize pathogens and respond in a highly specific manner based upon the unique antigen present on the invading pathogen, while concurrently remaining tolerant towards self-antigens. My study will focus on the specialized B cells of humoral immunity. B cells fight infection caused by extracellular pathogens through the generation and secretion of highly specific immunoglobulins (antibodies (Abs)).

II. *B Lymphocytes*

A. *Development*

B cells are continuously generated by hematopoietic stem cells (HSC) in the bone marrow. Self-renewing HSCs have the potential to generate erythroid, myeloid and lymphoid cell lineages. In order to differentiate, HSC must migrate to the necessary environment where they receive the appropriate cues and cytokines to initiate the expression of specific transcription factors [1]. For HSC to differentiate into B lymphoid progenitors, specific B cell lineage transcription factors must be expressed as well as those specific for the other cell lineages suppressed [2]. Specifically, the gene *Pu.1* is required for HSC commitment into the lymphoid lineages and further the *Ikaros* gene is responsible for the development of B and T lymphocytes [2]. In B cells the *Ikaros* gene encodes a family of transcription factors that control gene rearrangement, immunoglobulin (Ig) heavy and light chains, and the gene encoding $Ig\alpha$ [1]. As a B cell matures it progresses through many strictly controlled developmental stages. Each developmental stage is defined by the molecular changes that accompany random gene rearrangements that are required to make functional surface Ig [3]. Each surface Ig receptor that is generated maintains its own diversity for a specific antigen, which allows a broader response repertoire [4]. B cells undergo early development in the bone marrow

and stages are broken down into: Pro, Pre, Immature, and Mature B cells (see Figure 1).

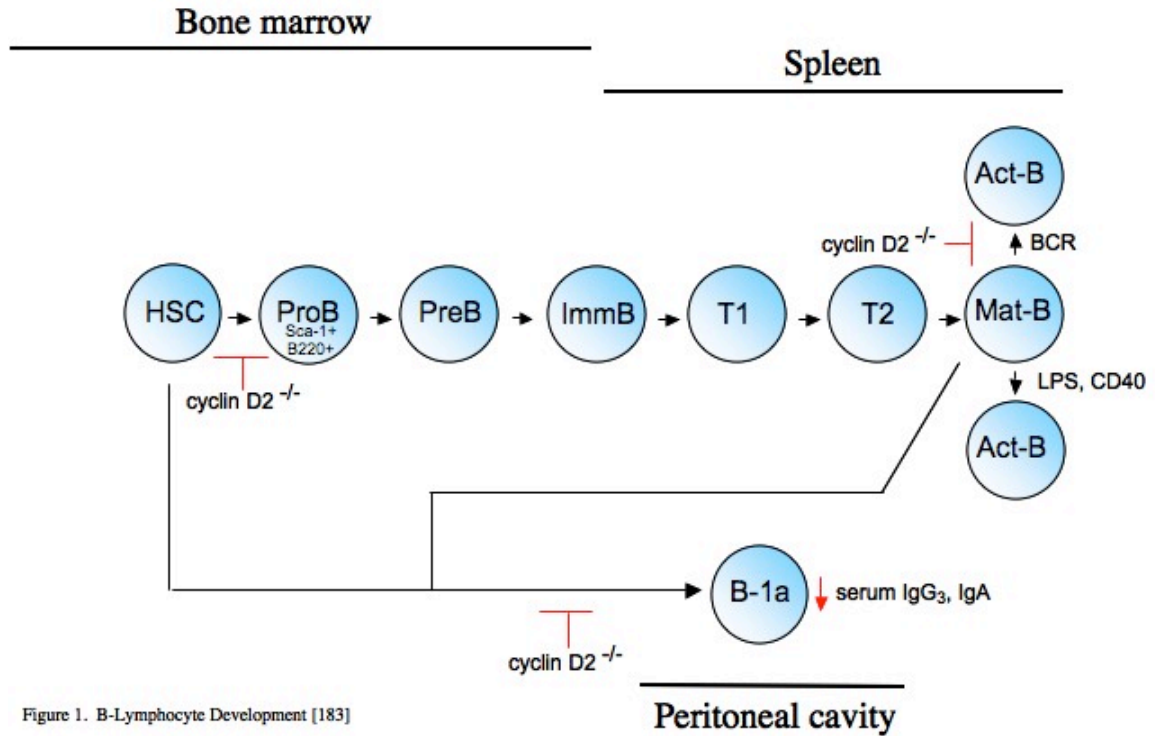


Figure 1. B-Lymphocyte Development [183]

Each stage is further classified based on distinct gene expression profiles, distinct expression of microRNA clusters, the presence of cell surface markers and receptors, and the assembly of a mature B cell receptor (BCR) [5]. All pro- and pre-B cells reside in the bone marrow, whereas immature cells migrate to the periphery where they undergo further maturation and become capable of recognizing self from non-self. At this stage the B cells are mature, but naïve because they have not encountered antigen. They are primed and ready to illicit an immune response provided the correct signals.

B. Activation and Terminal Differentiation

Activation of a B cell begins when a mature, naïve B cell (arrested in G_0 of the cell cycle) encounters antigen via the BCR and receives the necessary signals to begin cell division [6,7,8]. Activation of a B cell results in cell growth (*i.e.*, accumulation of cell volume and mass), a change in metabolism (discussed in detail in section III), an increase in the expression of class II major histocompatibility complex (MHC) molecules, an increase in the expression of IL-4 receptors (IL-4r), and finally, activation drives resting cells (G_0 of the cell cycle) into G_1 -phase. B-cells that begin to proliferate undergo clonal expansion and terminal differentiation into Ab secreting plasma cells. Each step is tightly controlled by cell cycle together with apoptosis. Cell cycle regulation is a major determinant of homeostasis during B cell development and differentiation [7]. Binding of an antigen causes the surface Ig on the B cell to become physically crosslinked [1,9]. Other surface proteins, $Ig\alpha$ and $Ig\beta$, associate with the surface Ig to form the functional BCR, which can either strengthen or inhibit the signal to proliferate [3,6, 8, 9]. Aggregation of the BCR complex recruits a number of tyrosine kinases that initiate three main intracellular signaling cascades, each resulting in changes of gene expression in the nucleus (see Figure 2) [1].

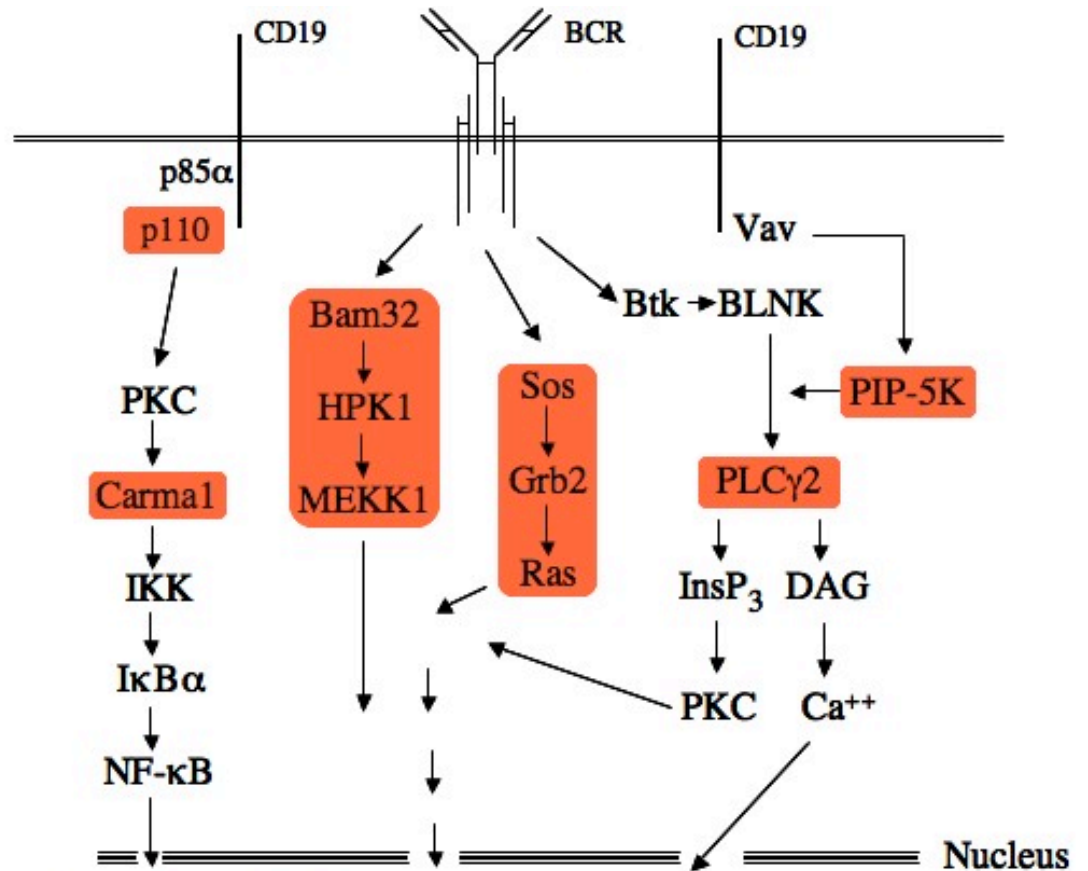


Figure 2. BCR-Induced Signal Transduction Pathways [183]

Studying and understanding BCR coupled signals and their cell cycle target is of interest because irregular cell cycle often leads to malignant transformation.

Following activation and proliferation, plasma cell precursors (plasmablast cells), or long-lived memory cells emerge from the germinal center (GC) and undergo terminal differentiation. Long lived, antigen specific memory cells are responsible for the secondary immune response should the same antigen invade the body again. This response is faster and more aggressive than the first because the memory cells are already primed specifically against that particular pathogen. Plasmablast cells travel to the bone

marrow where they give rise to mature plasma cells [6]. Mature plasma cells are terminally differentiated B cells that exit the cell cycle, never to proliferate again [10,11]. They are a very distinct subset of the B cell population and their primary role is to secrete copious amounts of antibody specific to the particular antigen [6,11,12].

III. Bioenergetics and Immune Function

A fundamental aspect of immune cell regulation is the prerequisite of metabolic substrates to support the bioenergetics associated with lymphocyte development, antigen (Ag)-driven clonal expansion, and acquisition of effector functions [13, 14]. For example, a recent publication demonstrates the requirement for glucose metabolism in supporting Notch-mediated survival of pre-T cells [15]. Recent studies performed in the Chiles' Lab suggest a model in which the modulation of glucose energy metabolism by signal input from surface receptors, influence the outcome of B-cell responses.

A. Energy Metabolism and B Lymphocyte Responses

As noted above, an important consequence of BCR signaling is the expression of cell surface molecules involved in B cell-T cell collaboration and in promoting cell cycle entry of B cells [16]. A hallmark of lymphocytes is their ability to respond immediately to Ag challenge, shifting from a quiescent state (G_0) to a highly active metabolic state within hours. During this period, transcriptional and translational programs are enacted to support growth and acquisition of effect functions [17,18,19]. Although a great deal of effort has been directed toward identifying signaling and gene expression programs that

link extrinsic signals to B cell responses, little is known about the acquisition of metabolic substrates, the regulation of nutrient metabolism, and the biological significance of such regulation to B lymphocyte development, survival, and function.

Early studies revealed that T cells generate most of their ATP from oxidizing glycolytic-derived metabolites (e.g., pyruvate) by the tricarboxylic acid (TCA) cycle in the mitochondria [13,20,21,22]. Based on recent studies by Craig Thompson and colleagues and the Chiles' Lab, a clearer picture has emerged of the metabolic responses of quiescent T- and B-lymphocytes to antigen receptor ligation [23,24]. B-lymphocytes, (like TCR- and CD28-stimulated T cells), rapidly increase glucose uptake and hyper-induce glycolytic flux in response to BCR cross-linking [23,24]. Pro-survival cytokines also mediate glucose energy metabolism in lymphocytes. To illustrate, IL-7 withdrawal from T cells results in a decline in glycolysis and triggering of apoptosis [25]. IL-7 has been shown to promote glucose transport-1 (Glut 1) surface trafficking and glucose uptake via a Stat5/Akt-dependent pathway [26]. Importantly, mammalian cells engineered to express surface Glut1 and the glycolytic enzyme, hexokinase I, resist cytokine-withdrawal induced apoptosis indicating an essential role for glucose metabolism in protecting mammalian cells from apoptotic death [25]. In our most recent findings we discovered that IL-4 induces glycolysis in naïve B cells [27]; inhibition of glycolytic flux is sufficient to trigger apoptosis, despite the presence of IL-4, suggesting that glycolysis is necessary for the pro-survival action of IL-4. Based on these and other studies, it is currently held that lymphocytes and hematopoietic cells depend on extrinsic growth factors, by virtue of their ability to regulate glucose uptake and metabolism, in

order to maintain viability and prevent cell death. The significance of this metabolic regulation beyond normal lymphocyte homeostasis is underscored by the various disease states that can result from growth factor excess (e.g., cancer or autoimmunity) or conditions of which growth factors are limiting (e.g., immunodeficiency).

B. Phosphatidylinositol 3-kinase (PI-3K)/Akt Controls B-Cell Glucose Energy

Metabolism

Classic biochemistry teaches that intermediary metabolism is homeostatically regulated, such that derepression of catabolic pathways occurs as a response to increased cellular ADP/ATP ratio. This ensures that adequate levels of ATP and/or metabolites are maintained to support biosynthetic reactions associated with cellular function. However, this has been revised based on studies of hormone-and growth factor-responsive tissues wherein extrinsic signals are required for the acquisition of extracellular nutrients and their metabolism [13,23,24,28-34]. Akt/PKB kinase has emerged as the link between the insulin receptor and increased glucose utilization as well as instructs cells to increase transcription and translation [35-37]. Naïve B lymphocytes do not enter the cell cycle and proliferate autonomously, but instead require extrinsic growth factors. For example, BCR cross-linking triggers activation of PI-3K, which plays an essential role in B cell growth and proliferation [38]. NF- κ B-and c-Myc-dependent gene expression programs lie downstream of PI-3K and have been implicated in B cell growth and survival [39-41]. It should not be surprising that signal transduction pathways possess the capacity to reprogram glucose metabolism in order to support B cell growth responses. Recent

finding by the Chiles' Lab point to a critical role for PI-3K signaling in orchestrating glucose carbon flow by regulating key glycolytic rate-limiting enzymes that control macromolecular synthetic demands imposed by BCR ligation [24].

C. ATP Citrate Lyase (ACL) and *de novo* Lipogenesis

Germane to my research, one of the biosynthetic fates of glucose is the conversion to lipids during *de novo* lipogenesis. *de novo* lipid synthesis is necessary for membrane production and lipid-based posttranslational modification of proteins. Briefly, glucose is converted to pyruvate by cellular glycolysis, imported into the mitochondria, decarboxylated to acetyl CoA, and condensed with oxaloacetate (OAA) into citrate (see Figure 3).

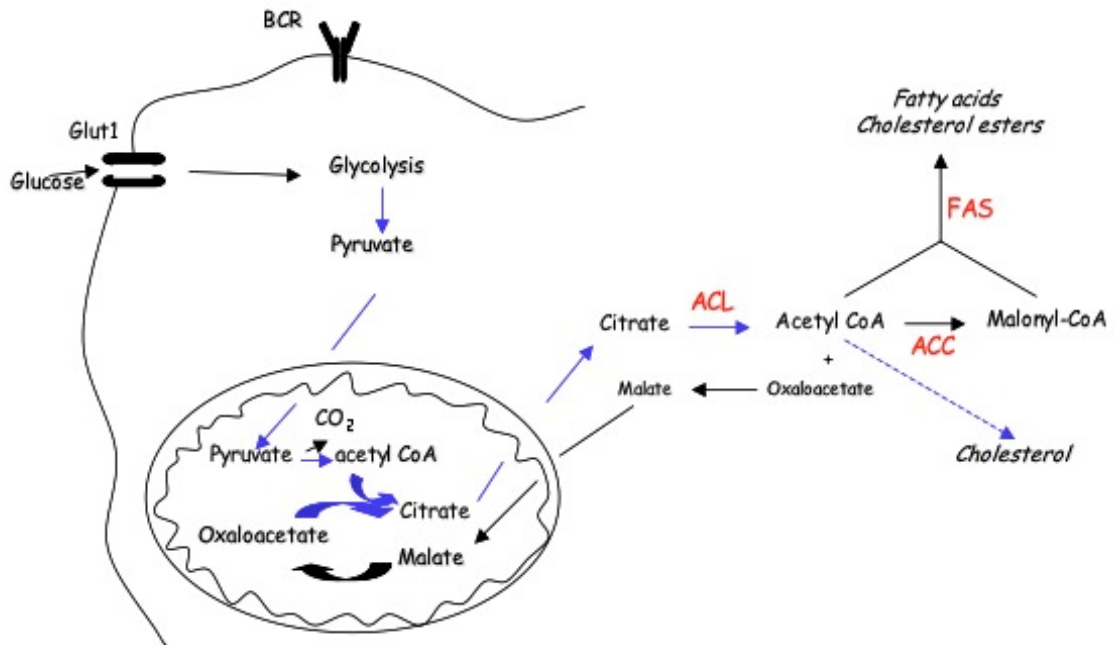


Figure 3. ACL and *de novo* Lipogenesis

Citrate is then either oxidized via the TCA cycle or exported from the mitochondria. Once exported from the mitochondria, cytosolic citrate is processed by ATP citrate lyase (ACL) to produce cytosolic acetyl CoA and regenerate OAA, which is the key step for the biosynthesis of fatty acids, cholesterol and acetylcholine [42-46].

ACL is a key homotetrameric enzyme linking glucose metabolism to lipid synthesis. Nutrients and hormones regulate the expression level and phosphorylation of ACL [44,46,47]. ACL is phosphorylated by GSK-3 on Thr⁴⁴⁶ and Ser⁴⁵⁰, and by PKA and Akt on Ser⁴⁵⁴ [48,49]. Phosphorylation on Ser⁴⁵⁴ abolishes the homotropic allosteric regulation by citrate and enhances the catalytic activity of the enzyme [47].

As evidence supports a role for PI-3K/Akt signaling in increased glucose uptake and glycolytic flux in B cells [24], we do not understand at this time how BCR signaling regulates glucose carbon flow into *de novo* lipogenesis. ACL is considered to be rate-limiting for glucose carbon flow into fatty acid and cholesterol synthesis and thus, its activation by PI-3K signaling in B cells may reflect an important regulatory mechanism by which the BCR reprograms glucose metabolism to support blastogenesis and perhaps, contribute to expansion of the endoplasmic reticulum and Golgi compartments, a prerequisite for synthesis, assembly and secretion of Ig. On a related point, plasma membrane cholesterol content has been implicated in regulating BCR signaling and B cell fate [50]. It is noteworthy that a growing body of evidence supports a critical role for ACL in cancer cell pathogenesis [51]. Knockdown of ACL leads to impairment of glucose-dependent lipid synthesis and a decrease in cytokine stimulated cell growth and

proliferation [45]. My research investigates the regulation and function of ACL in B cells stimulated through the BCR.

IV. *Cyclin D/cdk4/pRb Pathway in B Lymphocytes*

As mentioned earlier signaling through the BCR triggers B cell activation, which is a step necessary step for proliferation and differentiation. The decision to enter cell cycle is regulated by extracellular growth promoting and inhibiting signals [8,51]. It is necessary that the B cell is capable of translating these contrasting signals and coordinates them with the cell cycle machinery [8]. Understanding B cell cycle is necessary because many lymphoproliferative malignancies demonstrate a lack of responsiveness to extracellular signals, resulting in a loss of control over cell growth and proliferation a trademark of cell transformation [51].

The cell cycle is a series of events that a cell undergoes in order to grow and divide. It is coordinated with a complex network of tightly regulated proteins that must integrate extracellular signals to the intracellular cell cycle machinery in order to duplicate its genome. This investigation will focus on the biochemical signals that promote or inhibit the progression of the cell cycle at the first restriction point (R point) in G₁-phase. Passing through the R point is irreversible and it determines whether the cell is going to commit to S phase entry, revert back to quiescence, or initiate apoptosis [8]. It is also at the R point that the cell transitions from serum dependent to independent [51].

G₁-phase is noted for an increase in cell size (*i.e.*, growth), gene expression, and protein synthesis required for DNA synthesis. In a brief summary, progression through G₁-phase of the cell cycle is extensively regulated by a family of catalytic cyclin dependent kinases (cdks) that function together with their regulatory counterparts the D- and E-type cyclins [53]. The D-type cyclins (D1, D2, and D3) bind cdk4 and cdk6 in mid-G₁-phase, while cyclin E binds cdk2 in late-G₁-phase (see Figure 4) [54].

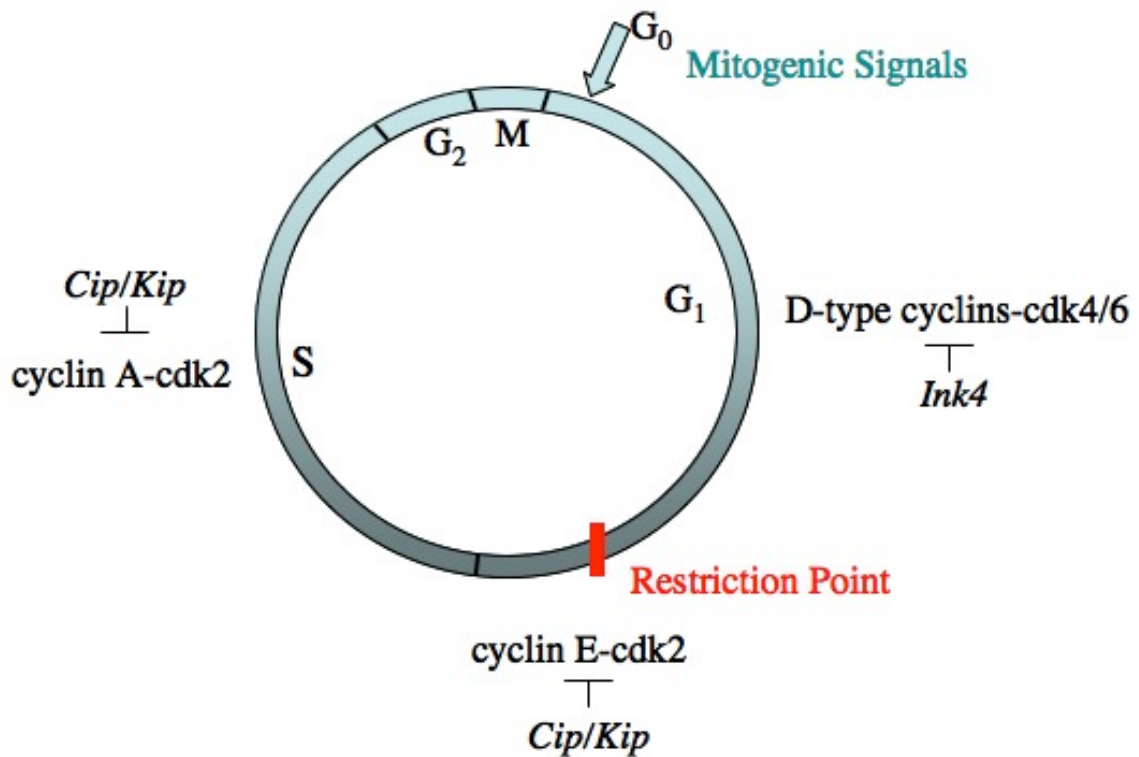


Figure 4. The Mammalian Cell Cycle [183]

Assembled complexes are transported into the nucleus where they must be phosphorylated by cdk-activating kinase (CAK) [53]. Together these complexes sequentially phosphorylate the retinoblastoma tumor suppressor protein (pRB) and pRB-related pocket proteins, p107 and p130 [53-55]. This in turn disrupts pRB association

with the E2F family of transcription factors, leading to the coordinated transcription of a variety of genes that are necessary for S-phase entry, nucleotide synthesis, DNA replication, and DNA repair [53,54,56]. E2F response genes include, *c-myc*, *B-myb*, *cdc2*, dihydrofolate reductase, thymidine kinase, and the promoter of the *E2F-1* gene itself [54,57]. Another gene in particular that E2F activates is cyclin E, which in turn binds cdk2 thereby activating the kinase complex and creating a positive feedback loop that ensures commitment to proliferation [53,58].

In addition to cyclin accumulation, the proper timing and duration of cdk activation are also controlled by regulation of cyclin-cdk assembly, subcellular localization, the action of cdk-inhibitors (cdki's, which will be discussed in section V), and posttranslational modifications of cyclin and cdk subunits [59,60]. The posttranslational modifications that yield active holoenzymes remain largely undefined; however, it has been established that maximal cdk activity is only achieved after nuclear import and subsequent phosphorylation by cdk-activating kinase (CAK) on Thr¹⁷² in cdk4/6 [61-63]. CAK activity appears to be constant throughout the cell cycle, but is induced in some cell types during G₁-S progression [63-65]. Phosphorylation on Tyr¹⁷ of cdk4 and cdk6 results in the inhibition of catalytic activity even in the presence of CAK-mediated phosphorylation [66,67]. Tyr¹⁷ phosphorylation is removed by the action of the Cdc25 family of protein phosphatases, which are subject to regulation at the protein level by extracellular signals [66,68-70]. The protein kinase responsible for Tyr¹⁷ phosphorylation has not been identified.

A. D-type Cyclins

In 1982, Tim Hunt first discovered cyclins while doing research using the sea urchin egg. He observed that certain proteins that were otherwise not detectable in the unfertilized eggs were synthesized early during fertilization and were later destroyed at certain stages of the cell cycle [71]. He called them cyclins and later he and others demonstrated that the cyclins bind and activate the cyclin-dependent kinases, which had been identified as a key cell cycle regulator by Paul Nurse. Both were awarded the Nobel Prize in 2001.

The D-type cyclins represent a unique protein in the cell cycle. Unlike other cyclins that are periodically induced throughout the cell cycle, the D-type cyclins are up regulated and controlled by extracellular mitogenic signals from the environment [53,54,72]. If there is a loss of extracellular stimulation prior to the R-point, D-type cyclins are degraded, which results in dephosphorylation of pRb and transition back into quiescence [59,73,74]. Therefore, the D-type cyclins are critical proteins that connect the extracellular environment with the cell cycle machinery in order to initiate genome replication [8,53]. In early embryogenesis of *Drosophila* where cell cycle precedes independently of extrinsic signals, the D-type cyclins are absent. On the other hand, constitutively active cyclin D pathways can override the necessary extracellular signals and cause a cell to enter the cell cycle prematurely, thereby contributing to oncogenic transformation [54,75,76].

The mammalian D-type cyclins (cyclin D1, D2, and D3) are encoded by three separate genes that share a high degree of amino acid homology and overlapping

expression patterns [60,77,78]. All three D-type cyclins have two highly conserved domains. The first domain is the cyclin box (~100 amino acids), which mediates binding to cdk and induces its active conformation [79]. The second conserved domain is a N-terminal LxCxE motif, which is critical for binding with pRb and is believed to play a role in orienting the cdk subunit [79]. My study will focus on cyclin D2 and D3, because there is no cyclin D1 in lymphoid lineages of mice. In splenic B-lymphocytes, BCR cross-linking induces endogenous cyclin D2 and cyclin D3 protein expression [80-82]. Studies performed in the Chiles' Lab demonstrated that NF- κ B signaling is required for BCR-induced cyclin D2 expression in B cells [83]. Further evidence shows MEK1/2-p42/44ERK and NF- κ B pathways link PI-3K activity to BCR-mediated cyclin D2 induction [83,84]. On the other hand, the regulation and function of cyclin D3 in B cell subsets is not well defined. The *cyclin D3* gene promoter contains multiple transcription factor recognition sites, including NF- κ B-binding sites, and B cells deficient in c-Rel exhibit diminished cyclin D3 induction in response to BCR cross-linking [85,86]. My study sought to elucidate the function of cyclin D3 in primary peritoneal B-1a cells and in the human diffuse large B cell lymphoma, OCI-LY18.

The ability to perform specific gene targeted knockouts in mice has allowed the direct study of the functions of the D-type cyclins. Gene targeting studies in mice where individual D-type cyclins are knocked out, show that the mice are viable and display limited abnormalities and phenotypes, suggesting high levels of functional redundancy [51,60,72,87]. Germane to my studies, cyclin D2 deficient mice are viable and display normal numbers of splenic B lymphocytes (B220⁺IgM⁺); however, they have a

significant reduction in the B-1a (CD5⁺) cell compartment [88-90]. In response to BCR cross-linking, B-lymphocytes from cyclin D2 deficient spleens exhibit impaired proliferation; however, that proliferation is not completely blocked is believed to be a result of redundancy with cyclin D3 in this tissue [88-90]. Cyclin D3 deficient mice are also viable, however they display a defect in the development of T-lymphocytes [88,89]. The molecular mechanisms of compensation between the D-type cyclins are unclear. Whether or not they are completely interchangeable or possess distinct biological functions remains to be revealed. In most tissues the remaining D-type cyclins that have not been knocked out are up regulated and appear to compensate for the targeted cyclin [51,72]. Mice with two D-type cyclins knocked out display the sum of the individual knock out phenotypes, while mice with all three D-type cyclins knocked out die at embryonic day 17.5 [72].

As mentioned above D-type cyclin genes share a high degree of homology with each other, however their expression profiles only partially overlap. Research studies have proposed that the specificity of each D-type cyclin lies within its tissue specific expression [60]. For example, cyclin D1 is observed in epithelium, while cyclin D3 is most ubiquitously expressed in lymphoid tissue [60,91]. A study published by Bartkova in 1998, demonstrates that the role of cyclin D3 is not fully redundant [76]. They revealed that in lymphocytes, cyclin D3 correlates with proliferation, thereby having the potential to be the driving force of oncogenesis in some lymphoid malignancies [76]. In a study of human B cells stimulated to proliferate, cyclin D3-cdk6 complexes were found to regulate proliferation, not cyclin D2 [92]. Of particular interest, gene expression

profiling studies have revealed that cyclin D3 expression is elevated in human GC B cells [93]. An important question is why cyclin D2 is not expressed in such highly proliferative cells. One possibility is that in this tissue specific setting, cyclin D2 is involved in the regulation of cell growth and not proliferation, which has been established in recent studies [51]. Therefore, the GC B cells actively repress cyclin D2 and growth, in order to rapidly proliferate [51]. This idea is supported by extensive D3 expression studies, which have demonstrated that tissue specific gene profiles for GC B cells favors proliferation, not growth. Lymphocytes are of the few cell types that show D3 expression in correlation with proliferation, which provides evidence for cell type-specific utilization of D-type cyclins [76,92,94].

As noted, D-type cyclins play an important role in growth and proliferation; as a result it is not surprising to find that abnormal expression can lead to deregulated growth and proliferation thereby becoming the root of several human cancers [87]. In many malignancies, overexpression of cyclin D proteins is observed [95]. Understanding the normal functions of the D-type cyclins is vital to gain insight into the role that these proteins are playing in human malignancies [95]. Studies have shown cyclin D1 is overexpressed and rearranged in breast cancer and mantle cell lymphoma, and a subset of multiple myeloma [91,95]. In mantle cell lymphoma the translocation involves cyclin D1 juxtaposed to the Ig heavy chain gene, which results in an overexpression of cyclin D1 in lymphoid cells, where typically only cyclins D2 and D3 are expressed [96]. Cyclin D2 is overexpressed in wide range of B cell malignancies and cyclin D3 the least studied of the three, is expressed in broad range of proliferating cells and is overexpressed in many

cancers [76,95]. Recent data suggests that in several hematological malignancies (myeloma, plasma cell leukemia, and diffuse large B cell lymphoma (DLBCL)), the overexpression of cyclin D3 has a genetic basis because t(6;14)(p21;q32) translocations of cyclin D3 and IgH genes have been detected [91].

V. Cyclin Dependent Kinase Inhibitors (cdki)

Cdk activity is negatively regulated by two families of inhibitory proteins: the INK4 family and the Cip/Kip family [53]. Cdk inhibitors not only maintain cell cycle control necessary for homeostasis, but they also have the potential to induce growth arrest and initiate apoptosis in cancer cells. The integrity of the pRB pathway appears to be compromised in most human cancers through an increased activity of the cyclin-cdk complexes and highly aggressive lymphomas often acquire alterations in their tumor suppressor pathways particularly affecting cdki's [91]. These inhibitors as they pertain to the immune system will be discussed in detail.

A. The INK4 Family

The INK4 family is comprised of p15^{INK4b} (p15), p16^{INK4a} (p16), p18^{INK4c} (p18), and p19^{INK4d} (p19). The four INK4 proteins are structurally similar. They contain pairs of anti-parallel α -helices stacked side by side called ankyrin repeats, which are connected by a series of hairpin motifs [97]. These structural regions bind the non-catalytic side of cdk4/6, which induces an allosteric rotation of 15° between the two lobes of cdk4/6, thereby altering the D-type cyclin and ATP binding sites [97]. Signals leading to INK4

synthesis are not fully understood. Studies have revealed that p15 is induced by TGF- β , p18/p19 is involved in development and terminal differentiation, and p16 is induced during senescence and is also a tumor suppressor [53,96].

p18 is an essential protein involved in terminal differentiation of mature B cells. It is expressed in many tissues and it is required for cell cycle arrest in B cells undergoing terminal differentiation into antibody secreting plasma cells [7]. A deficiency of p18 cannot be compensated by any other cdk, in particular p19, which has a similar expression pattern in B cells [11]. Studies demonstrate that p18 binds to cdk6, thereby arresting the cells in G₁ phase [10]. p18 knock out mice display lymphoproliferative disorders with enlarged lymph nodes with hyperplastic germinal centers and expansion of plasma cells [97], and p18^{-/-} B cells hyperproliferate in germinal centers never arresting in the cell cycle [7]. Cell cycle arrest mediated by p18 is therefore a prerequisite for the generation of functional plasma cells.

My study will focus on p16, which interacts with cdk4 and cdk6, thereby disrupting cyclin D and ATP binding, resulting in a block in cell cycle at the R point in G₁-phase [53]. Of the INK4 family of proteins, only p16 has gained credibility as a tumor suppressor gene. The *p16* gene is located in 9p21, which after *p53*, is the most frequently altered locus in human cancer [91]. Without p16 there is an increase in cyclin D-cdk4/6 activity followed by an increase in pRb activity, leaving the malignant cell with a growth and proliferation advantage [53,96]. Many tumors display an increase in cdk activity because of p16 inactivation. Specifically, p16 appears to play a role in regulating proliferation because it is either mutated or deleted in many human tumors of lymphoid

origin [98]. Studies in mice have revealed that deletions in p16 and p19 have led to spontaneous B cell lymphomas [10,89]. The importance of the interaction between cdk4 and p16 became apparent with the identification of a mutation in cdk4 in patients with familial melanoma [99,100]. This missense mutation results in a mutant cdk4 (R24C) protein that loses its affinity for p16 without affecting its ability to bind D-type cyclins and form a functional pRb protein kinase, thereby promoting tumor growth [99,100]. Induced expression of p16 in a tumor cell has been shown to block the binding of cdk4/6 with D-type cyclins, resulting in G₁-arrest [101]. This is under investigation as a therapeutic target.

p15 functions by binding cdk4, thereby preventing D-type cyclin binding or by disrupting already bound cyclin D-cdk4 complexes [53,54,56,80]. Studies by Chen-Kiang and colleagues have revealed that a frequent occurrence in the malignant plasma cells of Multiple Myeloma (MM) is inactivation of p15, thereby allowing aberrant proliferation [102]. It is proposed that the inactivation of p15 may contribute to MM pathogenesis by promoting the expansion of bone marrow myeloma precursors [102]. Studies have also revealed that mice deficient in p15 demonstrate lymphoproliferative disorders, splenic extramedullar hematopoiesis, hyperproliferation in germinal centers, and a reduction in serum antibody [89, 97]. Despite the potential role that p15 plays in plasma cell malignancies, the physiological role of p15 during terminal B cell differentiation remains to be characterized.

B. The Cip/Kip Family

The Cip/Kip protein family is made up of p21^{Cip1} (p21), p27^{Kip1} (p27), and p57^{Kip2} (p57). These proteins share a conserved N-terminal region, which mediates cyclin/cdk binding, and a non-conserved sequence region, which gives each protein its ability to perform different functions [103]. p21 is a downstream transcriptional target of p53 and data have shown that it mediates DNA damage induced cell cycle arrest [103]. p57 is believed to regulate cell cycle during embryonic development, while p27 is found in quiescent cells and is rapidly down regulated when the cells enter G₁-phase of the cell cycle and begin to proliferate [103]. Loss of Cip/Kip function has not been observed in many human cancers.

My study will characterize, in part, the role of p27 in cell cycle regulation in human LY18 cells. p27 plays two major roles in B cells; first, it is required for assembly and nuclear import of D-type cyclins-cdk complexes. Evidence for a noncatalytic function of these complexes is demonstrated in murine fibroblasts lacking p27 and p21 that failed to assemble cyclin D-cdk complexes [104]. In addition, cyclin D-cdk4 complexes play an important secondary noncatalytic function by sequestering Cip/Kip family members away from cdk2 complexes [53,72,105]. Finally, p27 is able to insert into the catalytic cleft of cdk2, thereby preventing the binding of ATP and cyclin E, and perturbing the cell cycle [103].

In lymphoid tissue, the expression of p27 is inversely related to proliferation. p27 expression is high in quiescent cells, whereas in proliferating cells (*i.e.*, germinal

centers) it is down regulated [91]. Studies in the immature B cell lymphoma cell line, WEHI 231, have identified p27 as a proapoptotic gene [106]. BCR-engagement leads to a signaling pathway that results in a decrease in c-Myc levels and an increase in p27 levels, which promotes apoptosis [106]. In lymphomas, typically the expression of p27 follows the same inverse relationship with proliferation; however, in some DLBCL a wide range of p27 expression often exists; ranging from an absence of p27 protein to an overexpression of p27 [91]. There does not seem to be any positive or negative correlation between p27 and proliferation in DLBCL.

Furthermore, studies have demonstrated that p27 deregulation in certain cancers leads to poor prognosis [107]. In B-cell Chronic Lymphocytic Leukemia (B-CLL), high expression of p27 is associated with an aggressive course and lower spontaneous cell death rate of cells in culture [91]. This suggests that p27 may be involved in the deregulation of apoptosis and that a mechanism of p27 inactivation other than down-regulation exists, which allows the tumor cells to overcome the antiproliferative activity of this cdki [91]. Restoration of p27 activity and stability may prove to be an effective therapy to induce cell cycle arrest in B cell cancers [107].

VI. *B-1 Lymphocytes*

A. *Development and Function*

Two B cell lineages, B-1 cells and conventional splenic B-2 cells (referred to as B cells in the earlier text) arise from lymphopoiesis (refer to Figure 1). Each subset is distinguished by numerous phenotypic and functional characteristics. B-1 cells are

distinguished from the more abundant conventional B-2 cells by the expression of the pan-T cell surface glycoprotein, CD5 [108]. Additional identifying phenotypic characteristics include sIgM^{hi}, sIgD^{lo}, CD43⁺, Mac1⁺, CD23⁻, and B220^{lo} [109,110]. Peritoneal B-1 cells are further subdivided into CD5⁺ (B-1a) or CD5⁻ (B-1b) cells. My study will focus on B-1a cells (referred to in the text as B-1). B-2 cells represent the majority of the B cell population and are found primarily in the lymph nodes and spleen. B-1 cells are a minor, unique subset of the B cell pool that arises first in ontogeny in the fetal omentum and later in the fetal liver and bone marrow, thereby predominating the B-cell repertoire early in life [1,108]. Concepts regarding the origin of B-1 cells have changed over the years. Early work suggested that B-1 cells exist as a separate lineage, distinct from conventional B and T cells [111]. Other studies suggest that there is only one B cell lineage, and that B-1 cells are derived by B cell receptor (BCR) signaling following interactions between surface Ig and (self-) antigen [112]. More than likely, elements of both lineage and differentiation play a role in producing B-1 cells [113]. In adult mice, B-1 cells make up the lymphocyte population in the peritoneal cavity and a small population in the spleen [114]. B-1 cells are maintained by self-replenishing, giving rise to their own progeny, in contrast to B-2 cells, which do not proliferate following maturation in the absence of exogenous stimulation.

B-1 cells are responsible for the majority of non-immune serum IgM and contribute substantial amounts of resting IgA [115,116]. The inherent and constitutive secretion of immunoglobulin by B-1 cells, in the absence of direct stimulation, distinguishes B-1 cells from B-2 cells. B-1 cell-derived immunoglobulin (Ig) generally

adheres more closely to the germline state than B-2 Ig, as a result of diminished somatic mutation and reduced length of non-templated N-insertions; thus, they are repertoire restricted [117-120]. It has been suggested that B-1 cells play an important role in the early immune response against a range of microorganisms by producing a natural antibody that provides a low affinity of protection [121-123].

B-1 cells are associated with many human disease states characterized by B-cell expansion. They exhibit the inclination for clonal expansion and for malignant transformation with age [8,124]. B-1 cells have been implicated in the pathogenesis of autoimmunity, because: a) increased number of B-1 cells are found in patients and animals with some autoimmune disorders; b) the elimination of B-1 cells reverses autoimmunity in some cases; and, c) B-1 cell Ig displays binding to self antigen [125-129]. Notably, B-1 cells represent the origin for human chronic lymphocytic leukemia (CLL), a B cell malignancy in which the cells express CD5. Furthermore, studies have also demonstrated that in aging mice, monoclonal expansion of B-1 cells resembles CLL [130].

B. Proliferation

Murine B-1 cells also differ from B-2 cells by the signals necessary to induce proliferation. B-1 cells are self-renewing, whereas B-2 cells arise continually from B cell precursors, but fail to proliferate following maturation without an exogenous stimulation. This suggests that the regulation of proliferation differs between these two B cell subsets. In *ex vivo* B-1 cells, BCR signaling fails to induce proliferation but does so in B-2 cells

[131,132]. Early studies performed in the Rothstein lab in the late 1980s in collaboration with work from the Chiles' Lab demonstrates that B-1 and B-2 cells differ significantly in their response to phorbol esters. B-1 cells rapidly enter S-phase in response to PMA, whereas B-2 cells require a combination of PMA and a calcium ionophore [131,132]. Thus, in relation to B-2 cells, B-1 cells are hyper-responsive to phorbol esters. This hyper-responsiveness to PMA is further manifested in the rapidity with which S-phase is attained; peak thymidine incorporation occurs 24-30 hours after B-1 cells are stimulated with PMA, but 54-60 hours after B-2 cells are mitogenically stimulated with PMA plus ionomycin [133]. These results, along with the propensity of B-1 cells for self-renewal, clonal expansion, and malignant transformation, demonstrate that B-1 cells differ from B-2 cells in the signaling requirements needed for proliferation and in the molecular mechanisms that control G₀-S-phase progression. In further support of this observation, PMA-stimulated B-1 cells express cyclins D2 and D3 in a non-overlapping manner during G₁-phase [65,134]. Specifically, cyclin D2 is rapidly upregulated in early G₁-phase, while cyclin D3 is upregulated after cyclin D2 degradation and peaks in parallel with pRb phosphorylation in late G₁-phase [134]. In B-2 cells, mitogenic activation leads to a coordinate, overlapping induction of both cyclin D2 and D3 [82,134]. Together these data suggest that cyclin D3 is uniquely positioned in B-1 cells to play a specific role

in mediating the transition from G₁-S phase (see Figure 5).

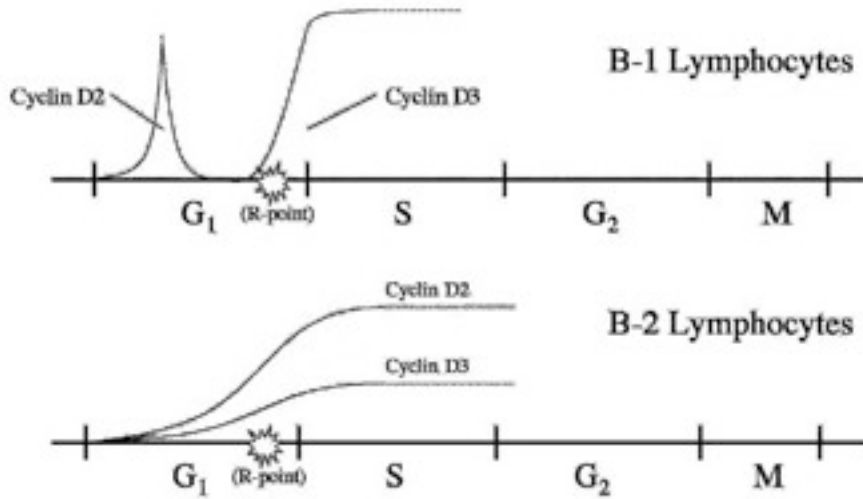


Figure 5. Cyclin D Expression in B-Lymphocytes

VII. Cyclin D/cdk4/pRb Pathway in B Cell Lymphoma

Understanding the cyclin D/cdk/pRb pathway and the other molecules involved in the G₁-S phase transition is of particular interest because they are altered in 80% or more of human malignancies [97]. Specifically, the genes encoding cdks involved in G₁-S phase progression are amplified in many DLBCL. For example, overexpression of cdk4 and cdk6 has been identified in DLBCL and lymphoid tumors, however the molecular studies of cdk4/6 are yet to be analyzed in detail [88,97,135]. The cdk2 gene is often overexpressed in many B cell malignancies and its inhibition is a potential target to inhibit tumor cell proliferation [136]. High levels of cyclin E have been associated with many different human cancers, particularly, breast cancer, leukemia, and Non-Hodgkin's lymphoma [58,137]. Also, transgenic mouse models in which cyclin E is overexpressed

develop malignant diseases as a result of accelerated G₁-phase of the cell cycle [58,137]. The role of cyclin E in tumorigenesis has only recently begun to be unfolded.

It is also important to note that in tumor cells, knockdown of G₁-phase proteins often results in no phenotype. The high levels of other proteins may compensate, thereby allowing cell cycle progression in malignant cells. It is possible that particular cyclins and cdk's have redundant functions and can compensate for the deficiency of a specific protein. For example, studies have revealed that cyclin E has been shown to not only overcome a deficiency of other G₁-cyclins in yeast, but also does so in higher mammals such as mice [58]. In 1999, Geng et al replaced cyclin D1 with cyclin E in a knock-in mouse study [138]. Cyclin E was able to rescue all phenotypic manifestations of the cyclin D1 deficiency [138]. This compensatory action has also been observed in human breast cancer [139]. Furthermore, studies have revealed that cdk2 activity can also be dispensable for cancer cell proliferation [140]. High levels of cdk4 activity in these cells may compensate for the lack of cdk2 during cell cycle progression [140].

VIII. Non-Hodgkin's Lymphoma

Non-Hodgkin's lymphoma (NHL) is a group of heterogeneous lymphoproliferative malignancies. Currently, in the United States, there are an estimated 66,000 new cases of NHL and 19,000 deaths [141]. There are many different types of NHL, which are first classified as B or T cell origin as well as slowly growing or aggressive. My study will focus on B cell origin NHL that accounts for approximately 85% of NHL in adults [141].

A large part of understanding the biology of a malignant cell is gleaned from its non-malignant counterpart—the normal, untransformed cell. This holds true with B cell malignancies. The malignant cell often resembles a normal B cell during a specific stage of B cell differentiation. B-cell lymphomas retain normal physiologic and phenotypic properties of the healthy B cell while also developing pathological abnormalities [142]. This is a useful tool used in the classification and diagnosis of lymphoma.

My study will focus on DLBCL, the most common type of NHL in adults, accounting for approximately 30-40% of cases [93,142-144]. DLBCL is an aggressive, mature B cell malignancy. Patients typically receive (and can be cured) by anthracycline-based chemotherapy. However, the response to treatment is often highly variable.

A. Diffuse Large B-Cell Lymphoma

Diffuse large B cell lymphoma (DLBCL) is a heterogeneous group of lymphomas characterized by its diffuse pattern of growth. It affects people of all ages and typically appears as an aggressive, rapidly growing nodal mass often times with extranodal sites present [94,142]. The malignant population is made up of large cells with big distinct nucleoli and little cytoplasm.

Gene expression profiling of DLBCL reveals two molecular classifications: germinal center (GC)-like and activated DLBCL [93,142,144]. My study will focus on GC-like DLBCL, which display a distinct gene expression profile that is preserved in normal GC B cells. There is evidence that suggests most if not all DLBCL's develop within the GC or at a later stage of B cell differentiation [93,142,145]. Furthermore,

gene-profiling studies reveal that the rearranged immunoglobulin genes in DLBCL have mutations that resemble what is normally found during somatic hypermutation, which normally occurs only within GC's [93,145].

Often times, the presentation of a malignancy is a result of uncontrolled cell proliferation as a result of deregulated apoptosis; however, DLBCL is just the opposite. It is observed that the increased proliferation and cell accumulation are a consequence of deregulated cell cycle [135]. DLBCL's commonly display several translocations; t(14;18) and t(3;14) juxtapose BCL-2 and BCL-6, respectively with the immunoglobulin heavy chain on 14q32 and overexpression of the genes *CDK2* in 12q13.3 and *CDK4* in 12q14.1 along the 12q region [146-149].

B. OCI-LY18

My study will focus on the human GC-like DLBCL, OCI-LY18 (LY18). LY18 cells were established (1988) in a 56-year-old male, who relapsed with stage IIIB, high-grade non-Hodgkin's lymphoma of diffuse large cell immunoblastic type [150]. The cell line was established from the patient's pleural fluid and the cells are characterized as of a large size with a high nuclear to cytoplasm ratio and one or more nucleolus [150]. LY18 cells are further identified based on the immunophenotypic characterization, CD10⁺, CD19⁺, CD20⁺, CD21⁻, CD23⁻, as well as IgM and light chain λ [150]. The cell line carries a three-way translocation involving bands 8q24, 14q32, and 18q21, which lead to an alteration of myc-IgH genes [150]. MYC induces proliferation by inducing the genes for cell cycle progression, such as *cdk4*, cyclin D1, D2, and E and it suppresses the

inhibitors p15 and p21 [135]. Approximately 6% of DLBCL have c-MYC translocations and they are under the control (like the LY18 cells) of the Ig enhancer [135]. The Ig enhancers are responsible for the inappropriately high transcription rate of the translocated c-myc allele. The detailed function of c-Myc is not yet completely understood, but it is believed to involve the promotion of both cell proliferation and apoptosis [151]. The Bcl-2 gene is germline in LY18 cells (it is typically rearranged in DLBCL) and the Bcl-6 gene is only moderately expressed with no translocations.

Of particular interest, I have found that LY18 cells only express cyclin D3. In studying lymphoid malignancies, cyclin D3 has been identified as a potential oncogene because it is frequently overexpressed in certain human lymphoid cancer subsets (e.g. B-CLL) [94,95,152]. In 2002, a study analyzed the clinical significance of cyclin D3 expression in DLBCL and revealed that increased expression levels of cyclin D3 were at advanced stages and had a lower overall survival [152]. Overall, cyclin D3 expression is associated with poor clinical outcome in patients with DLBCL [152].

IX. Summary/Aims of Study

A. Chapter 1: The role of cyclin D3 in growth and proliferation in primary peritoneal B-1a cells

In summary, in B-1 cells, but not B-2 cells, stimulated expression of cyclin D2 and D3 is temporally distinct. Taken together, these observations suggest that cyclin D3 is uniquely positioned in B-1 cells to mediate transition through the G₁-S boundary, which may reflect its role in conventional B-2 cells where cyclin D3 expression overlaps

with that of cyclin D2. To investigate the role of cyclin D3-cdk complexes in G₀-S phase progression in normal B-1 cells, I used protein transduction technology to specifically block assembly and activation of cyclin D3 holoenzyme complexes in normal peritoneal B-1 cells. I also examined the proliferative responses of B-1 cells from cyclin D3-deficient mice.

B. Chapter 2: Cyclin D3-cdk4/6 complexes are dispensable in the growth and survival of the human Diffuse Large B-cell Lymphoma, OCI-LY18; evidence for redundancy by cyclin E

Typically, there are two or three D cyclins expressed in overlapping roles in normal and malignant cells [76]. Therefore, targeting only one D-type cyclin is not useful due to compensation by the remaining cyclins. LY18 cells express only cyclin D3, which out of the D-type cyclins is the least characterized. This leaves a unique opportunity to target cyclin D3-cdk4/6 complexes in LY18 cells and to further elucidate the role of cyclin D3 in malignant lymphomas as well as in normal, healthy B cells. To investigate the role of cyclin D3-cdk complexes in G₀-S-phase progression in LY18 cells, I used protein transduction technology and RNA interference to specifically block assembly and activation of cyclin D3 holoenzymes. The literature and clinical trial studies have revealed that small molecule inhibitors of cdk4 may provide a promising therapeutic strategy in treatment of human DLBCL's. With that in mind I also used a small molecular inhibitor to further examine the role of cyclin D3-cdk4/6 in LY18 cells.

C. Chapter 3: The regulation and function of ATP citrate lyase (ACL) by extrinsic signals in splenic B-lymphocytes

In summary, B-lymphocytes rapidly increase glucose uptake and hyper-induce glycolytic flux in response to BCR cross-linking [23,24], and in our most recent findings we discovered that IL-4 induces glycolysis in naïve B cells [27]. A high glycolytic rate may reflect a requirement to provide sufficient levels of glycolytic intermediates to support macromolecular synthesis, associated with B lymphocyte activation. As evidence supports a role for PI-3K/Akt signaling in increased glucose uptake and glycolytic flux in B cells [24], it is not understood at this time how BCR signaling regulates glucose carbon flow into *de novo* lipogenesis. Foremost, I hypothesize that glucose-directed *de novo* lipogenesis in B cells requires a PI-3K-dependent step that results in activation of ATP citrate lyase (ACL) via a post-translational mechanism. With this in mind, my studies sought to understand more fully the regulation and biological significance of ACL activation as instructed by the BCR and by signaling input from IL-4. Furthermore, I will examine the role of PI-3K/Akt signaling pathway in the regulation of ACL enzyme activity. Here I will use specific PI-3K chemical inhibitors as well as PI-3K deficient-mice.

MATERIALS AND METHODS

Reagents and Antibodies

Anti-cyclin D1 (DCS-6), anti-cyclin D2 (DCS-3.1), and anti-cyclin D3 (DCS-22) antibodies (Abs) were purchased from Thermo Fisher Scientific (Fremont, CA). Anti- β actin (AC-15) Ab was purchased from Sigma-Aldrich (St. Louis, MO). Anti-phospho-pRb^{Ser807/811} Ab, anti-phospho-cdk2^{Thr160} Ab, anti-total pRb, anti-phospho-ATP-citrate lyase^{Ser454} Ab, anti-ATP-citrate lyase Ab, and anti-hsp90 Ab were obtained from Cell Signaling Technologies (Beverly, MA). Anti-cdk4 (C-22) Ab, anti-cdk6 (C-21) Ab, anti-cdk2 (M2) Ab, and anti-p27 (C19) Ab, Protein G agarose, anti-mouse IgG-coupled HRP, and anti-mouse cdk4 Ab were purchased from Santa Cruz Biotechnology (Santa Cruz, CA). Anti-phospho-pRb^{Thr821} (44-582G) Ab was purchased from Invitrogen Corporation (Carlsbad, CA). Fluorescent-labeled Abs for FACS was obtained from BD Pharmingen (San Diego, CA). Rabbit complement and Lympholyte M were purchased from Accurate Chemical and Scientific (Westbury, NY). All other chemicals were obtained from Sigma-Aldrich. Fluorescent-labeled Abs directed against B220, CD5, CD23, Mac-1, CD4, CD8, CD3, and CD14 for FACS and flow cytometric analysis were obtained from BD Pharmingen. Electrochemiluminescence (ECL) reagents were obtained from Kirkegaard and Perry Laboratories (Gaithersburg, MD). F(ab')₂ fragments of goat anti-mouse IgM were obtained from Jackson ImmunoResearch Labs (West Grove, PA). Murine IL-4 was from R&D Systems (Minneapolis, MN). Phorbol 12-myristate 13-acetate (PMA) and Lipopolysaccharides (LPS) from *Salmonella typhosa* (source strain

ATCC 10749) were obtained from Sigma-Aldrich and used at 300 ng/ml and 25 µg/ml, respectively. Soluble rCD40L was obtained from transfected J558L cells that secrete a chimeric CD40L/CD8α fusion protein and prepared as previously described [153,154]. Anti-CD8α Ab was obtained from the supernatant of 53-6-72 hybridoma cells and was used to cross-link rCD40L [154]. CD40L was used at 1/10 dilution of supernatant and anti-CD8α Ab was used at 1/40 dilution of supernatant. 2-Bromo-12,13-dihydro-5H-indolo[2,3-a]pyrrolo[3,4-c]carbazole-5,7(6H)-dione, (cyclin dependent kinase 4 inhibitor, cdk4i), Carbobenzoxy-L-leucyl-L-leucyl-L-leucinal (MG-132), Wortmannin (WT), and LY294002 (LY) were obtained from Calbiochem-NovBiochem, Corp. (San Diego, CA). siGENOME SMARTpool siRNA was purchased from Thermo Dharmacon Scientific (Chicago, IL): p27, cyclin D3, cyclin E, cdk4, cdk6, cdk2, and control (Table 1).

Preparation of Murine B-1a and B-2 Lymphocytes and Cell Culture

The cyclin D3-deficient mice were obtained from Dr. Piotr Sicinski (Dana-Faber Cancer Center, Boston MA; see *Cancer Cell* 4:451). p85α-deficient mice (BALB/cAnNTac-Pik3r1 N12, back crossed nine times) and BALB/cByj mice were purchased from The Jackson Laboratory (Bar Harbor, ME) and housed at Boston College. The studies described below were reviewed and approved by institutional animal care and use committees at both institutions. Mice were cared for and handled at all times in accordance with National Institutes of Health and University guidelines. Unseparated cells were obtained by peritoneal washout and splenic disruption and stained with immunofluorescent Abs directed against B220 and CD5, and were subjected to

FACS at 4°C using a Mo-Flo flow cytometer (DakoCytomation, Carpinteria, CA) to yield purified peritoneal B-1 (B220⁺CD5⁺) and splenic B-2 (B220⁺CD5⁻) cells, including the use of an anti-CD8 “dump” channel for B cell purification. Sort-purified B cell populations were re-analyzed by immunofluorescent staining with Abs directed against CD3 and CD14. Sort-purified peritoneal B-1a cells and splenic B-2 cells were found to be $\geq 95\%$ (SEM $\pm 0.98\%$) and $\geq 96\%$ (SEM $\pm 0.84\%$) pure, respectively. In addition, both populations contained less than 1.8% and 1.2% CD3⁺ or CD14⁺ cells, respectively. Mature B-2 cells were isolated from spleens of mice 8-12 weeks. T-lymphocytes were depleted with anti-Thy-1.2 plus rabbit complement (Accurate Chemical and Scientific), macrophages (and other adherent cells) were removed by plastic adherence, and red blood cells and nonviable cells were removed by sedimentation on Lympholyte M (Accurate Chemical and Scientific). Small dense B cells were further isolated following centrifugation through a discontinuous Percoll gradient as described [24]. B-cells were cultured in RPMI 1640 medium supplemented with 10% heat-inactivated fetal bovine serum (FBS), penicillin (100 U/ml), streptomycin (100 $\mu\text{g/ml}$), 2-mercaptoethanol (50 μM), and glutamine (2 mM), and incubated at 37 °C in a 5% CO₂ atmosphere at 95% humidity. Dr. Raju Chaganti (Memorial Sloan-Kettering Cancer Center, New York, NY) kindly provided the human GC-like DLBCL cell line OCI-LY18 (LY18). The cells were maintained in RPMI 1640 medium supplemented with 10% heat-inactivated fetal bovine serum (FBS), penicillin (100 U/ml), streptomycin (100 $\mu\text{g/ml}$), 2-mercaptoethanol (50 μM), and glutamine (2 mM) at a cell density of 5×10^5 to 1×10^6 cells/ml (at 37 °C in a 5% CO₂ atmosphere at 95% humidity) [155].

TAT Peptides

TAT-p16 peptides were synthesized by the Biotechnology and Genomics Research Center (Utah State University, Logan, UT). The 32-mer peptides contain an NH₂-terminal 11 residue TAT protein transduction domain (YGRKKRRQRRR) immediately followed by a glycine residue and either a 20-mer wild-type p16 sequence (DAAREGFLATLVVLHRAGAR) or a charge-match control sequence (ARGRALTAHVDRDLGEFVAAL), as described [156,157]. TAT-p27 fusion proteins were kindly provided by Dr. Mira Grdisa (Rudjer Boskovic Institute, Zagreb, Croatia) [158]. Each fusion protein was coupled to an 11-amino-acid peptide (YGRKKRRQRRR) consisting of the NH₂-terminal HIV TAT protein transduction domain immediately followed by a glycine residue and either a full-length wild-type TAT-p27 fusion protein (TAT-p27 WT), a functional truncated N-terminal-TAT-p27 protein (TAT-N'p27), or an inactive point mutant-TAT-p27 protein (TAT-ptMut-p27) [159].

Flow Cytometry

For cell cycle phase analysis, B cells (10^5) were resuspended in 300 μ l of PBS containing 0.1% (v/v) Triton X-100, 200 μ g/ml DNase-free RNase A, and 20 μ g/ml propidium iodide [108]. B cell fluorescence was then acquired with a BD FACSCanto flow cytometer (BD Biosciences). DNA synthesis was measured by BrdU incorporation according to the manufacturer's instructions (BD Biosciences Pharmingen). For apoptosis measurements, LY18 cells (10^5) were collected, washed in PBS and then resuspended in 0.5 ml binding buffer (10 mM HEPES, pH 7.4, 140 mM NaCl, 2.5 mM CaCl₂) containing

5 μ l of FITC-conjugated-Annexin V and 5 μ l PI (50 μ g/ml). Cells were incubated at room temperature for 15 mins and then analyzed by flow cytometry. For cell viability measurements, 5×10^5 cells were collected by centrifugation at 400 x g for 8 mins, washed in FACS buffer (1 x PBS containing 0.5% BSA and 0.01% sodium azide), and resuspended in FACS buffer containing 5 μ g/ml PI. Samples were incubated on ice for 10 mins then analyzed by flow cytometry using a BD FACSCanto flow cytometer with BD FACS Diva software (BD Biosciences). Standard deviations for all flow cytometry analysis were between 5-10% unless otherwise specified in the figure legends.

Proliferation Assay

To measure proliferation, B cells ($1-2 \times 10^4$ in 0.2 ml) were cultured in quadruplicate and stimulated as indicated in the figure legends. DNA synthesis was measured by incubating B cells with 0.5 μ Ci [3 H]thymidine (20 Ci/mmol; New England Nuclear, Waltham, MA) during the last 6 hrs of culture. Cells were then harvested onto glass fiber filters and [3 H]thymidine incorporation into DNA was quantitated by liquid scintillation spectroscopy.

Western Blotting

LY18 cells and B cells were solubilized in Triton X-100 buffer (20 mM Tris (pH 7.4), 100 mM NaCl, 0.1% Triton X-100) containing 2.5 μ g/ml leupeptin/aprotinin, 10 mM β -glycerophosphate, 1 mM PMSF, 1 mM NaF, and 1 mM Na_3VO_4 . Insoluble debris was removed by centrifugation at 15,000 x g for 15 mins (4°C). Lysate protein was

separated by electrophoresis through a 7.5%, 10%, or 12% polyacrylamide SDS gel (SDS-PAGE) and transferred to an Immobilon-P membrane. The membrane was blocked in TBS-T (20 mM Tris (pH 7.6), 137 mM NaCl, and 0.05% Tween 20) containing 5% nonfat dry milk for 60 mins and then incubated overnight (4°C) with primary Ab at 1 µg/ml in TBS-T. The membrane was washed several times in TBS-T, incubated with a 1/2,500 dilution of anti-rabbit or anti-mouse IgG-coupled HRP Ab (60 mins) and developed by ECL. Autoradiograms were scanned with Adobe Photoshop 7.0 (Adobe Systems, Inc., San Jose, CA) and the mean density of each band was analyzed by the ImageJ program (NIH, Bethesda, MD).

Fluorescence Microscopy

B cells were centrifuged at 600 x g for 10 mins onto glass slides by Cytospin. For imaging D-type cyclins, lymphocytes (2.5×10^5) were fixed with methanol for 10 mins at -20°C and then permeabilized with 0.1% Triton X-100 at room temperature. Cells were blocked for 30 mins with 2% BSA in PBS and then washed several times with PBS. Detection of cyclin D2 and cyclin D3 was performed by incubating cells with 1:50 anti-cyclin D2 or anti-cyclin D3 mAbs at 4°C, respectively. After several washes with PBS, cells were incubated with a 1:200 FITC-conjugated Affinipure goat anti-mouse Ab (Jackson ImmunoResearch Laboratories, West Grove, PA) for 2 hrs at room temperature. The slides were then dried, mounted with Aqua Polymount, and immunofluorescence images were captured with a Leica confocal microscope.

Nucleofection

LY18 cells were transfected using the Amaxa nucleofection technology™ (Amaxa, Koeln, Germany). Cells were resuspended in solution V from nucleofector kit V, following the Amaxa guidelines for cell line transfection. Briefly, 2×10^6 cells/condition were centrifuged at 90 x g at room temperature for ten minutes. LY18 cells were then resuspended in 100 μ l of pre-warmed solution V and mixed with 200, 300, or 400 pmol of siRNA. The LY18 cell suspension was transferred into the provided cuvette and nucleofected with an Amaxa Nucleofector (Amaxa). LY18 cells were transfected using the X-001 pulsing parameter and were immediately transferred into wells containing 37 °C, pre-warmed culture medium (Optimem supplemented with 10% FCS) in a 6-well plate. After transfection, cells were cultured from 2 to 48 hrs and analyzed by flow cytometry using a BD FACSCanto flow cytometer with BD FACS Diva software (BD Biosciences).

Lipid Isolation, Purification, and Quantification

Total lipids were isolated and purified from lyophilized B-lymphocytes by using modifications of previously described procedures [160,161]. B cells (6×10^6) were stimulated as specified in the figure legends. At several time points the cultures were pulsed for 3 hrs with 6 μ Ci/ml D-[6-¹⁴C] glucose (New England Nuclear). B cells were collected and total lipids extracted in chloroform: methanol (1:1 v/v); the neutral and acidic lipids were then separated from the total lipids by using DEAE-Sephadex (A-25;

Pharmacia Biotech, Upsala, Sweden) column chromatography as previously described [162-164]. The total lipid extract, suspended in solvent A ($\text{CHCl}_3:\text{CH}_3\text{OH}:\text{H}_2\text{O}$, 30:60:8 by vol), was then applied to a DEAE-Sephadex column (1.2 ml bed volume) that had been equilibrated with solvent A. The column was washed twice with 20 ml of solvent A, and the entire neutral lipid fraction, consisting of the initial eluent plus washes, was collected. This fraction contained cholesterol, phosphatidylcholine, phosphatidylethanolamine, ceramide, sphingomyelin, and cerebrosides. The acidic lipids were then eluted from the column with 30 ml of solvent B ($\text{CHCl}_3:\text{CH}_3\text{OH}:0.8 \text{ M Na acetate}$, 30:60:8 by vol). This fraction contained the gangliosides and other less hydrophilic acidic lipids, including free fatty acids, cardiolipin, phosphatidylserine, phosphatidylinositol, phosphatidic acid, and sulfatides. Folch partitioning will remove any unincorporated glucose and the gangliosides from the neutral and acidic fractions, respectively [165]. The concentration of neutral and acidic lipids will be determined by scintillation counting using 1219 Rackbeta Counter (LKB Wallac).

High-Performance Thin-Layer Chromatography

All lipids were analyzed qualitatively by high-performance thin-layer chromatography (HPTLC) according to previously described methods [160-162,164]. Lipids were spotted on 10×20 cm Silica gel 60 HPTLC plates (E. Merck, Darmstadt, Germany) using a Camag Linomat V auto-TLC spotter (Camag Scientific Inc., Wilmington, NC). For the analysis of neutral lipids, 4000 dpm were spotted per lane. To enhance precision, an internal standard (oleoyl alcohol) was added to the neutral and

acidic lipid standards and samples as previously described [162,164]. Purified lipid standards were purchased from Matreya Inc. (Pleasant Gap, PA, USA) or Sigma (St. Louis, MO, USA) or were a gift from Dr. Robert Yu (Medical College of Georgia, Augusta, GA, USA). For neutral phospholipids, the plates were developed to a height of either 4.5 cm, respectively, with chloroform:methanol:acetic acid:formic acid:water (35:15:6:2:1 by vol), then developed to the top with hexanes:diisopropyl ether:acetic acid (65:35:2 by vol) as previously described [162,163]. Neutral and acidic lipids were visualized by charring with 3% cupric acetate in 8% phosphoric acid solution, followed by heating in an oven at 160-170°C for 7 mins. The percentage distribution of the individual radiolabeled lipid bands was determined by scanning the plates using a Bioscan imaging system as previously described [166]. These experiments were carried out in collaboration with Dr. Thomas Seyfried, Department of Biology, Boston College.

ATP Citrate Lyase (ACL) Enzyme Activity

ACL activity was measured via the malate dehydrogenase coupled method [167]. B cells (8×10^6) were stimulated as specified in the figure legends and solubilized in RIPA buffer (25 mM Tris (pH 7.6), 150 mM NaCl, 1% NP-40, 1% sodium deoxycholate, 0.1% SDS) containing 2.5 µg/ml leupeptin/aprotinin, 10 mM β-glycerophosphate, 1 mM PMSF, 1 mM NaF, and 1 mM Na₃VO₄. Insoluble debris was removed by centrifugation at 15,000 x g for 15 mins (4°C). Whole cell lysates were added at a 1:19 ratio to the reaction mixture containing 100 mM Tris-HCL (pH 8.7), 20 mM potassium citrate, 10 mM MgCl₂, 10 mM DTT, 0.5 U/ml malate dehydrogenase, 0.33 mM CoASH, 0.14 mM

NADH, and 5 mM ATP (all from Sigma). Change in absorbance at 340 nm was read every 30 secs over 12 mins on a spectrophotometer. Change in absorbance in the absence of exogenous ATP was subtracted from change in absorbance in the presence of ATP.

**Chapter 1: The role of cyclin D3 in the proliferation of primary peritoneal
B-1a cells**

RESULTS

TAT-p16 peptidyl mimetics disrupt endogenous D-type cyclin-cdk4/6 complexes in ex vivo peritoneal B-1a cells

Lane and coworkers [156] established that a 20-mer peptide composed of the third ankyrin repeat of the p16^{INK4a} tumor suppressor protein specifically bound to cdk4 and cdk6 and blocked cdk4/6 mediated pRb phosphorylation. With this technology available, our approach for studying the role of cyclin D3-cdk4/6 complexes in B-1a cell proliferation was to precisely target cyclin D3-cdk4/6 complexes by transducing p16^{INK4a} peptidyl mimetics into *ex vivo* cells. For efficient transduction the p16^{INK4a} peptidyl mimetic was coupled to an 11-mer peptide consisting of the NH₂-terminal HIV TAT protein domain (denoted as TAT-p16 wild type) [157]. Flow cytometry and confocal microscopy revealed transduction of nearly 100% of B-1a cells that had been incubated with the TAT-p16-FITC peptide [124].

To validate peptide efficiency *ex vivo*, PMA-stimulated B-1a cells, which express cyclin D3-cdk4 complexes as demonstrated by immunoreactive cyclin D3 in nondenatured anti-cdk4 immunoprecipitates, were transduced with 10 μ M TAT-p16 wild-type peptides (Figure 1A, Control) [80]. B-1a cells were transduced with TAT-p16 wild-type peptide at 14 hours after PMA-stimulation, before cyclin D3 induction, prevented cyclin D3-cdk4 complex formation (Figure 1A, p16 WT). The control (charge-matched) TAT-p16 (TAT-p16 mutant) peptide, that cannot bind cdk4 or cdk6, did not effect cyclin D3-cdk4 complex formation (Figure 1A, p16 Mut). When

evaluating the effects of TAT-p16 peptides on cyclin D3-cdk6 complexes similar results were observed (data not shown). To further evaluate the efficiency of TAT-p16 peptides, asynchronously growing murine Bal17 B cells were analyzed. Bal17 B cells constitutively express assembled cyclin D2-cdk4 complexes (Figure 1B, Control). TAT-p16 wild-type peptide disrupted cyclin D2-cdk4 complexes in Bal17 B cells and TAT-p16 mutant peptide had no measurable effect (Figure 1B). To be sure that transduction of TAT-p16 peptides is specific for cyclin D3-cdk4/6 complexes, we measured cdk-activating kinase-mediated Thr¹⁶⁰ phosphorylation on cdk2. This phosphorylation event serves as an indicator for the presence of cyclin E-cdk2 complexes in the nucleus. PMA-stimulated B-1a cells transduced with TAT-p16 wild-type peptide, before cyclin E-cdk2 assembly did not effect Thr¹⁶⁰ phosphorylation of cdk2 (Figure 1C, PMA). B-1a cells that were not stimulated with PMA did not express active cyclin E-cdk2 complex assembly (Figure 1C, M).

Transduction of TAT-p16 wild-type peptide into normal peritoneal B-1a cells inhibits proliferation

Cyclin D2 and cyclin D3 expression in PMA-stimulated B-1a cells does not overlap [80, 134]. As a result we were able to directly evaluate the contribution of cyclin D3-cdk4/6 holoenzymes in B-1a cell proliferation, by blocking the assembly of temporally expressed cyclin D3-cdk4/6 complexes, with transduction of the TAT-p16 wild-type peptide into B-1a cells at 14 hours after stimulation with PMA. The 14-hour time window was chosen because it is when cyclin D2 protein is undetectable and cyclin

D3 protein is not induced until 17 hours post PMA-stimulation. B cell activation was also achieved by stimulation with lipopolysaccharide (LPS) or CD40L. LPS is a major component of the cell wall on gram-negative bacteria, which induces polyclonal B cell activation (T cell independent) regardless of BCR antigen specificity [168]. CD40L is a T cell membrane protein, which binds the CD40 receptor on B cells and stimulates (T cell dependent) B cell division [168]. PMA-, LPS-, and CD40L-stimulated B-1a cells treated with TAT-p16 wild-type peptide exhibited a greater than 70% reduction in tritiated thymidine incorporation in comparison to control and TAT-p16 mutant peptide treated B-1a cells (Figure 2A). Nonstimulated B-1a cells incubated with TAT-p16 peptides did not have any effect on the base-line tritiated thymidine incorporation (Figure 2A, Media). To support these data, we also analyzed the cell cycle positions of B-1a cells by propidium iodide staining and flow cytometry. The percentage of PMA-stimulated B-1a cells treated with TAT-p16 wild-type peptide in S+G₂/M phase of the cell cycle was reduced by 70% in comparison to B-1a cells transduced with TAT-p16 mutant peptide (Figure 2B, PMA). Similar results were obtained with LPS- or CD40L-stimulated B-1a cells (Figure 2B, LPS, CD40L). TAT-p16 mutant peptide transduced into PMA-stimulated B-1a cells had a minimal effect on the percentage of cells in S+G₂/M-phase of the cell cycle in comparison to control B-1a cells (Figure 2B, PMA). Similar results were obtained with LPS- or CD40L-stimulated B-1a cells (Figure 2B, LPS, CD40L).

D-type cyclin-cdk4/6 complexes directly phosphorylate pRb on Ser^{807/811}. To establish endogenous pRb phosphorylation levels in B-1a cells treated with TAT-p16 wild-type peptide, whole cell extracts were prepared and immunoblotted with anti-

phospho-pRb^{Ser807/811} Ab. B-1a cells that were not stimulated and therefore not proliferating, did not express measurable pRb phosphorylation (Figure 3, M). PMA-stimulated B-1a cells demonstrated abundant endogenous phospho-pRb^{Ser807/811} (Figure 3, PMA). Endogenous phospho-pRb^{Ser807/811} was measurably inhibited in B-1a cells treated with TAT-p16 wild-type peptide, but not TAT-p16 mutant peptide (Figure 3, p16 WT, p16 Mut). Total protein levels of pRb were not affected by treatment of TAT-p16 peptides (Figure 3, pRb). These data demonstrate that in PMA-stimulated B-1a cells, TAT-p16 wild-type peptide inhibits phosphorylation of pRb on the D-type cyclin-cdk4/6 specific Ser^{807/811} site.

Cyclin D3-deficient mice have normal peripheral B-1 and B-2 lymphocyte compartments

The results above demonstrate that PMA-stimulated B-1a cells require cyclin D3-cdk4/6 complexes for proliferation. Given these data, we were interested in understanding whether B-1a cell development and proliferation were affected by loss of cyclin D3 [95]. The cyclin D3-deficient mice were a generous gift of our collaborator, Dr. Peter Sicinski (Dana-Farber Cancer Institute, Boston, MA). These mice are viable and exhibit a normal life span, however, the impact of cyclin D3 loss on proliferation and function of the peritoneal B-1 cells has not been examined. Thus, cyclin D3-deficient mice offer a unique model to test our hypothesis in non-manipulated *ex vivo* B-1a cells. First, we analyzed the splenic and peritoneal lymphoid compartments to confirm that cyclin D3 was absent in cyclin D3-deficient mice. Total murine splenocytes were

isolated and stimulated to induce the expression of cyclin D2 and cyclin D3 in B- and T- lymphocytes [80,82,86]. Splenic cells of wild-type mice express both cyclin D2 and cyclin D3, whereas in cyclin D3-deficient lymphocytes only cyclin D2 expression was induced and not cyclin D3 (Figure 4, S). The total number of lymphocytes was decreased in cyclin D3-deficient spleens as compared with wild-type littermate spleens (Figure 5A). Immunofluorescent staining revealed that this was a result of a decrease in the number of B-2 cells in cyclin D3 deficient spleens (Figure 5B, B-2S). On the other hand there was no difference between wild-type littermates and cyclin D3-deficient mice in the total number of peritoneal cells, and, more specifically, the number of B-1a cells (B-1aP; CD5⁺B220^{low}Mac-1⁺), B-1b cells (B-1bP; CD5⁻B220^{low}Mac-1⁺), B-2 cells (B-2P; B220⁺CD23⁺), T cells (T-P; B220⁻CD5⁺Mac-1⁻), and macrophages (M0-P; forward scatter high, Mac-1⁺), recovered by peritoneal washout (Figure 5A and 5C). Thus, by several measures, the development and function of cyclin D3-deficient peritoneal B-1a cells appears unaltered.

We next evaluated the role of cyclin D3 in peritoneal B-1a proliferation induced by PMA. In contrast to the results obtained when cyclin D3-cdk4/6 complex assembly was prevented by transduction of TAT-p16 wild-type peptide into normal B-1a cells, we found that cyclin D3-deficient B-1a cells responded comparably to wild-type B cells stimulated with PMA (Figure 6). In addition, the proliferation of cyclin D3-deficient B-1a cells in response to LPS was similar to wild-type B-1a cells (Figure 6). In data not shown, similar results were obtained with B-1a cell populations stimulated with CD40L.

Deregulation of cyclin D2 expression in cyclin D3-deficient B-1a cells

At 4 hours, PMA-stimulated cyclin D3-deficient B-1a cells expressed endogenous cyclin D2 protein levels that measured approximately 4.5-fold (based on scanning densitometry of the ECL exposed film obtained after Western blot of B-1a lysates) greater than that of parallel PMA-stimulated B-1a cells from control wild-type mice (Figure 7A).

Indirect immunofluorescence microscopy of endogenous expression of cyclin D2 protein was analyzed in cyclin D3-deficient B-1a cells to further provide evidence that cyclin D2 may act to compensate for the loss of cyclin D3. As expected, nonstimulated B-1a cells did not express detectable cyclin D2 or cyclin D3 (Figure 8, M); the weak fluorescence signal detected in non-stimulated B-1a cells was similar in intensity to that of parallel B-1a cells stained with a control isotype mAb (data not shown). PMA-stimulated wild-type B-1a cells expressed cyclin D2 and cyclin D3, at 4 and 21 hours, respectively, in a non-overlapping manner (Figure 8). In contrast, immunofluorescent staining of cyclin D2 in cyclin D3-deficient B-1a cells revealed that cyclin D2 was expressed at both 4 and 21 hours post-PMA stimulation (Figure 8). These results suggest that in PMA-stimulated cyclin D3-deficient B-1a cells, cyclin D2 remains elevated throughout the G_0/S -phase interval, where as in wild-type B-1a cells, cyclin D2 protein is induced in a rapid and transient manner.

To assess whether or not cyclin D2 protein was functional in cyclin D3-deficient B-1a cells, we measured the levels of endogenous pRb phosphorylation on cyclin D-cdk4/6-targeted residues, detected by Western blotting (Figure 7B). At 21 hours

following PMA stimulation, cyclin D3-deficient B-1a cell lysates expressed levels of pRb phosphorylation comparable to wild-type B-1a cells stimulated with PMA (Figure 7B). It is important to note that cyclin D1 was not expressed in PMA stimulated cyclin D3-deficient B-1a cells (data not shown). Further evidence that PMA-induced proliferation of B-1a cells in the absence of cyclin D3 may result from compensation by cyclin D2 was obtained by transduction of TAT-p16 wild-type peptide into cyclin D3-deficient B-1a cells, wherein only cyclin D2 expression is detectable. TAT-p16 wild-type peptide treated B-1a cells resulted in an ~80% reduction of PMA-stimulated tritiated thymidine incorporation compared to control and TAT-p16 mutant transduced B-1a cells (Figure 9), suggesting that cyclin D2 protein is functional in the absence of cyclin D3.

Turnover of endogenous cyclin D2 and cyclin D3 protein expression levels in PMA treated B-1a cells

The induction of D-type cyclins by mitogens is controlled, in part, through *de novo* transcription and increased translation, whereas, D-type cyclin turnover is controlled via ubiquitin-mediated proteasome degradation [74,60]; however, our knowledge of these events is limited. To begin to understand the molecular mechanisms underlying the sustained expression of cyclin D2 in cyclin D3-deficient B-1a cells, we examined the protein turnover of cyclin D2 and cyclin D3 in PMA-stimulated B-1a cells. To determine the turnover of cyclin D2 and cyclin D3, we measured the levels of endogenous cyclin D2 and cyclin D3 in PMA-stimulated B-1a cells in the presence of cycloheximide a protein synthesis inhibitor. Endogenous cyclin D2 expression, induced

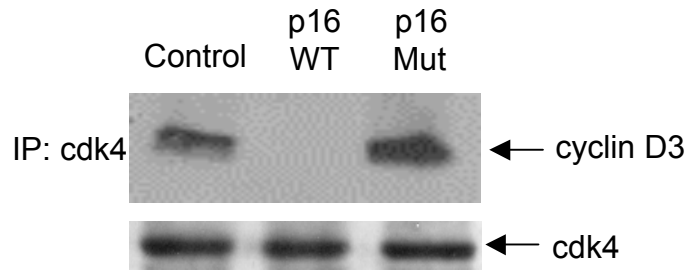
by PMA, turned over within 40 minutes of cycloheximide treatment, as detected by Western Blotting (Figure 10A). Similar results were observed with the expression of endogenous cyclin D3 in PMA-stimulated B-1a cells treated with cycloheximide, however, cyclin D3 turned over after 120 minutes (Figure 10B). Proteins are targeted for degradation by ubiquitination and the proteasome pathway, which can be blocked with MG132, a specific proteasome inhibitor. Pretreatment of PMA-stimulated B-1a cells with MG132 followed by cycloheximide inhibited the turnover of cyclin D2 (Figure 10A). Similar results were observed with cyclin D3 in PMA-stimulated B-1a cells pretreated with MG132 followed by cycloheximide (data not shown). These results confirm that D-type cyclin turnover is controlled via ubiquitin-mediated proteasome degradation in PMA-stimulated B-1a cells, however it appears that the rate of cyclin D2 and cyclin D3 turnover may be different.

FIGURES AND LEGENDS

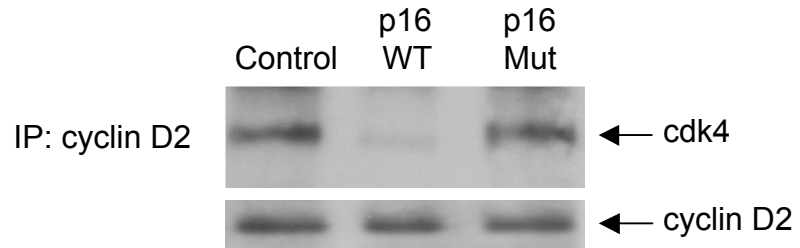
Figure 1. TAT-p16 wild-type peptide blocks formation of cyclin D3-cdk4 complexes in B-1a cells. *A*, Peritoneal B-1a cells were stimulated with 300 ng/ml PMA to induce the expression of cyclin D3 and assembly of cyclin D3-cdk4 complexes (Control). In parallel sets of B-1a cells, 10 μ M TAT-p16 wild-type (p16 WT), or TAT-p16 mutant (p16 Mut) peptides were added at 14 hrs after PMA, before cyclin D3 induction. At 20 hrs, B-1a cells were collected and immunoprecipitated (IP) with 1.5 μ g of anti-cdk4 Ab as described [134]. The immune complexes were separated by SDS-PAGE and Western blotted with anti-cyclin D3 Ab. The blot was also probed with anti-cdk4 Ab to ensure that equal amounts of cdk4 were immunoprecipitated. *B*, Asynchronously growing Bal17 B cells were similarly treated with the TAT-p16 peptides for 4 hrs; B cells were then collected, immunoprecipitated (IP) with 1.5 μ g of anti-cyclin D2 Ab, and the immune complexes were analyzed by Western blot with anti-cdk4 Ab. The blot was also probed with anti-cyclin D2 Ab to ensure that equal amounts of cyclin D2 were immunoprecipitated. *C*, B-1a cells were cultured in media alone (M) or stimulated with 300 ng/ml PMA for 24 hrs to induce cyclin E-cdk2 assembly. Where indicated, 10 μ M TAT-p16 wild-type (p16 WT) or TAT-p16 mutant (p16 Mut) peptides were added during the last 4 hrs of PMA treatment. Phosphorylation of cdk2 on Thr¹⁶⁰ was detected by Western blotting with an anti-phospho cdk2^{Thr160} Ab. The blot was stripped and reprobed with an anti- β -actin Ab. The data are representative of two independent experiments.

Figure 1

A.



B.



C.

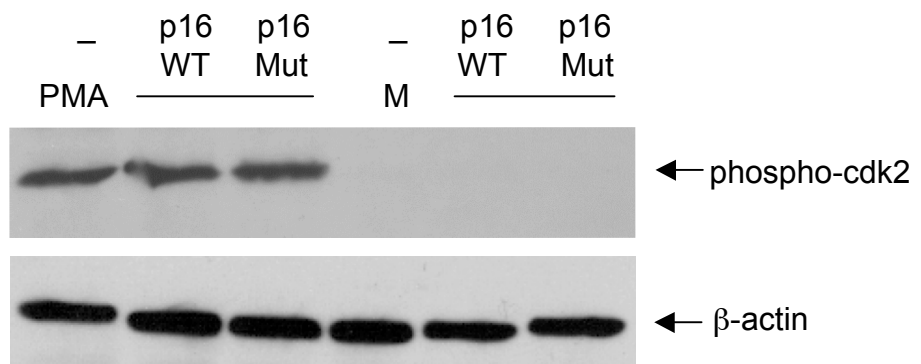
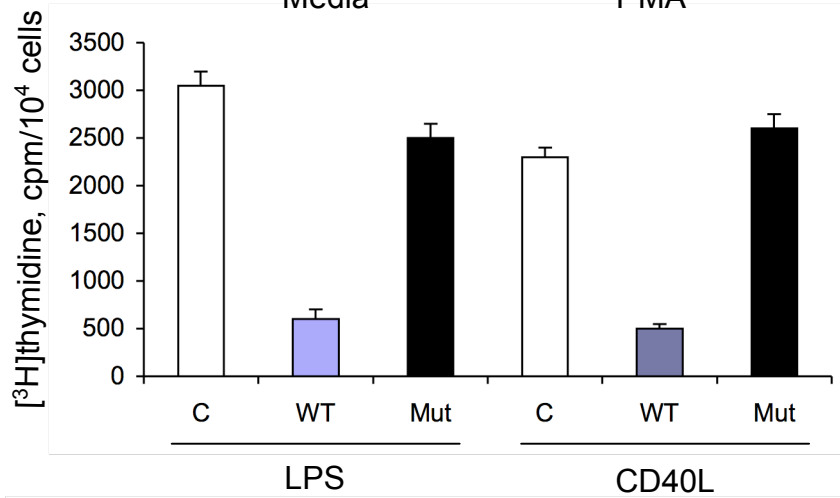
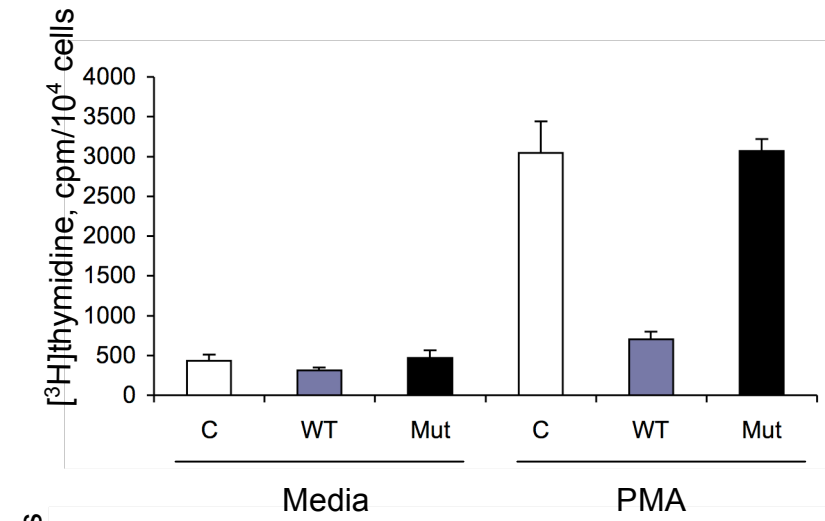


Figure 2. TAT-p16 wild-type peptide inhibits DNA synthesis in B-1a cells in response to PMA, LPS, or CD40L. B-1a cells were cultured in media alone, 300 ng/ml PMA, 25 µg/ml LPS, or CD40L for 24 hrs. Where indicated, 10 µM TAT-p16 wild-type (WT) or TAT-p16 mutant (Mut) peptides were added at 14 hrs postmitogen addition. Control (C) denotes B-1a cells cultured in the absence of added peptides. *A*, DNA synthesis was monitored by tritiated thymidine incorporation. Mean results are shown, along with lines indicating standard errors of the means ($n = 4$). *B*, For cell cycle analysis, B-1a cells were stained with propidium iodide and 10,000 cells were analyzed by flow cytometry as described in *Materials and Methods*. The data are represented as the percentage of B-1a cells in the S+G₂/M-phase of the cell cycle. The data are representative of three independent experiments.

Figure 2

A.



B.

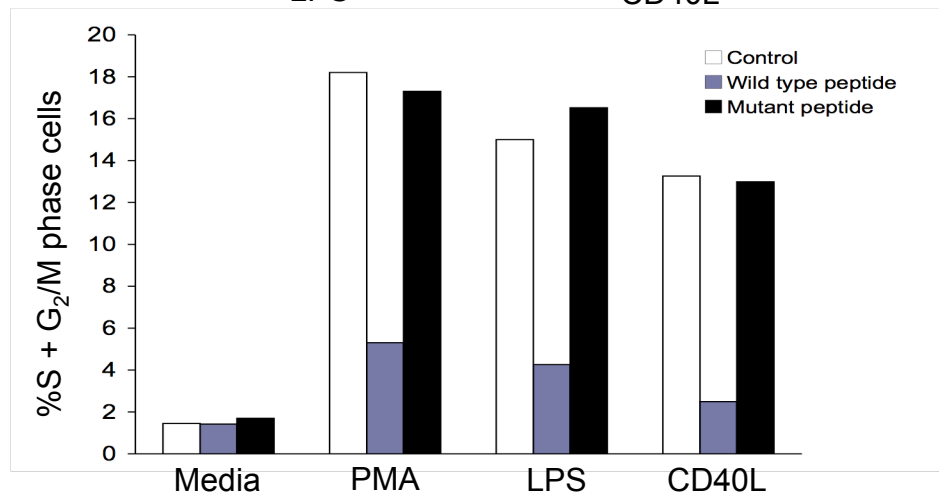


Figure 3. TAT-p16 wild-type peptide inhibits pRb^{Ser807/811} phosphorylation in B-1a cells in response to PMA. B-1a cells were cultured in media alone (M) or stimulated with 300 ng/ml PMA in the absence or presence of 10 μ M TAT-p16 wild-type (WT) or TAT-p16 mutant (Mut) peptides. Whole cell extracts were prepared, and Western blotting was performed with an anti-phospho-pRb^{Ser807/811} Ab. The blot was stripped and reprobed with anti-pRb Ab.

Figure 3

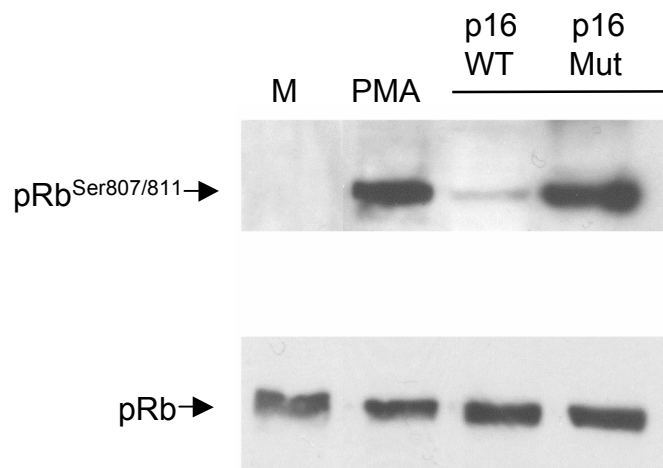


Figure 4. D-type cyclin expression in B-1a cells in wild-type and cyclin D3-deficient mice. Total splenic lymphocytes were isolated from wild-type (+/+) and cyclin D3-deficient mice (-/-) and were either left untreated (M) or were stimulated (S) with a mitogenic combination consisting of 300 ng/ml PMA plus 400 ng/ml ionomycin and 25 μ g/ml LPS. At 24 hrs, lymphocytes were collected, detergent extracts were prepared, and then Western blotting was performed with anti-cyclin D2 or anti-cyclin D3 Abs. The blot was stripped and reprobed with an anti- β -actin Ab to verify equal loading of each lane.

Figure 4

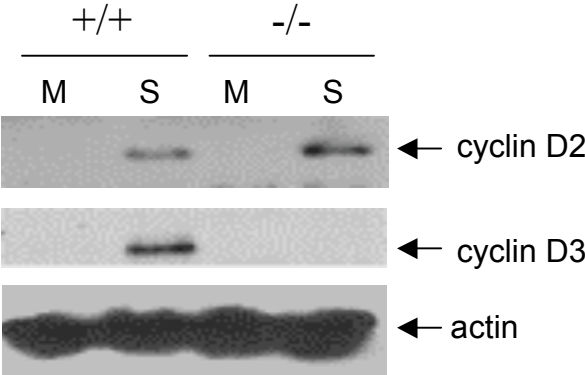


Figure 5. Initial characterization of B-1a cell lymphoid compartments in wild-type

and cyclin D3-deficient mice. *A*, Peritoneal washout (peritoneum) and spleen cell

suspensions (spleen) were obtained from cyclin D3-deficient mice (-/-) and wild-type littermate control animals (+/+), and total cell numbers were determined. Mean results

are shown, along with lines indicating SEs of the mean ($n = 6$). *B*, Spleen cell

suspensions were obtained from cyclin D3-deficient mice (-/-) and littermate control mice (+/+). The distribution of splenic T cells (T-S; B220⁻CD5⁺), B-2 cells (B-2S;

B220⁺CD5⁻), and MZ cells (MZ-S; CD21^{high}CD23^{low}) was determined by

immunofluorescent staining and flow cytometric analysis and converted to cell number

based on initial cell counts. Mean numbers of cells in each lymphoid population are

shown, along with lines indicating standard errors of the means ($n = 6$ except for MZ-S

where $n = 2$ and the line depicts the range of values). *C*, Peritoneal washout cells were

obtained from cyclin D3-deficient (-/-) and littermate control mice (+/+). The

distribution of peritoneal B-1a cells (B-1aP; B220^{low}CD5⁺Mac-1⁺), B-1b cells (B-1bP;

B220^{low}CD5⁻Mac-1⁺), B-2 cells (B-2P; B220⁺CD23⁺), T cells (T-P; B220⁻CD5⁺Mac-1⁻),

and macrophages (M0-P; forward and side scatter high, Mac-1⁺) was determined by

immunofluorescent staining and flow cytometric analysis and converted to cell number

based on initial cell counts. Mean numbers of cells in each lymphoid population are

shown, along with lines indicating standard errors of the means ($n = 6$). Experiments

were performed in collaboration with Dr. Joseph Tumang, Ph.D., The Feinstein Institute

for Medical Research (Manhasset, NY).

Figure 5

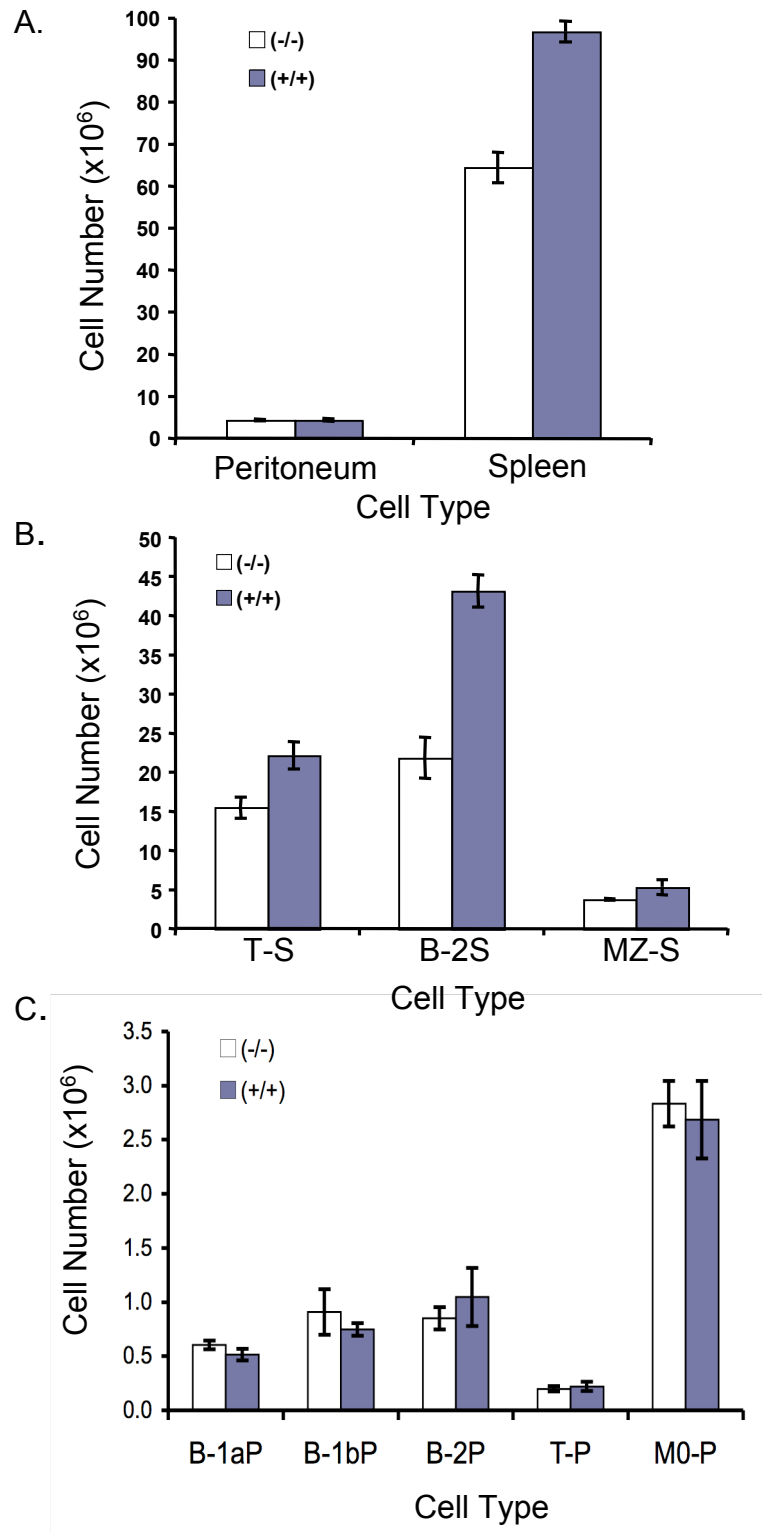


Figure 6. DNA synthesis in B-1a cells in cyclin D3-deficient mice. B-1a cells from wild-type (WT) or cyclin D3-deficient (KO) were cultured in media alone (inset) or stimulated with 300 ng/ml PMA or 25 μ g/ml LPS for the times indicated. Incorporation of tritiated thymidine was assessed for the final 6 hrs of culture as described in *Materials and Methods*. Results represent mean values of triplicate cultures with lines indicating standard errors of the means. The data are representative of three independent experiments.

Figure 6

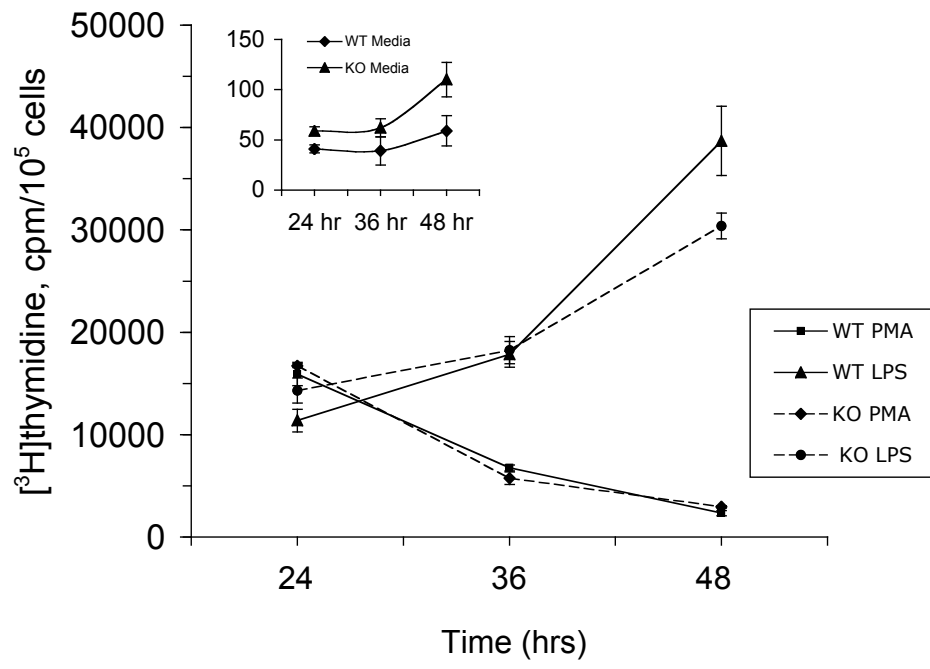


Figure 7. Expression of cyclin D2 is elevated in PMA stimulated cyclin D3-deficient

B-1a cells. *A*, B-1a cells were isolated from wild type (+/+) and cyclin D3-deficient mice

(-/-) and cultured in media alone (M) or stimulated with 300 ng/ml PMA (P) for 4 hrs.

Whole cell extracts were prepared and Western blotting was performed with anti-cyclin

D2 Ab. The blot was stripped and re-probed with anti- β -actin Ab. *B*, Parallel B-1a cells

were cultured in media alone (M) or stimulated with 300 ng/ml PMA (P) for 21 hrs and

then Western blotted with anti-phospho-pRb^{Ser807/811} Ab.

Figure 7

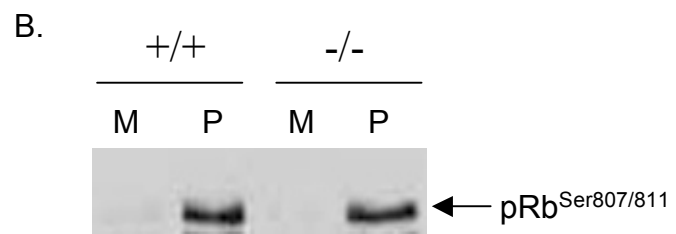
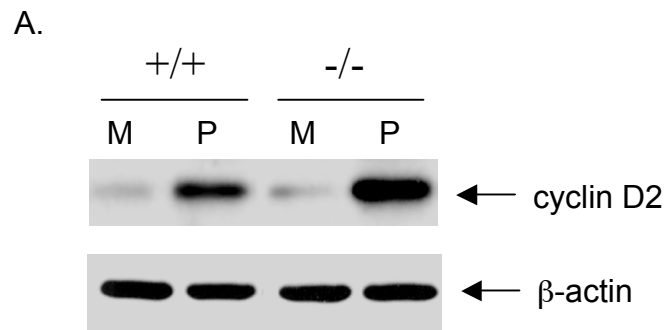


Figure 8. Cyclin D2 compensates for the loss of cyclin D3 in PMA stimulated cyclin D3-deficient B-1a cells. B-1a cells from wild-type (cyclin D3^{+/+}) and cyclin D3-deficient (cyclin D3^{-/-}) mice were cultured in media alone (M) or stimulated with 300 ng/ml PMA for 4 and 21 hrs. B-1a cells were collected and prepared for indirect immunofluorescence staining of cyclin D2 and cyclin D3 as described in the *Materials and Methods*. The data are representative of two independent experiments.

Figure 8

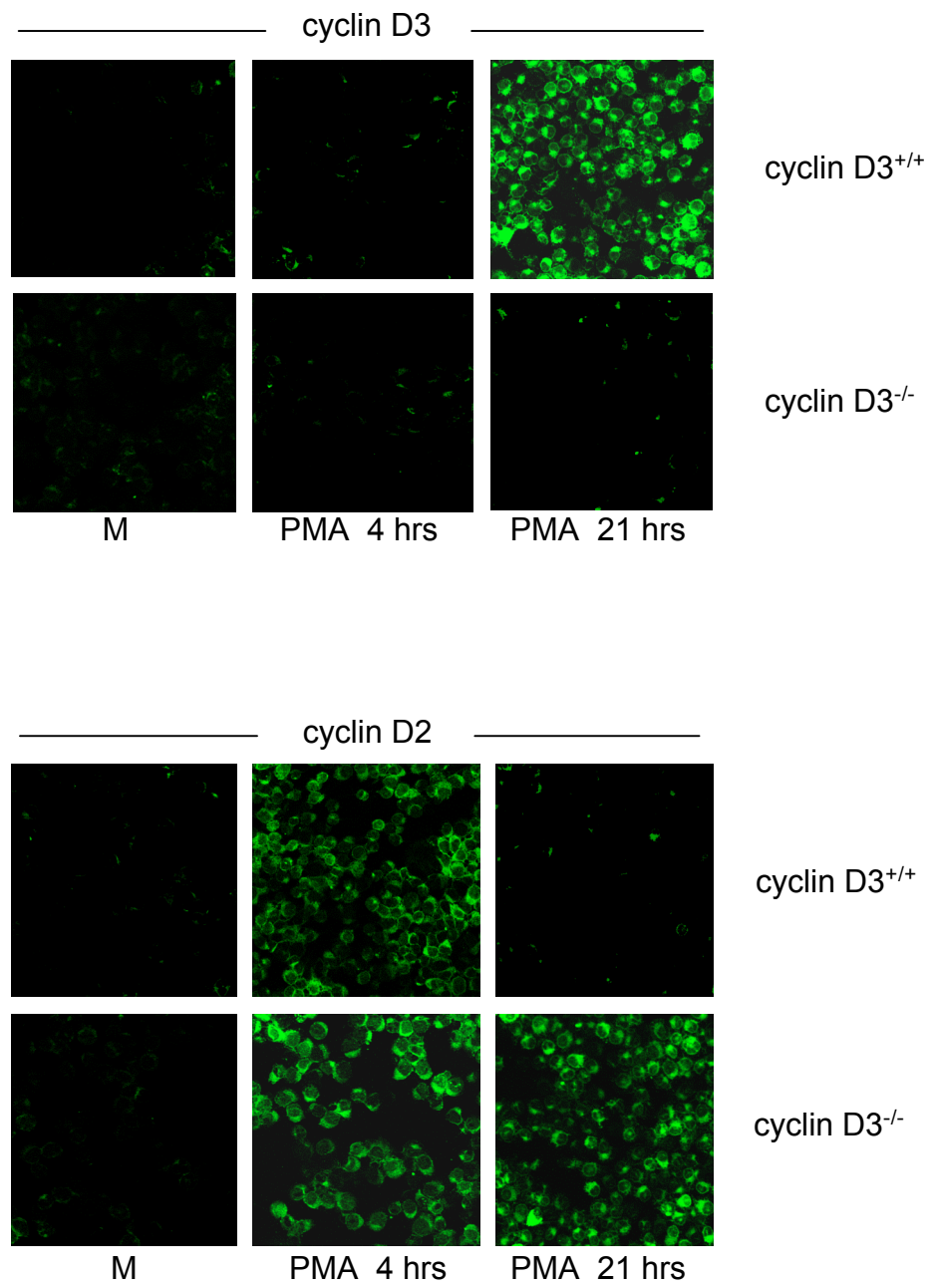


Figure 9. TAT-p16 wild-type peptide inhibits DNA synthesis in PMA stimulated cyclin D3-deficient B-1a cells. Cyclin D3-deficient B-1a cells were cultured in media alone or stimulated with 300 ng/ml PMA for 24 hrs. Where indicated, 10 μ M TAT-p16 wild-type (WT) or TAT-p16 mutant (Mut) peptides were added together with PMA. C denotes control B-1a cells cultured in the absence of added peptide. DNA synthesis was monitored by tritiated thymidine incorporation. Results represent mean values of triplicate cultures with lines indicating standard errors of the means. The data are representative of two independent experiments.

Figure 9

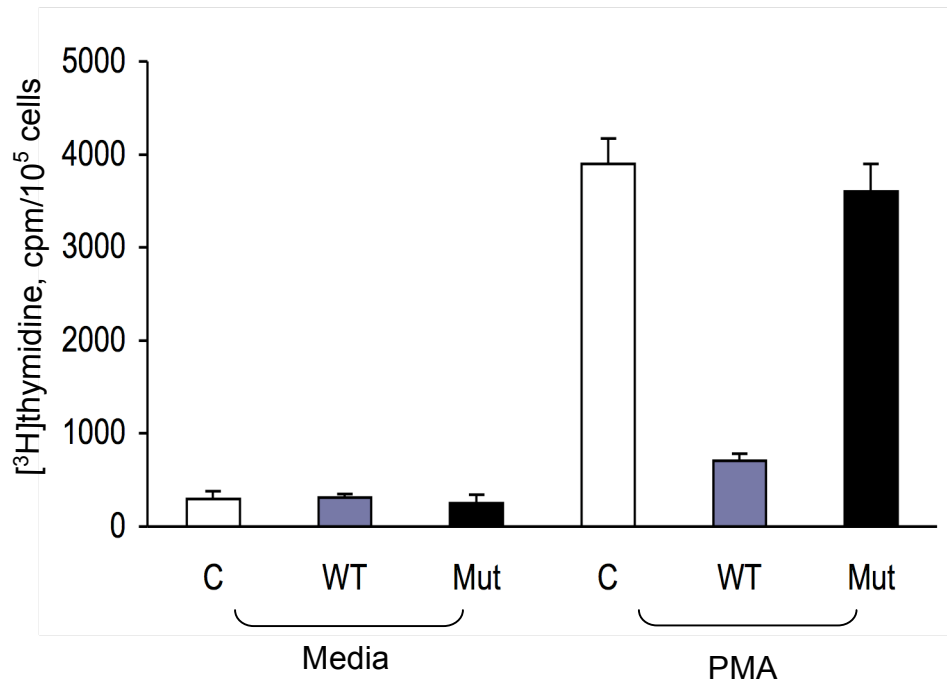
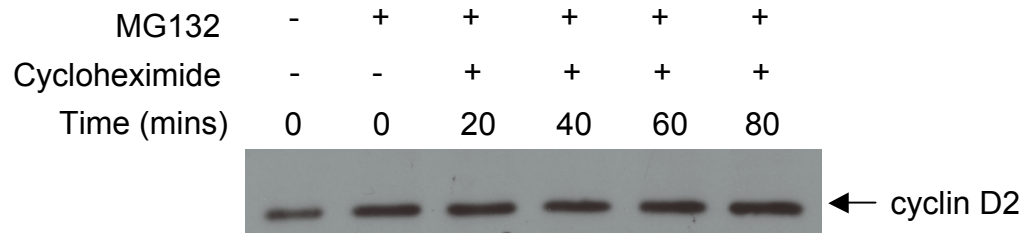
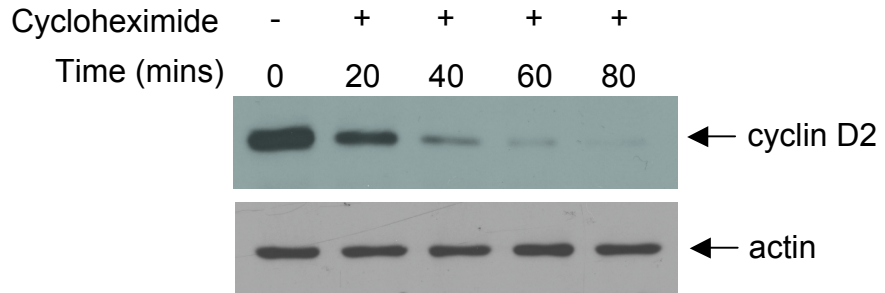


Figure 10. Cycloheximide decreases endogenous cyclin D2 and cyclin D3 in PMA

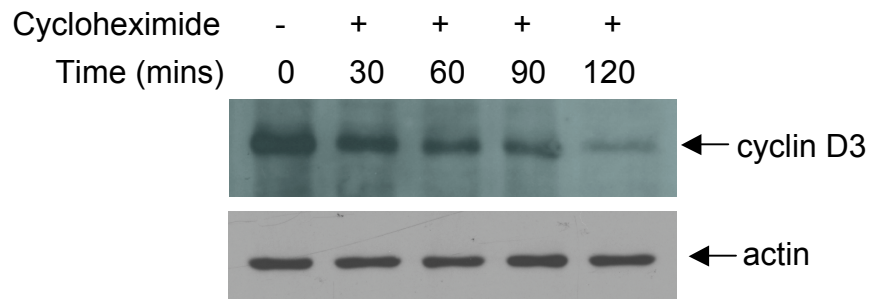
treated B-1a. *A*, B-1a cells stimulated with 300 ng/ml PMA. At 3.5 hrs, cells were incubated with 10 μ g/ml cycloheximide in the presence or absence of 25 μ M MG132. Whole cell extracts were prepared, and Western blotting was performed with an anti-cyclin D2 Ab. The blot was stripped and reprobed with anti-actin Ab. *B*, B-1a cells were stimulated with 300 ng/ml PMA. At 21 hrs, cells were incubated in the presence or absence of 10 μ g/ml cycloheximide. Whole cell extracts were prepared, and Western blotting was performed with an anti-cyclin D3 Ab. The blot was stripped and reprobed with anti-actin Ab to verify equal loading of each lane.

Figure 10

A.



B.



Chapter 2: Cyclin D3-cdk4/6 complexes are dispensable in the growth and survival of the human Diffuse Large B-cell Lymphoma, OCI-LY18; evidence for redundancy by cyclin E

RESULTS

Human LY18 cells uniquely express cyclin D3

DLBCL are described as having an increase in cell proliferation and accumulation as a consequence of deregulated cell cycle [135]. To begin to evaluate the regulation of proliferation in human LY18 cells we examined endogenous protein expression of the relevant G₁-phase proteins in asynchronously growing LY18 cells. LY18 cells constitutively express cdk4, cdk6, cdk2, phospho-pRb^{Thr821}, phospho-pRb^{Ser807/811}, and pRb (Figure 11). It is important to note that phosphorylation on Ser^{807/811} and Thr⁸²¹ of pRb indicates the specific target residues of D-type cyclin-cdk4/6 and cyclin E-cdk2 kinase activity, respectively. Interestingly, LY18 cells did not express p27 (Figure 11) or any other cdk-inhibitors (*i.e.*, p21 or p16) (data not shown). Typically, normal and malignant B cells express more than one D-type cyclin in an overlapping manner [76], however, unique to LY18 cells they only constitutively express cyclin D3, and not cyclin D1 or D2 (Figure 11). As positive controls (where indicated), asynchronously growing human HeLa cells and murine A20 lymphoma cells were analyzed. HeLa cells constitutively express cyclin D1, while A20 cells constitutively express cyclin D2, cyclin D3, and p27 (Figure 11). Further analysis revealed that constitutively expressed cyclin D3 forms complexes with cdk4 in proliferating LY18 cells, as demonstrated by immunoreactive cdk4 in nondenatured anti-cyclin D3 immunoprecipitates isolated from exponentially growing LY18 cells as detected by Western blotting (Figure 12, Media). By contrast, LY18 cells did not form cyclin D3-cdk4 complexes in nondenatured

immunoprecipitates lacking anti-cyclin D3 as evidence by immunoreactive cdk4 (Figure 12, Control). Similar results were observed by immunoreactive cdk6 in nondenatured anti-cyclin D3 immunoprecipitates in proliferating LY18 cells (data not shown). Collectively, these results demonstrate the relatively high protein expression levels of the G₁-phase proteins, particularly cyclin D3. Also, cyclin D3, the only D-type cyclin expressed in LY18 cells, forms active complexes with cdk4/6.

Transduction of TAT-p16 wild-type peptide into LY18 cells inhibits proliferation resulting in apoptosis

We sought to directly evaluate the contribution of cyclin D3-cdk4/6 complexes in LY18 cell proliferation. Since endogenous cyclin D3 is expressed in human LY18 cells and its expression does not overlap with cyclin D1 or cyclin D2, we were able to directly evaluate the contribution of cyclin D3-cdk4/6 complexes in LY18 cell cycle progression. Our strategy to assess the role of these holoenzymes in LY18 cells was to precisely target cyclin D3-cdk4/6 complexes by transducing p16^{INK4a} peptidyl mimetics (TAT-p16 wild-type peptide) into proliferating LY18 cells. We first analyzed cell cycle progression in LY18 cells by propidium iodide staining and flow cytometry. Transduction of TAT-p16 mutant peptide into LY18 cells had a minimal effect on the percentage of LY18 cells in sub-G₀/G₁-phase of cell cycle in comparison to untreated (M) LY18 cells (Figure 13A). By contrast, LY18 cells treated with TAT-p16 wild-type peptide for 24 hours, exhibited an increase in the percentage of LY18 cells in sub-G₀/G₁-phase of the cell cycle by 86% in comparison to LY18 cells transduced with TAT-p16 mutant peptide (Figure 13A).

Similar results were observed in LY18 cells transduced with TAT-p16 wild-type peptide at 12 and 48 hours; specifically, at 12 hours there was a 74% increase and at 48 hours a 89% increase in hypodiploid DNA, in comparison to LY18 cells transduced with TAT-p16 mutant peptides (Figure 13A).

D-type cyclin-cdk4/6 complexes directly phosphorylate pRb on Ser^{807/811}. To establish endogenous pRb phosphorylation levels in LY18 cells treated with TAT-p16 wild-type peptide, whole cell extracts were prepared and Western blotting performed with anti-phospho-pRb^{Ser807/811} Ab. Untreated LY18 cells constitutively express abundant endogenous phospho-pRb^{Ser807/811}, which was inhibited in LY18 cells treated with TAT-p16 wild-type peptide, but not TAT-p16 mutant peptide (Figure 14). These data demonstrate that in LY18 cells, TAT-p16 wild-type peptide inhibits phosphorylation of pRb on the D-type cyclin-cdk4/6 specific Ser^{807/811} site. Collectively, the observed results suggest that following treatment with TAT-p16 peptides, cyclin D3-cdk4/6 complexes are inhibited, thereby disrupting cdk4/6 kinase activity and its phosphorylation on pRb^{Ser807/811} in LY18 cells.

The results above demonstrate that disruption of cyclin D3-cdk4/6 complexes in LY18 cells results in an increase in the percentage of hypodiploid DNA. To further evaluate these results we were interested in determining whether LY18 cells were undergoing apoptosis. The presence of apoptotic cells was confirmed by annexin V-FITC/PI staining. LY18 cells treated with TAT-p16 wild-type peptide for 24 hours, demonstrated ~100% increase in the percentage of apoptotic cells in comparison to untreated (M) LY18 cells (Figure 13B, WT). In contrast, transduction of TAT-p16

mutant peptide into LY18 cells had a minimal effect on the percentage of annexin V-FITC/PI positive cells in comparison to untreated LY18 cells (Figure 13B, Media, Mut). It is important to note that the percentages of hypodiploid DNA (34.8%) (Figure 13A) and annexin V-FITC/PI positive cells (78.2%) (Figure 13B) differ at 24 hours as a result of the way the LY18 cells were gated. In measuring apoptosis, LY18 cells that were undergoing early apoptosis (annexin V-FITC positive, PI negative) were combined with the cells that were dead (annexin V-FITC positive, PI positive) (Figure 13B). The percentage of hypodiploid DNA observed in Figure 13A represents the percentage of LY18 cells that were dead. To summarize, disruption of cyclin D3-cdk4/6 complexes, mediated by transduction of TAT-p16 peptides, inhibits LY18 cell proliferation resulting in apoptosis.

Cyclin dependent kinase 4 inhibitor (cdk4i) inhibits proliferation in LY18 cells by inducing G₁ cell cycle arrest

Small-molecular inhibitors have been documented by researchers as a potentially useful class of therapeutic agents in NHL's [151]. Many small molecular inhibitors, specifically, cdk inhibitors have been used in ongoing clinical trials and preclinical testing [151]. To further assess the role of cyclin D3-cdk4/6 complexes in LY18 cell proliferation, in corroboration with our previous findings with TAT-p16 peptides, our strategy was to specifically disrupt cyclin D3-cdk4/6 complexes with the cyclin dependent kinase 4 inhibitor, 2-bromo-12,13-dihydro-5H-indolo[2,3-a]pyrrolo[3,4-c]carbazole-5,7(6H)-dione, which will be referred to as cdk4i (Figure 15A). Cdk4i has

previously been shown to inhibit cdk4 (IC_{50} of 0.076 μ M), and at greater concentrations cdk2 (IC_{50} of 0.52 μ M) and cdk1 (IC_{50} of 2.1 μ M), as determined by inhibition of Rb phosphorylation [169,170]. Cdk4i is a cell permeable compound that inhibits tumor cell growth and proliferation by blocking Rb phosphorylation and inducing G_1 -phase cell cycle arrest [169,170]. We initially sought to monitor cell viability by treating LY18 cells with cdk4i. Here, LY18 cells were cultured in the absence or presence of varying concentrations of cdk4i and the number of viable cells was measured over time. Treatment of LY18 cells with 5 μ M cdk4i did not result in a measurable decrease in viable cells in comparison to untreated (Media) LY18 cells over the 72-hour time period observed (Figure 15B). In contrast, LY18 cells incubated with 10 μ M and 25 μ M, demonstrated a time and dose dependent decrease in viable cells in comparison to untreated (Media) LY18 cells (Figure 15B). These data suggest that at increased concentrations, cdk4i is potentially inhibiting cdk4/6, cdk2 and cdk1, or is toxic to LY18 cells.

Next we measured the effects of treating LY18 cells with cdk4i on cell cycle progression. Analysis of DNA content by propidium iodide staining and flow cytometry [108], revealed that incubation of LY18 cells with 5 μ M and 10 μ M cdk4i resulted in an increase in the percentage of cells in G_1 -phase of the cell cycle in comparison to untreated LY18 cells (Media) (Figure 16). Specifically, from 57.4% in media cells to 76.0% and 79.1% in 5 μ M cdk4i treated cells and 71.0% and 69.0%, in 10 μ M cdk4i treated cells at 24 and 48 hours, respectively (Figure 16). Also observed was a decrease in S-, and G_2 /M-phases of the cell cycle in 5 μ M and 10 μ M cdk4i treated LY18 cells

(Figure 16). For example, at 48 hours media LY18 cells went from 12.1% S-phase and 26.0% G₂/M-phase to 3.8% S-phase and 10.5% G₂/M-phase in 5 μM cdk4i treated LY18 cells (Figure 16). Interestingly, treatment of LY18 cells with 25 μM cdk4i resulted in a decrease in G₁-phase and an increase in G₂/M-phase of the cell cycle at 24 hours (Figure 16). Control (media) cells went from 57.4% in G₁-phase and 26.0% in G₂/M-phase to 33.2% in G₁-phase and 46.7% in G₂/M-phase with treatment of 25 μM cdk4i (Figure 16). These observed results suggest that at higher concentrations cdk4i is inhibiting cdk2 and cdk1. To avoid these results the remaining experiments were performed with 5 μM cdk4i.

To obtain further evidence that cdk4i blocks cell cycle progression in LY18 cells we sought to measure the levels of DNA synthesis in cdk4i treated cells. In corroboration with the above results, 5 μM cdk4i inhibits DNA synthesis in LY18 cells over 48 hours in comparison to untreated (stained media) LY18 cells, as determined by BrdU incorporation (Figure 17). Specifically, proliferating LY18 cells used as a positive control, incorporated 62.5% BrdU (Figure 17, stained media), while LY18 cells treated with cdk4i demonstrated a 36.2%-7.3% decrease in BrdU incorporation from 15-48 hours, respectively. Of note, unstained media LY18 cells were used as a negative control and did not receive BrdU. In summary, cdk4i treatment of LY18 cells inhibits cell cycle progression, which corresponds to a decrease in DNA synthesis.

Cdk4i affects endogenous G₁-phase protein expression levels

To investigate the impact of cdk4i on LY18 cells, we re-examined endogenous protein expression profiles that were first observed in Figure 11 following treatment with cdk4i. The expression levels of endogenous G₁-proteins in LY18 cells treated with 5 μM cdk4i were analyzed by Western blotting performed with specific antibodies against each individual protein. Endogenous cyclin D3 and cdk4 protein expression levels began to decrease at 18 hours and were almost undetectable at 48 hours (Figure 18). Endogenous cdk6 protein expression did not show any measurable differences within 48 hours of cdk4i treatment in LY18 cells (Figure 18). Phosphorylation of pRb on Ser^{807/811} specifically detects cyclin D-cdk4/6 mediated phosphorylation of pRb. To determine the status of endogenous pRb phosphorylation in cdk4i treated LY18 cells, whole cell extracts were prepared and immunoblotted with an anti-phospho-pRb^{Ser807/811} Ab. Untreated LY18 cells express relatively abundant phosphorylation of endogenous pRb on Ser^{807/811} (Figure 19, Time 0, -). In contrast, phosphorylation of constitutive pRb on Ser^{807/811} in LY18 cells was inhibited ~24 hours after incubation with cdk4i and continued to decrease over 48 hours (Figure 19, +). These results suggest that cdk4i inhibits cyclin D3 and cdk4, thereby blocking constitutive pRb phosphorylation on the D-type cyclin-cdk4/6 site in LY18 cells.

Endogenous cyclin E and cdk2 form complexes later in G₁-phase of cell cycle to further promote pRb phosphorylation and proliferation. The phosphorylation of cdk2 on Thr¹⁶⁰ is an indicator of active cyclin E-cdk2 complexes [171]. Once activated cyclin E-cdk2 complexes phosphorylate pRb on Thr⁸²¹, the cyclin E-cdk2 specific site. To

determine the status of endogenous phospho-cdk2^{Thr160} in cdk4i treated LY18 cells, whole cell extracts were prepared and immunoblotted with an anti-phospho-cdk2^{Thr160} Ab. It is important to note that cdk4i has been shown to inhibit cyclin E-cdk2 complexes at higher concentrations [169,170]. Untreated LY18 cells express relatively abundant phosphorylation of endogenous cdk2 on Thr¹⁶⁰ (Time 0, -), which was inhibited following incubation with cdk4i (+) (Figure 20). Specifically, a measurable decrease in phospho-cdk2^{Thr160} was observed beginning at 12 hours, which continued to decrease to barely detectable levels at 48 hours. Cdk2 levels were not affected by treatment with cdk4i (Figure 20). Interestingly, the Western blot of phospho-cdk2^{Thr160} and cdk2 express two distinct bands. The cdk2 protein is closely related to cdc2 (cdk1), which is a proliferation marker that is significant in the G₂-M transition. We speculate that the cdk2 Ab is cross-reactive with cdk1, as a result of the shared homology between the two proteins. The nature of these immunoreactive bands needs to be clarified. LY18 cells undergoing proliferation displayed constitutive phospho-pRb^{Thr821} expression. In contrast, results demonstrated that cdk4i disrupted active cyclin E-cdk2 complexes and blocked constitutive pRb phosphorylation on the cyclin E-cdk2 site in LY18 cells (Figure 19). Phosphorylation of pRb on Thr⁸²¹ was inhibited in LY18 cells within 18 hours and was undetectable by 48 hours (Figure 19). In summary, our results suggest that cdk4i disrupts cyclin D3-cdk4/6 complexes in LY18 cells, resulting in a decrease in cyclin D3 and cdk4 protein levels, which eventually inhibits the phosphorylation of pRb on the cyclin D-cdk4/6 target residue Ser^{807/811}. In addition, our findings suggest that downstream of cyclin D3-cdk4 complexes there is decrease in active cyclin E-cdk2

complexes, by means of the observed decrease in phospho-cdk2^{Thr160} and phospho-pRb^{Thr821}.

Cdk4i induces p27 expression: transduction of TAT-p27 fusion proteins or siRNA-mediated knockdown of endogenous p27 has no measurable effect on LY18 cell cycle progression

The Cip/Kip family member, p27, plays a role in negative regulation of G₁-phase progression by inhibiting cyclin E-cdk2 complexes, thereby causing cells to accumulate in G₁-phase of the cell cycle [158]. Upon investigation, we found that untreated LY18 cells do not express endogenous p27, which is not uncommon for proliferating cells (Figure 11) [135]. However, following 5 μ M treatment with cdk4i, LY18 cells display a time-dependent increase in endogenous p27 protein expression (Figure 21, +). Specifically, at 18 hours post cdk4i treatment, LY18 cells begin to express p27, which increases dramatically by 48 hours (Figure 21). These results suggest that the upregulated expression of p27, which is consistent with loss of cyclin E-cdk2 activity, is contributing to the cell cycle arrest observed in cdk4i treated LY18 cells. Germane to these findings, the literature reports that in many normal and tumor cells, cell cycle progression is dependent on the balance of sequestered p27 by cyclin D-cdk complexes and free p27, which is able to bind and inhibit cyclin E-cdk2 complex activity [92,106,135,172]. Taken together, we investigated the role of p27 in LY18 cells by introducing exogenous p27 via transduction with TAT-p27 fusion proteins. Grdisa and coworkers [158] demonstrated that in different human tumor cell lines, transduction of

TAT-fusion proteins affected proliferation, specifically, causing G₁-phase arrest in certain cell types [158,159]. To mediate efficient p27 protein transduction in LY18 cells, full-length p27 fusion proteins were coupled to an 11-amino-acid peptide consisting of the NH₂-terminal HIV TAT protein transduction domain [159]. A bacterial expression vector, pTAT-HA, was constructed, to produce genetic in-frame TAT fusion proteins [159].

To evaluate the role of exogenous p27, in the absence of cdk4i, on cell viability we transduced full-length wild-type TAT-p27 fusion proteins (TAT-p27 WT), functional truncated N-terminal-TAT-p27 fusion proteins (TAT-N³p27), or inactive point mutant-TAT-p27 fusion proteins (TAT-ptMut-p27), into asynchronously growing LY18 cells [158,159]. Assuming that the increased expression of endogenous p27 plays a role in cdk4i-mediated LY18 cell cycle arrest, we expected to observe LY18 cells arresting in G₁-phase following transduction of exogenous p27 (TAT-p27 WT and TAT-N³p27). The negative control, TAT-ptMut-p27, should have no effect on LY18 cell cycle progression. Transduction of 150 nM of TAT-p27 fusion proteins did not measurably alter LY18 cell viability in contrast to untreated LY18 cells (Media) (Figure 22A). Specifically, all LY18 cells remained greater than 90% viable over 72 hours (Figure 22A). The minor decrease in cell viability between 48 and 72 hours is due to LY18 cells exhausting their media supply, as the cultures were not passed during the course of the experiment. LY18 cells were first transduced with 150 nM of the TAT-p27 fusion proteins because that is the dose that has been shown to inhibit cell proliferation in different cell lines *in vitro* [158]. To be sure that LY18 cells do not require a higher

concentration of TAT-p27 fusion proteins, we performed the above experiment measuring LY18 cell viability with increased concentrations of TAT-p27 fusion proteins. Similarly, transduction with 300 nM and 450 nM TAT-p27 WT, TAT-ptMut-p27, or TAT-N'p27 fusion proteins into LY18 cells had no measurable effect on LY28 cell viability in comparison to untreated (media) cells at 48 hours (Figure 22B). As observed above, LY18 cells under all conditions remained greater than 90% viable.

To evaluate the role of exogenous p27 in LY18 cell cycle progression we analyzed DNA content by propidium iodide staining and flow cytometry [108]. Transduction of 150 nM TAT-p27 WT, TAT-ptMut-p27, or TAT-N'p27 fusion proteins, into LY18 cells did not measurably alter the percentage of cells in G₁- or S+G₂/M-phases of the cell cycle (Figure 23A, 23B). Specifically, under all conditions, ~50% of LY18 were in G₁-phase of the cell cycle whereas 40-50% of LY18 cells were in S+G₂/M-phase of the cell cycle (Figure 23). Again, the minor decrease of LY18 cells observed in the S+G₂/M phase between 48 and 72 hours was a direct result of proliferating LY18 cells exhausting their media supply. In summary, there are no measurable phenotypes observed in LY18 cells transduced with exogenous TAT-p27 fusion proteins. Our results suggest that LY18 cells do not require the upregulation of p27 for cell cycle arrest. Of note, it is also possible that TAT-p27 fusion proteins are not getting into the LY18 cells or they are entering the cells and being degraded.

As a second, independent means to investigate the role of endogenous p27 in cdk4i treated LY18 cells, we investigated the function of p27 using RNA interference. Unlike the first experiment, where LY18 cells were not treated with cdk4i, in the

following experiments we used cdk4i to induce the expression of p27, followed by p27-specific siRNA to target p27 for knockdown. See Table 1 for a complete list of siRNA target sequences. In several control experiments, we found that between 200 pmol and 400 pmol siRNA was able to reduce endogenous p27 below measurable levels as detected by Western blotting. p27 protein abundance was reduced 24-72 hours after nucleofection of cdk4i treated LY18 cells with p27 specific siRNA, in comparison to untransfected (M) or control siRNA transfected cells (Figure 24A). It is important to note that the negative control siRNA used in all experiments was a non-targeting 20-25 nucleotide sequence. Next, we examined the effect of p27 siRNA on cdk4i treated LY18 cell viability. siRNA-mediated knockdown of endogenous p27 had no measurable effect on cdk4i treated cell viability over 72 hours (Figure 24B). Untreated cells remained over 90% viable, while p27 siRNA treated and cdk4i treated cells were ~85% viable (Figure 24B).

To evaluate the role of siRNA-mediated depletion of p27 on cell cycle progression in cdk4i treated LY18 cells, we analyzed DNA content by propidium iodide staining and flow cytometry [108]. siRNA-mediated knockdown of endogenous p27 in cdk4i treated LY18 cells had no significant effect on the percentage of cells in G₁-phase of the cell cycle, in comparison to LY18 cells treated with cdk4i alone (Figure 25A). In agreement with the results noted in Figure 16, at 24 hours cdk4i treated LY18 cells arrest in G₁-phase (77.8%) in comparison to untreated LY18 cells (44.9%) (Figure 25A). siRNA-mediated knockdown of p27 in cdk4i-treated LY18 cells had minimal effects on the percentage of LY18 cells in G₁-phase (71%) in comparison to cdk4i treated LY18

cells (77.8%) at 24 hours (Figure 25A). Similar results were observed at 48 and 72 hours. Furthermore, there were no significant differences observed in the percentage of LY18 cells in S+G₂/M-phase of cdk4i treated LY18 cells and siRNA-mediated p27 depleted, cdk4i treated cells (Figure 25B). Collectively, these results suggest that cdk4i-induced expression of endogenous p27 is dispensable for cell cycle arrest in LY18 cells.

siRNA knockdown of individual, endogenous G₁-phase proteins had no measurable effect on cell cycle progression in LY18 cells

Cyclin D3 is overexpressed in many human cancers. Targeting cyclin D3 and inhibiting its expression is a novel therapeutic approach to understand tumor cell cycle progression, specifically in lymphoid malignancies [95]. The observed results indicate that cyclin D3-cdk4/6 complexes are required for LY18 cell proliferation and inhibition of these complexes with TAT-p16 wild-type peptides or cdk4i results in G₁-phase accumulation. With this in mind, we were interested in determining whether LY18 cell proliferation would be affected by the loss of cyclin D3, being that it is the only D-type cyclin expressed in these cells. The dispensable nature of p27 induction in LY18 cells also suggests a role for cyclin D3. To this end, we targeted endogenous cyclin D3 specifically with siRNA (Table 1). To confirm the depletion of endogenous cyclin D3 after nucleofection with specific cyclin D3 siRNA, whole cell extracts were prepared and Western blotting performed. Cyclin D3 protein expression was decreased at 10 and 24 hours following transfection compared with untransfected LY18 cells (Media) and control siRNA (C) (Figure 26A). Of note, a non-targeting control siRNA (C) was used in

this experiment as a negative control at 24 hours and it did not measurably affect cyclin D3 protein expression (Figure 26 and Figure 27). Important to this study, we wanted to confirm that no other D-type cyclins were present in LY18 cells and to ensure that knockdown of endogenous cyclin D3 did not result in an increased expression of either cyclin D1 or cyclin D2 (*i.e.*, upregulated in a compensatory manner). To do this we analyzed cyclin D1 and cyclin D2 expression levels in untreated cells, cyclin D3 siRNA treated cells, and control siRNA treated LY18 cells. There was no observable expression of cyclin D1 or cyclin D2 (Figure 26A). Thus, cyclin D3 siRNA-mediated knockdown decreases cyclin D3 protein levels without inducing the expression of cyclin D1 or cyclin D2.

Next, we examined the viability of siRNA-mediated knockdown of endogenous cyclin D3. Note that there was no cdk4i used in the experiments to follow as only RNA interference was used to elucidate the role of G₁-phase proteins in asynchronously growing LY18 cells. Over 48 hours there was no measurable effect on LY18 cell viability (Figure 26B). Specifically, untreated (Media) LY18 cells and control- or cyclin D3-siRNA LY18 cells remained ~90% viable. To further measure the impact of cyclin D3 knockdown we analyzed cell cycle progression in LY18 cells treated with cyclin D3 siRNA. SiRNA-mediated knockdown of cyclin D3 did not result in G₁-phase cell cycle arrest in LY18 cells over 48 hours (Figure 27). For example, 24 hours post transfection with cyclin D3 specific siRNA, 53.5% of LY18 cells were in G₁-phase in comparison to 41.7% in control siRNA and 45.5% in untreated (Media) LY18 cells (Figure 27, 24 hrs). A similar trend was observed at 10 and 48 hours. Not surprisingly, there were also no

measurable differences in S+G₂/M-phases of the cell cycle in cyclin D3-depleted LY18 cells (Figure 27). Specifically, at 24 hours 42.3% of cyclin D3 siRNA treated LY18 cells were in S+G₂/M-phases in comparison to 49.8% in untreated (Media) cells and 54.4% in control siRNA treated LY18 cells (Figure 27). Similar values were observed at 10 and 48 hours. These data suggest that siRNA targeted depletion of cyclin D3 in LY18 cells does not induce cell cycle arrest.

To corroborate the above cell cycle data we measured DNA synthesis by BrdU incorporation. siRNA-mediated knockdown of cyclin D3 did not significantly affect DNA synthesis in asynchronously growing LY18 cells (Figure 28). At 24 hours post cyclin D3 siRNA transfection, BrdU incorporation was reduced 27.9% in comparison to untreated (Media) LY18 cells (Figure 28). At 10 and 48 hours, a 14% and 16.2% decrease in BrdU incorporation, respectively, was observed in contrast to untreated (M) LY18 cells (Figure 28). In corroboration with the cell cycle data, DNA synthesis is not measurably altered in siRNA-mediated cyclin D3 depleted LY18 cells.

To determine the status of endogenous pRb phosphorylation in LY18 cells treated with cyclin D3 siRNA, whole cell extracts were prepared and immunoblotted with anti-phospho-pRb^{Ser807/811} Ab and anti-phospho-pRb^{Thr821} Ab, that specifically detect cyclin D3-cdk4/6- and cyclin E-cdk2-mediated phosphorylation of pRb. siRNA knockdown of endogenous cyclin D3 did not measurably reduce the phosphorylation of pRb on Thr⁸²¹ or Ser^{807/811} (Figure 29, cyclin D3). These data imply that cyclin D3 is dispensable for cell cycle progression in LY18 cells.

Given the results that knockdown of endogenous cyclin D3 has no measurable affect on LY18 cell cycle progression, we decided to knockdown all relevant G₁-phase proteins, individually and in combination (for the complete list of the protein specific siRNAs that were used and their target sequences refer to Table 1). Of note, a non-targeting control siRNA (C) was used in all the following experiments as a negative control at either 24 or 48 hours and it did not measurably affect any protein expression levels. In summary, individual knockdown of the G₁-phase proteins did not significantly alter cell cycle progression in LY18 cells.

To begin, endogenous cdk4 or cdk6 were individually targeted with specific siRNA to each. Importantly, in many control experiments endogenous cdk4 and cdk6 protein expression was decreased with siRNA treatment at 200 or 400 pmol. To confirm the depletion of endogenous cdk4 or cdk6 in LY18 cells transfected with cdk4 or cdk6 specific siRNA, whole cell extracts were prepared and immunoblotting performed. Cdk4 and cdk6 protein expression levels were decreased at 24 and 48 hours following transfection in comparison to untreated (Media) and control siRNA LY18 cells (Figure 30A and Figure 31A, respectively). To confirm the specificity of the cdk4 target siRNAs we observed endogenous protein levels of cdk6 and cdk2 in cdk4 depleted LY18 cells. Cdk4 siRNA was specific for only endogenous cdk4 protein and did not reduce endogenous cdk6 or cdk2 (Figure 30A). Similar results were observed with cdk6 siRNA, as it did not affect endogenous cdk4 or cdk2 (data not shown) (Figure 31A). In summary, cdk4 siRNA and cdk6 siRNA exhibit specific knockdown of endogenous cdk4 and cdk6, respectively, in LY18 cells.

We next examined the viability and cell cycle progression of siRNA-mediated knockdown of endogenous cdk4 or cdk6 in LY18 cells. Over the observed 48 hours there was no measurable effects on LY18 cell viability (Figure 30B and Figure 31B, respectively). Specifically, the viability in untreated, cdk4 siRNA (200 or 400 pmol) treated, and control siRNA treated LY18 cells was ~88% at 24 hours and ~91% at 48 hours (Figure 30B). LY18 cells that were transfected with siRNA-specific for cdk6 displayed viable cells greater than 90% in all conditions (Figure 31B). Individual knockdown of either cdk4 or cdk6 had no measurable effects on G₁- or S+G₂/M-phases of the cell cycle in comparison to LY18 cell controls (Figure 32 and Figure 33, respectively). At 48 hours, 51.0% of cdk4 siRNA treated LY18 cells were in G₁-phase and 45.5% in S+G₂/M-phase; similarly, 53.1% of untreated (Media) cells and 53.8% control siRNA cells were in G₁-phase, while 39.8% of untreated (Media) cells and 41.5% control siRNA cells were in S+G₂/M-phase (Figure 32). Approximately the same percentages were observed at 24 hours. Furthermore, we observe the same results with cdk6 siRNA (Figure 33). These results indicate that cdk4 or cdk6 depletion in LY18 cells is not enough to affect cell cycle progression.

To determine the status of endogenous pRb phosphorylation in LY18 cells treated with cdk4 or cdk6 siRNA, whole cell extracts were prepared and immunoblotted with anti-phospho-pRb^{Ser^{807/811}} Ab and anti-phospho-pRb^{Thr⁸²¹} Ab. As stated previously, phosphorylation of pRb on Ser^{807/811} and on Thr⁸²¹ are the respective target residues of cyclin D3-cdk4/6- and cyclin E-cdk2. In corroboration with the above data, siRNA knockdown of endogenous cdk4 or cdk6 did not measurably reduce the phosphorylation

of pRb on Thr⁸²¹ or Ser^{807/811} (Figure 29, cdk4, cdk6). These data imply that individually, cdk4 and cdk6 are dispensable for cell cycle progression in LY18 cells.

Given that the observed results suggest that, individually, cyclin D3, cdk4, and cdk6 are dispensable for LY18 cell cycle we sought to examine endogenous cyclin E and cdk2 proteins. Cyclin E-cdk2 complexes function in late G₁-phase to promote S-phase entry and cell cycle progression. Endogenous cyclin E or cdk2 were individually targeted with specific siRNA to each. To confirm the depletion of cyclin E and cdk2 in LY18 cells transfected with cyclin E or cdk2 specific siRNA, whole cell extracts were prepared and Western blotting performed. Cdk2 protein expression was decreased at 24 and 48 hours following transfection compared with untransfected and control siRNA treated LY18 cells (Figure 34A). Cyclin E siRNA treated LY18 cells also showed a decrease in endogenous cyclin E protein levels at 24 and 48 hrs (data not shown). Subsequently, we examined the viability and cell cycle progression of siRNA-depleted cyclin E or cdk2 to investigate their impact on LY18 cell proliferation. Over 48 hours there were no measurable differences on LY18 cell viability (Figure 34B and Figure 35). LY18 cells treated with cdk2 or cyclin E siRNA remained ~ 90 % viable, similarly to control cells (Figure 34B and Figure 35).

Finally, we sought to examine cell cycle progression in LY18 cells treated with cyclin E or cdk2 siRNA. Individual knockdown of either cyclin E or cdk2 had no measurable effects on G₁- or S+G₂/M-phases of the cell cycle in comparison to LY18 cell controls (Figure 36 and Figure 37, respectively). At 24 hours, 62.9% of cyclin E siRNA treated LY18 cells were in G₁-phase and 31.5% in S+G₂/M-phase; similarly, 51.5% of

untreated (Media) LY18 cells and 46.5% control siRNA LY18 cells were in G₁-phase, while 43.9% of untreated (Media) cells and 50.3% control siRNA LY18 cells were in S+G₂/M-phase (Figure 36). Approximately, the same percentages were observed at 48 hours. Not surprisingly, at 24 hours, 47.3% of cdk2 siRNA treated LY18 cells were in G₁-phase and 48.8% in S+G₂/M-phase; similarly, 51.5% of untreated (Media) cells and 46.5% control siRNA cells were in G₁-phase, while 43.9% of untreated (Media) cells and 50.3% control siRNA cells were in S+G₂/M-phase (Figure 37). Approximately, the same percentages were observed at 48 hours. These results suggest that cyclin E or cdk2 depletion in LY18 cells does not affect proliferation.

To determine the status of endogenous pRb phosphorylation in LY18 cells treated with cdk4 or cdk6 siRNA, whole cell extracts were prepared and immunoblotted with anti-phospho-pRb^{Ser807/811} Ab and anti-phospho-pRb^{Thr821} Ab. In agreement with the above data, siRNA knockdown of either endogenous cyclin E or cdk2 did not measurably reduce the phosphorylation of pRb on Thr⁸²¹ or Ser^{807/811} (Figure 29, cyclin E, cdk2). These data imply that individually, cyclin E and cdk2 are dispensable for cell cycle progression in LY18 cells.

siRNA knockdown of a combination of G₁-phase cyclin dependent kinases impairs proliferation of LY18 cells by inducing G₁ cell cycle arrest

Using RNA interference on individual G₁-proteins did not result in an observable phenotype in LY18 cells. Given the structural similarities of the cyclins and cyclin dependent kinase proteins, we wanted to investigate the possibility that the proteins not

targeted by siRNA are functionally compensating for the depleted proteins in LY18 cells. This would explain the observed normal proliferation in siRNA-transfected cells. To begin we nucleofected LY18 cells with both cdk4 and cdk6 (cdk4/6) specific siRNAs. Combined cdk4/6 siRNA-treated LY18 cells exhibited a decrease in endogenous cdk4 and cdk6 protein expression levels (data not shown), however, had no measurable effect on LY18 cell viability in comparison to untreated LY18 cells and cells transfected with control siRNA (Figure 38). Specifically, under all conditions LY18 cells remained greater than 89% viable. To further assess the depletion of cdk4/6 in LY18 cells we examined cell cycle progression at 24 and 48 hours post transfection. siRNA-mediated knockdown of both endogenous cdk4 and cdk6 resulted in an increase in the percentage of LY18 cells in G₁-phase and a decrease in the percentage of cells in S+G₂/M-phases of the cell cycle (Figure 39). Note that in all instances where S and G₂/M phases were combined, the individual percentages of S- and G₂/M-phase followed the same trend. At 48 hours post transfection of cdk4/6 siRNA, 55.4% of control cells compared to 75.8% of LY18 cells treated with cdk4/6 siRNA were in G₁-phase, while the percentage of cells in S+G₂/M-phase decreased from 40.1% to 19.5% (Figure 38). Similar results were observed at 24 hours (Figure 39). These data demonstrate that depletion of cdk4 and cdk6 results in a G₁-phase accumulation.

Next, we sought to measure the effects of siRNA-mediated knockdown of both cdk6 and cdk2 in LY18 cells. Considering that cdk4 and cdk6 appear to be redundant in LY18 cells, it is likely that cdk2 also functions similarly. siRNA-mediated knockdown of endogenous cdk6 and cdk2 had no detectable effect on LY18 cell viability, as all cells

were greater than 90% viable (Figure 40A). Interestingly, there was an increase in the percentage of cells in G₁-phase and a decrease in the percentage of LY18 cells in S+G₂/M-phase of the cell cycle (Figure 40B). Evaluation at 48 hours post transfection of cdk6/2 siRNA demonstrated that 73.8% of LY18 cells were in G₁-phase in comparison to 59.4% of untreated control LY18 cells (Figure 40B). The percentage of cells in S+G₂/M-phase decreased from 35.0% in control cells, to 18.6% in cdk6/2 siRNA-treated LY18 cells (Figure 40B). Similar results were observed at 24 hours (Figure 40B). These data demonstrate that depletion of cdk6 and cdk2 results in a G₁-phase accumulation.

To determine the status of endogenous pRb phosphorylation in LY18 cells treated with cdk6 and cdk2 siRNA, whole cell extracts were prepared and immunoblotted with anti-phospho-pRb^{Ser807/811} Ab and anti-phospho-pRb^{Thr821} Ab. Interestingly, the data revealed a decrease in the phosphorylation of pRb on the D-type cyclin-cdk4/6 specific site, but not on the cyclinE-cdk2 specific site (Figure 29, cdk2/6). These data imply that, individually, cdk6 and cdk2 are dispensable for cell cycle progression, however, combined they arrest LY18 cells in G₁-phase of the cell cycle. Of particular interest, it appears that siRNA-mediate knockdown of cdk2/6 effects early G₁-phase phosphorylation of pRb on the cyclin D3-cdk4/6 specific target residue.

Cdk4/6 or cdk6/2 siRNA-mediated knockdowns resulted in a significant G₁ arrest in LY18 cells. Collectively, these data suggest that siRNA knockdown of individual cdk proteins are compensated by the remaining, non-targeted cdks. To test this hypothesis, we knocked down endogenous cdk4, cdk6, and cdk2 (cdk4/6/2), simultaneously in LY18 cells. siRNA-mediated knockdown of endogenous cdk4/6/2 had no measurable effect on

the viability in LY18 cells; all cells remained greater than 90% viable within 48 hours of nucleofection (Figure 41A). Furthermore, we assessed cell cycle progression in cdk4/6/2-depleted LY18 cells. A significant increase in the percentage of LY18 cells in G₁-phase of cell cycle was observed (Figure 41B). At 48 hours, 86.7% of cdk4/6/2 siRNA treated LY18 cells accumulated in G₁-phase in comparison to 55.2% of control cells (Figure 41B, 48 hrs). As a direct result of LY18 cells arresting in G₁-phase, there was a significant decrease in LY18 cells in S+G₂/M-phase. At 48 hours, 8.6% of cdk4/6/2 siRNA treated LY18 cells were in S+G₂/M-phase in comparison to 40.0% of control cells (Figure 41B, 48 hrs). It is important to note that at 24 hours similar results were observed. Also, control siRNA treatment had a minimal effect on the percentage of G₁ or S+G₂/M-phase LY18 cells in comparison to untreated (Media) LY18 cells. These data demonstrate that without G₁-phase cdks, LY18 cells cannot progress through the cell cycle.

To determine the status of endogenous pRb phosphorylation in LY18 cells treated with cdk4/6/2 siRNA, whole cell extracts were prepared and immunoblotted with anti-phospho-pRb^{Ser^{807/811}} Ab and anti-phospho-pRb^{Thr⁸²¹} Ab. Interestingly, the data displayed a significant decrease in the phosphorylation of pRb on Ser^{807/811} and Thr⁸²¹, in comparison to the individual cdk siRNA knockdowns (Figure 29, cdk4/6/2). These data demonstrate that cdk4, cdk6, and cdk2, are individually dispensable for cell cycle progression, however combined they arrest LY18 cells in G₁-phase of the cell cycle. Collectively, these results suggest that cdk4, cdk6, and cdk2 can play compensatory roles in LY18 cells. Of particular interest, it appears that siRNA-mediate knockdown of

cdk4/6/2 inhibits cyclin D3-cdk4/6 and cyclin E-cdk2 specific phosphorylation of pRb on their respective target residues Ser^{807/811} and Thr⁸²¹. These data suggest that these holoenzyme complexes are not functional without cdk.

siRNA-mediated knockdown of endogenous cyclin D3 in combination with cyclin E in LY18 cells inhibits proliferation by inducing G₁ cell cycle arrest

Since cyclin D3 knockdown with cyclin D3 specific siRNA does not have an observable phenotype in LY18 cells we wanted to examine the possibility of a compensatory mechanism by cyclin E. In the literature cyclin E has been shown to compensate for a lack of D-type cyclins and contributes to tumor proliferation [139]. We investigated this hypothesis with RNA interference. Both cyclin D3 and cyclin E protein levels were decreased in LY18 cells transfected with cyclin E and cyclin D3 siRNA (data not shown). The viability of siRNA-mediated knockdown of cyclin D3 and cyclin E resulted in no measurable effect in LY18 cells, as all cells remained greater than 90% viable over 48 hours (Figure 42).

Next we sought to examine cell cycle progression and proliferation in LY18 cells treated with cyclin D3 and cyclin E siRNA. At 48 hours post transfection, 83.1% of cyclin D3 and cyclin E depleted cells were accumulated in G₁-phase in comparison to 59.4% of untransfected control LY18 cells (Figure 43A, 48 hrs). There was also a significant decrease in LY18 cells in S+G₂/M; at 48 hours, 9.0% of cyclin D3/E siRNA treated cells were in S+G₂/M-phase in comparison to 35.0% of untransfected control LY18 cells (Figure 43A, 48 hrs). We observed similar results at 24 hours. It is important

to note that control siRNA treatment had a minimal effect on the percentage of G₁ or S+G₂/M-phase LY18 cells in comparison to untreated (Media) LY18 cells. Finally, we examined DNA synthesis in LY18 cells following siRNA depletion of endogenous cyclin D3 and cyclin E by BrdU incorporation. BrdU incorporation was reduced from 50.3% to 21.7% in cyclin D3 and cyclin E depleted cells at 24 and 48 hours, respectively, in comparison to untransfected LY18 cell controls (90.4% at 24 hours and 63.4% at 48 hours) (Figure 43B). The observed decrease in DNA synthesis was a direct result of LY18 cells accumulating in G₁-phase of the cell cycle. These data demonstrate that without G₁-phase cyclins, LY18 cells cannot progress through the cell cycle or proliferate.

To determine the status of endogenous pRb phosphorylation in LY18 cells treated with cyclin D3 and cyclin E siRNA, whole cell extracts were prepared and immunoblotted with anti-phospho-pRb^{Ser^{807/811}} Ab and anti-phospho-pRb^{Thr⁸²¹} Ab. Interestingly, the data displayed a significant decrease in the phosphorylation of pRb on Ser^{807/811} and Thr⁸²¹, in comparison to the individual cyclin siRNA knockdowns (Figure 29, cyclin D3/E). These data imply that cyclin D3 and cyclin E are individually dispensable for cell cycle progression; however, combined they arrest LY18 cells in G₁-phase of the cell cycle and inhibit DNA synthesis. Collectively, these data suggest that cyclin E can compensate for siRNA-mediated depletion of cyclin D3 and vice versa.

FIGURES AND LEGENDS

Figure 11. Protein expression profiles of relevant G₁ proteins reveals LY18 cells uniquely express cyclin D3. Asynchronously growing HeLa cells, A20 B cells, and LY18 B cells were cultured in media alone for 24 hrs. Whole cell extracts were prepared and Western blotting was performed with anti-cyclin D1 Ab, anti-cyclin D2 Ab, anti-cyclin D3 Ab, anti-cdk2 Ab, anti-cdk4 Ab, anti-cdk6 Ab, anti-p27 Ab, anti-phospho-pRb^{Thr821} Ab, anti-phospho-pRb^{Ser807/811} Ab, and anti-pRb Ab. The blot were stripped and re-probed with anti-hsp90 Ab to verify equal loading of each lane.

Figure 11

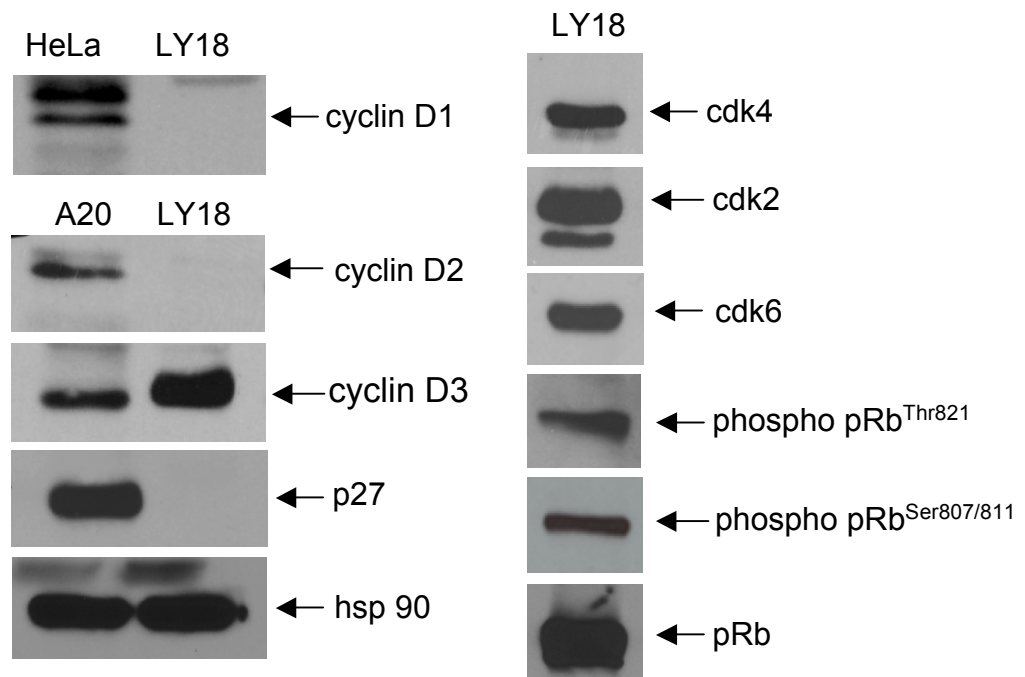


Figure 12. Cyclin dependent kinase 4 (cdk4) forms complexes with cyclin D3 in LY18 cells. LY18 cells were cultured in media alone. At 24 hrs, LY18 cells were collected and immunoprecipitated (IP) with 1.5 μ g of anti-cyclin D3 Ab and non-immune serum IgG (control) as described [80]. The immune complexes were separated by SDS-PAGE and Western blotted with anti-cdk4 Ab.

Figure 12



Figure 13. TAT-p16 wild-type peptide causes an increase in hypodiploid DNA resulting in apoptosis in LY18 cells. LY18 cells cultured in media alone (M) or in the presence of 20 μ M TAT-p16 wild-type (WT) or 20 μ M TAT-p16 mutant (Mut) peptides for various lengths of time. *A*, For cell cycle analysis, LY18 cells were stained with propidium iodide and analyzed by flow cytometry as described in *Materials and Methods*. The data are represented as the percentage of LY18 cells in sub-G₀/G₁-phase of the cell cycle. The data are representative of 10,000 cells. *B*, At 24 hrs, LY18 cells were stained with Annexin-V and analyzed by flow cytometry as described in *Materials and Methods*. The data are represented as the percentage of LY18 cells in the quadrants positive for Annexin-V/FITC and propidium iodide. The data are representative of 10,000 cells.

Figure 13

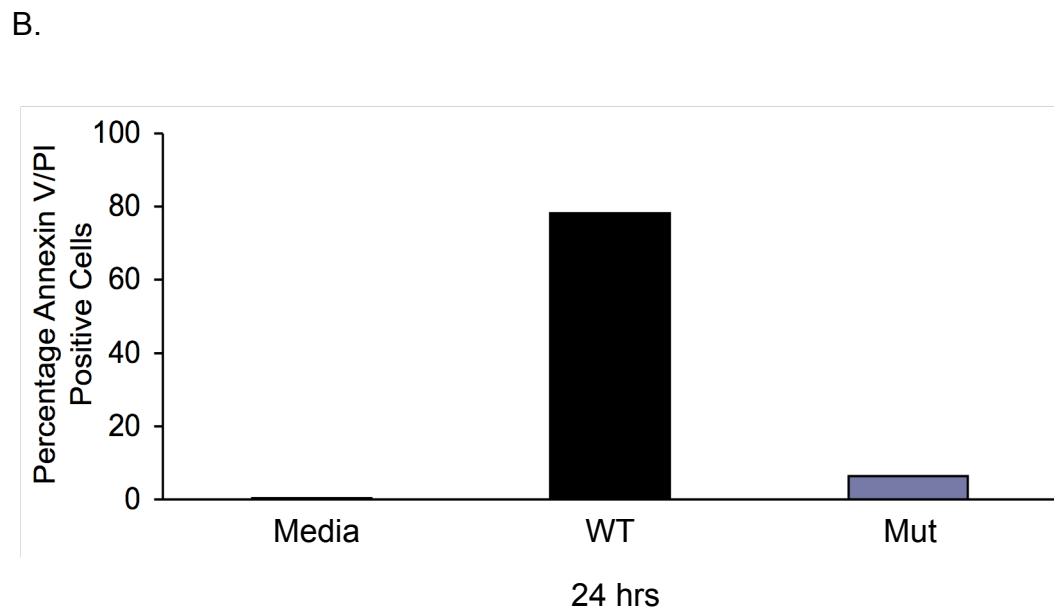
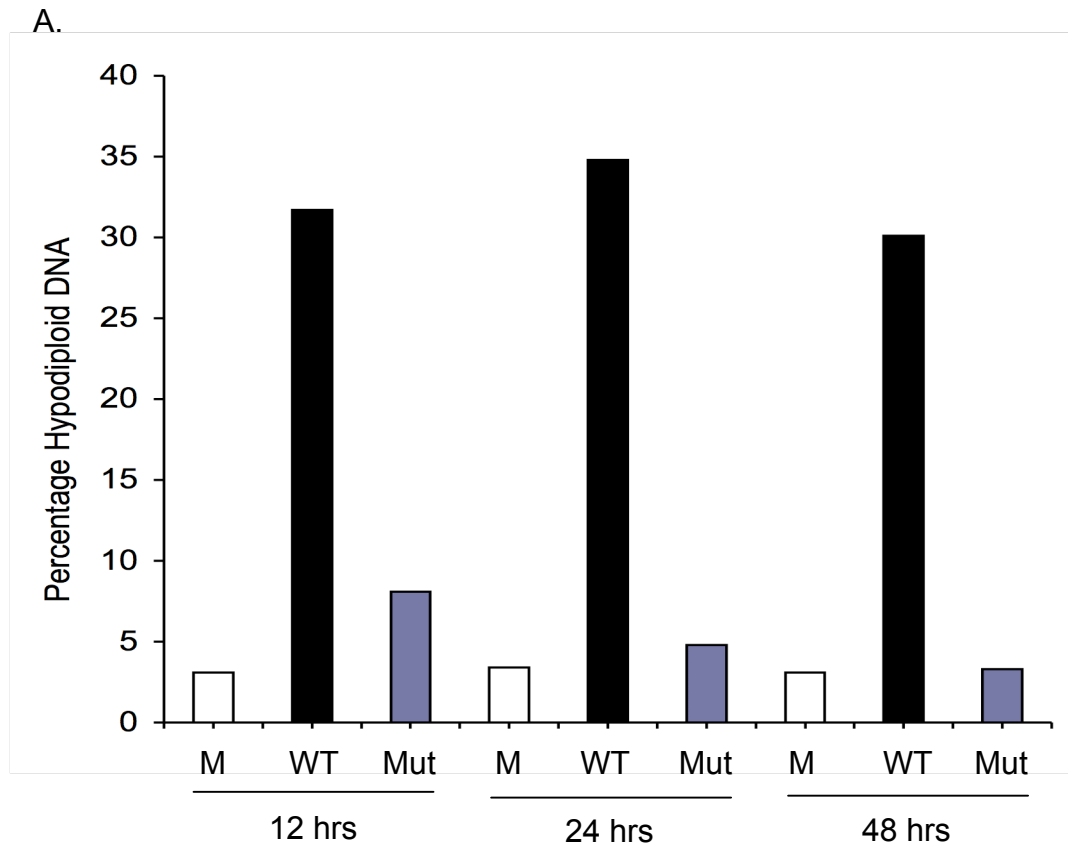


Figure 14. TAT-p16 wild-type peptide inhibits pRb^{Ser807/811} phosphorylation in LY18 cells. LY18 cells were cultured in media (M) alone or in the presence of 20 μ M TAT-p16 wild-type (p16 WT) or 20 μ M TAT-p16 mutant (p16 Mut) peptides. At 90 mins, whole cell extracts were prepared and Western blotting performed with an anti-phospho-pRb^{Ser807/811} Ab.

Figure 14

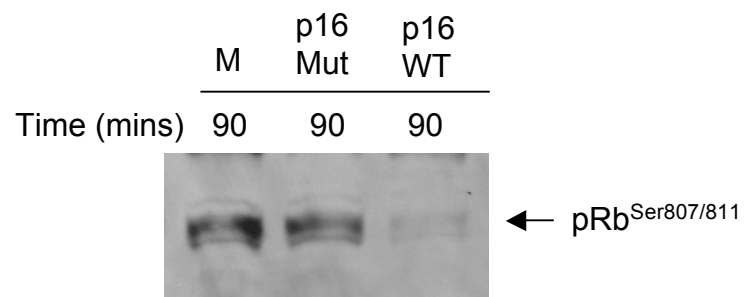


Figure 15. Treatment of LY18 cells with the cyclin dependent kinase 4 inhibitor (cdk4i) causes a decrease in viable cells. *A*, Structure of the cyclin dependent kinase 4 inhibitor (cdk4i). *B*, LY18 cells were cultured in media alone (DMSO solvent control) or in the presence of 5 μ M, 10 μ M, or 25 μ M cdk4i. At the indicated times, LY18 cells were collected and cell viability was determined by propidium iodide staining. Samples were analyzed by flow cytometry as described in *Material and Methods*. The data are represented as the percentage of LY18 cells that are negative for propidium iodide staining. The data are representative of 10,000 cells.

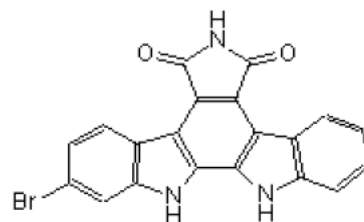
Figure 15

A.

Molecular Formula:



Structure:



B.

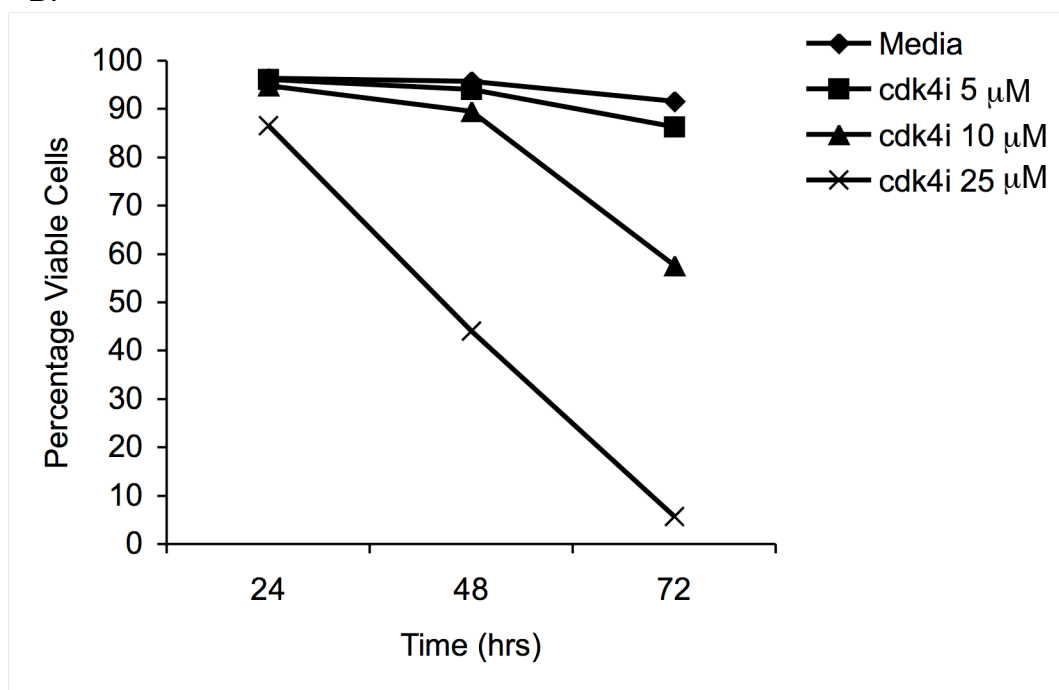


Figure 16. Cyclin dependent kinase 4 inhibitor (cdk4i) blocks cell cycle progression in LY18 cells. LY18 cells were cultured in media alone (DMSO solvent control) or in the presence of 5 μ M, 10 μ M, or 25 μ M cdk4i. At the indicated times, LY18 cells were stained propidium iodide and cell cycle analyzed by flow cytometry as described in *Materials and Methods*. The data are presented as the number of cells (counts) versus propidium iodide (PI-A), with percentages represented by black bars, indicating LY18 cells in G₁, S, or G₂/M-phase of the cell cycle, respectively. The data are representative of 10,000 cells.

Figure 16

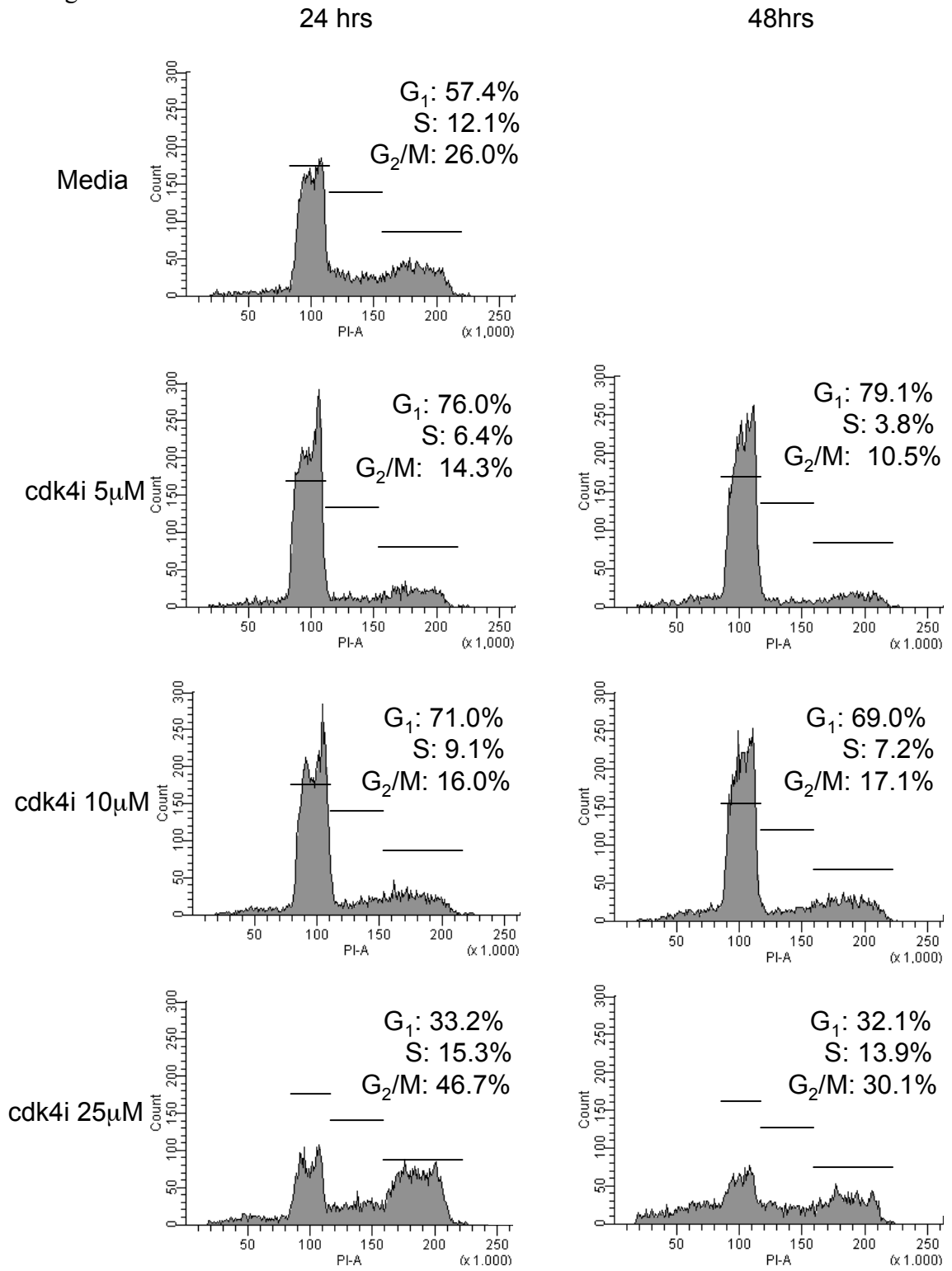


Figure 17. Cyclin dependent kinase 4 inhibitor (cdk4i) inhibits DNA synthesis in LY18 cells. LY18 cells were cultured in media alone (DMSO solvent control) or in the presence of 5 μ M cdk4i for various lengths of time. DNA synthesis was monitored by BrdU incorporation and analyzed by flow cytometry as described in *Materials and Methods*. The data are representative of 10,000 cells and are presented as cell number (counts) versus BrdU (FITC-A). The bars reflect the percentage of BrdU positive LY18 cells.

Figure 17

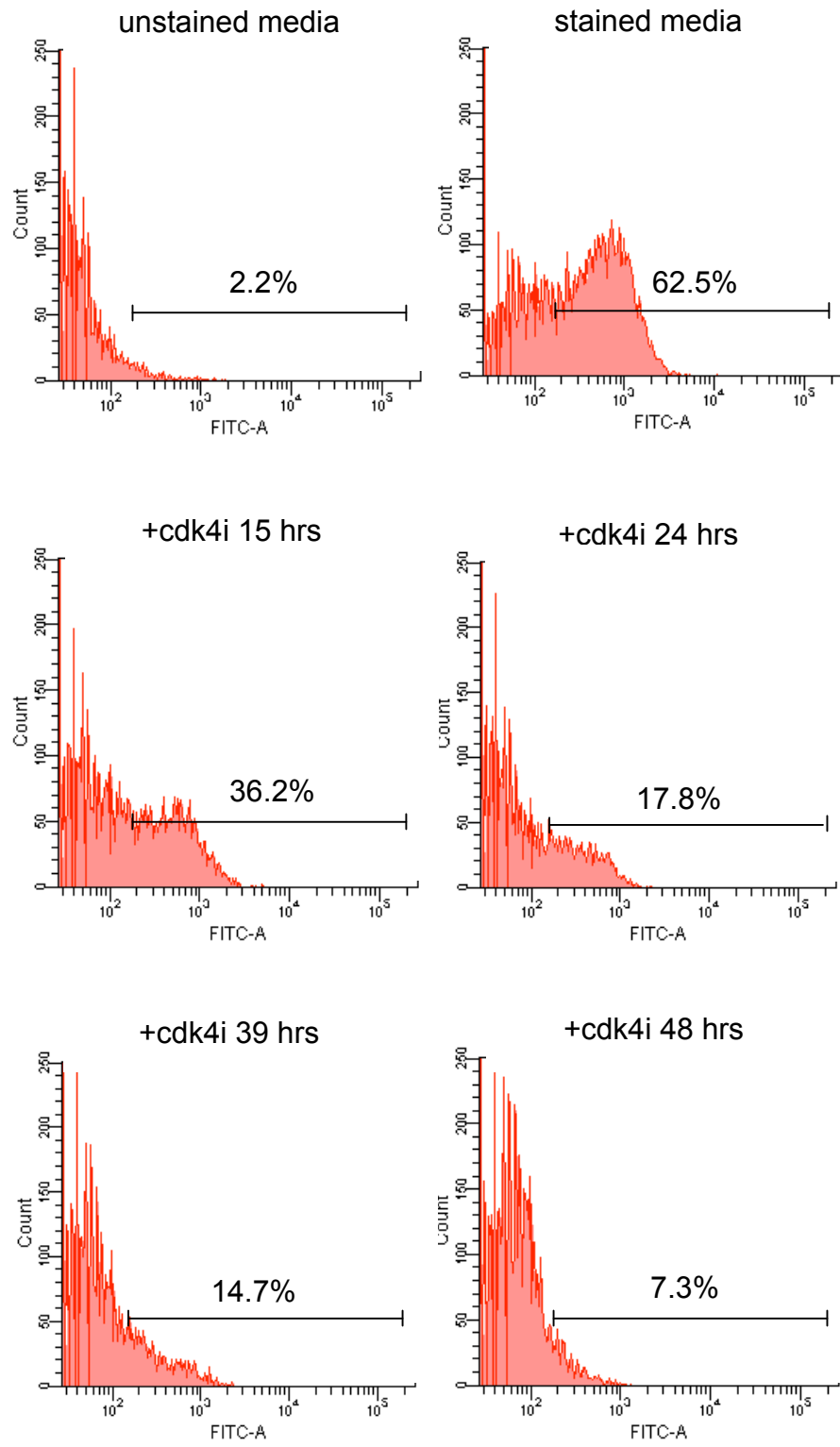


Figure 18. cdk4 and cyclin D3 protein expression decreases over time in cyclin dependent kinase 4 inhibitor (cdk4i) treated LY18 cells. LY18 cells were cultured in the absence (0 hrs, -) or in the presence (+) of 5 μ M cdk4i for various lengths of time. Whole cell extracts were prepared and Western blotting performed with anti-cdk4, anti-cdk6, or anti-cyclin D3 Abs. The blot was stripped and reprobed with anti-hsp90 Ab to verify equal loading of each lane. The densometric data (arbitrary) shown under the western blots are presented as fold changes as compared with their respective control.

Figure 18

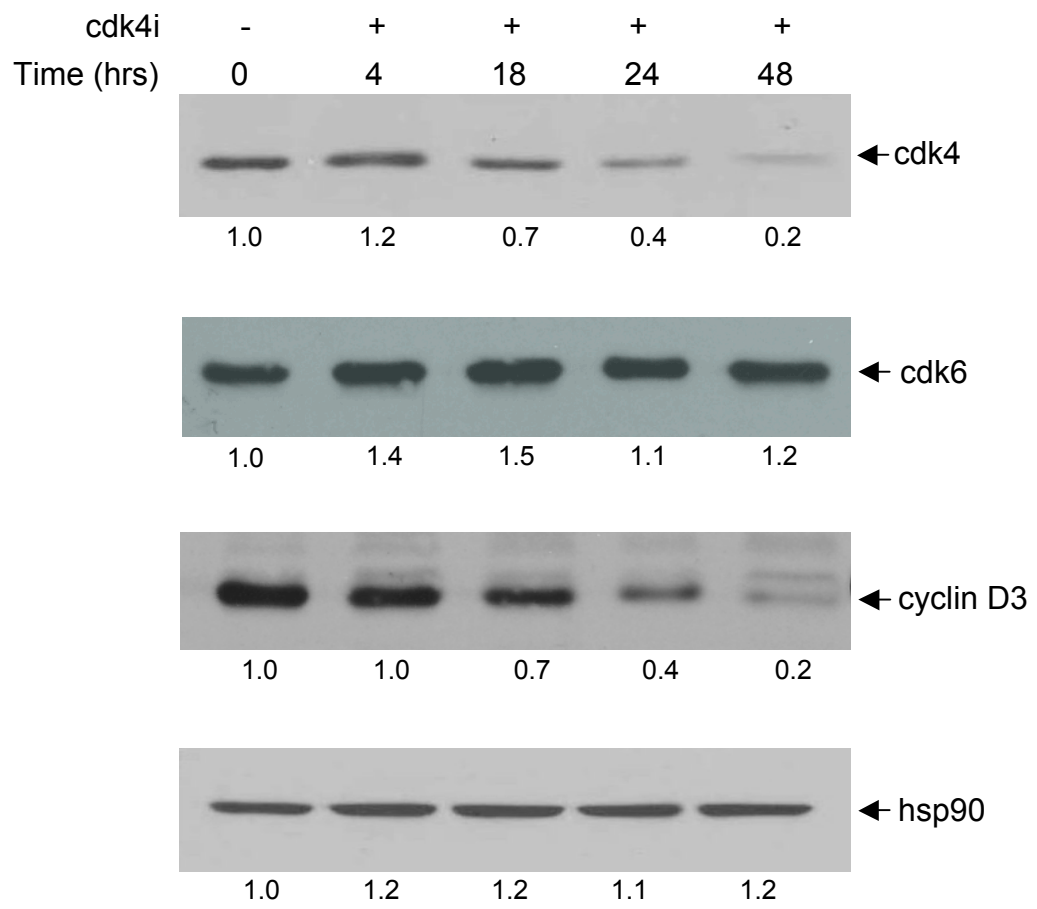


Figure 19. Cyclin dependent kinase 4 inhibitor (cdk4i) inhibits constitutive pRb^{Ser807/811} and pRb^{Thr821} phosphorylation in LY18 cells. LY18 cells were cultured in the absence (0 hrs, -) or in the presence (+) of 5 μ M cdk4i for various lengths of time. Whole cell extracts were prepared and Western blotting performed with anti-phospho-pRb^{Ser807/811} or anti-phospho-pRb^{Thr821} Abs. The blot was stripped and reprobed with anti-hsp90 Ab to verify equal loading of each lane. The densometric data (arbitrary) shown under the western blots are presented as fold changes as compared with their respective control.

Figure 19

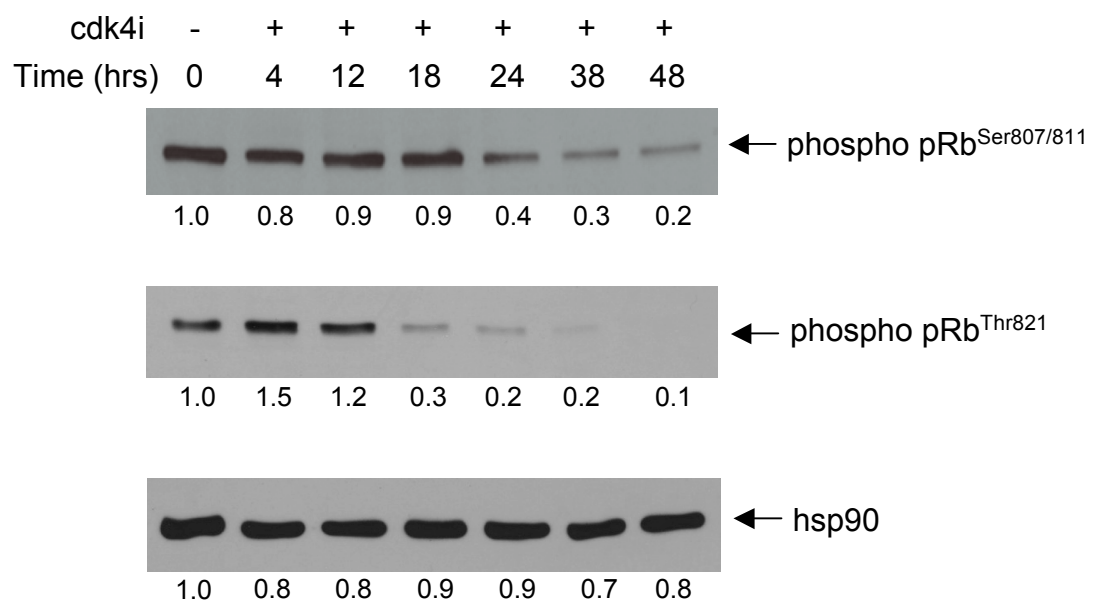


Figure 20. Cyclin dependent kinase 4 inhibitor (cdk4i) inhibits cdk2^{Thr160}

phosphorylation, but does not effect total cdk2 levels in LY18 cells. LY18 cells were cultured in the absence (0 hrs, -) or in the presence (+) of 5 μ M cdk4i for various lengths of time. Whole cell extracts were prepared and Western blotting performed with anti-phospho-cdk2^{Thr160} or anti-cdk2 Abs. The blot was stripped and reprobed with anti-hsp90 Ab to verify equal loading of each lane. The densometric data (arbitrary) shown under the western blots are presented as fold changes as compared with their respective control.

Figure 20

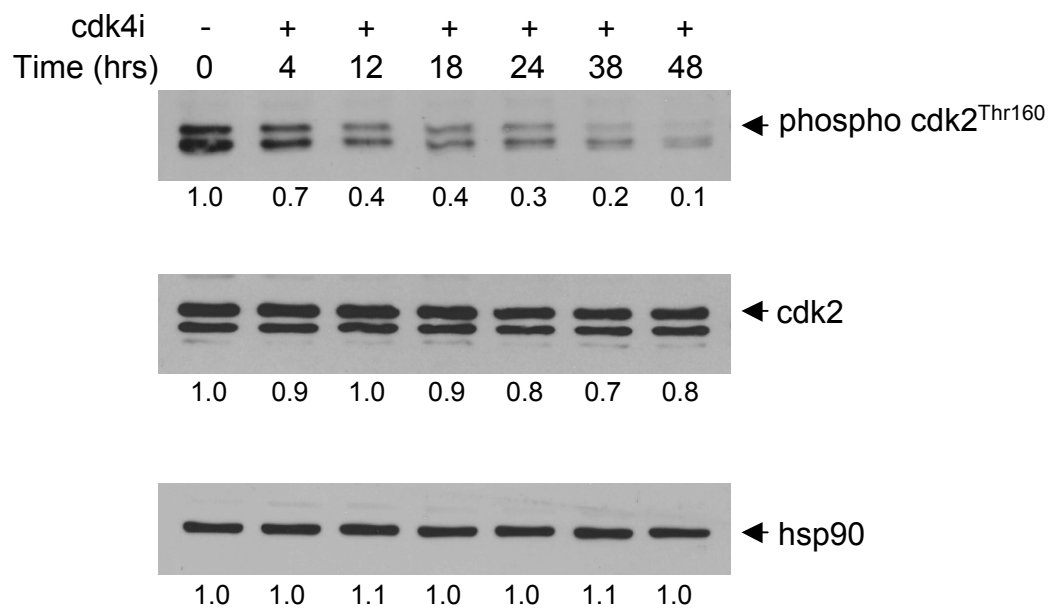


Figure 21. LY18 cells treated with cyclin dependent kinase 4 inhibitor (cdk4i) results in a time-dependent increase in endogenous p27 protein expression. LY18 cells were cultured in the absence (0 hrs, -) or in the presence (+) of 5 μ M cdk4i for various lengths of time. Whole cell extracts were prepared and Western blotting performed with anti-p27 Ab. The blot was stripped and reprobed with anti-hsp90 Ab to verify equal loading of each lane. The densometric data (arbitrary) shown under the western blots are presented as fold changes as compared with their respective control.

Figure 21

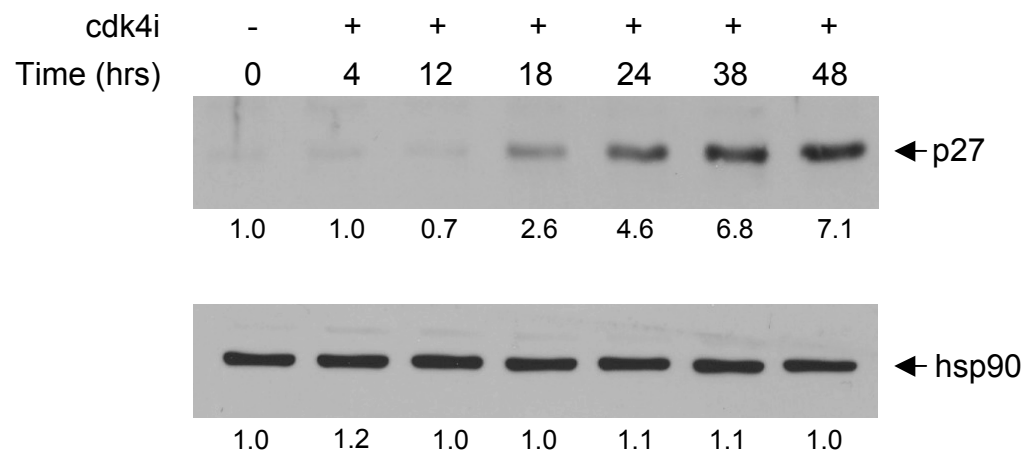
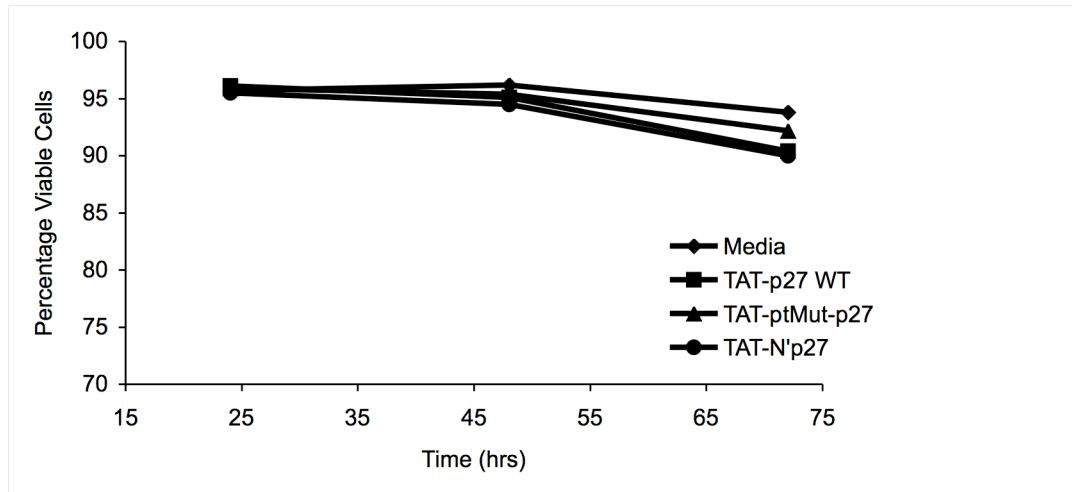


Figure 22. TAT-p27 fusion proteins do not measurably alter LY18 cell viability. *A*, LY18 cells were cultured in media alone, or where indicated with 150 nM TAT-p27 wild-type (WT), 150nM TAT-ptMut-p27, or 150nM TAT-N'p27 fusion proteins. At the indicated times, LY18 cells were collected and cell viability was determined by propidium iodide staining. Samples were analyzed by flow cytometry as described in *Material and Methods*. The data are represented as the percentage of LY18 cells that are negative for propidium iodide staining. The data are representative of 10,000 cells. *B*, LY18 cells were cultured in media alone, or where indicated with 300 nM or 450 nM TAT-p27 wild-type (WT), 300 nM or 450 nM TAT-ptMut-p27, or 300 nM or 450 nM TAT-N'p27 fusion proteins. At 48 hrs, LY18 cells were collected and viability was determined by propidium iodide staining. Samples were analyzed by flow cytometry as described in *Material and Methods*. The data are represented as the percentage of LY18 cells that are negative for propidium iodide staining. The data are representative of 10,000 cells.

Figure 22

A.



B.

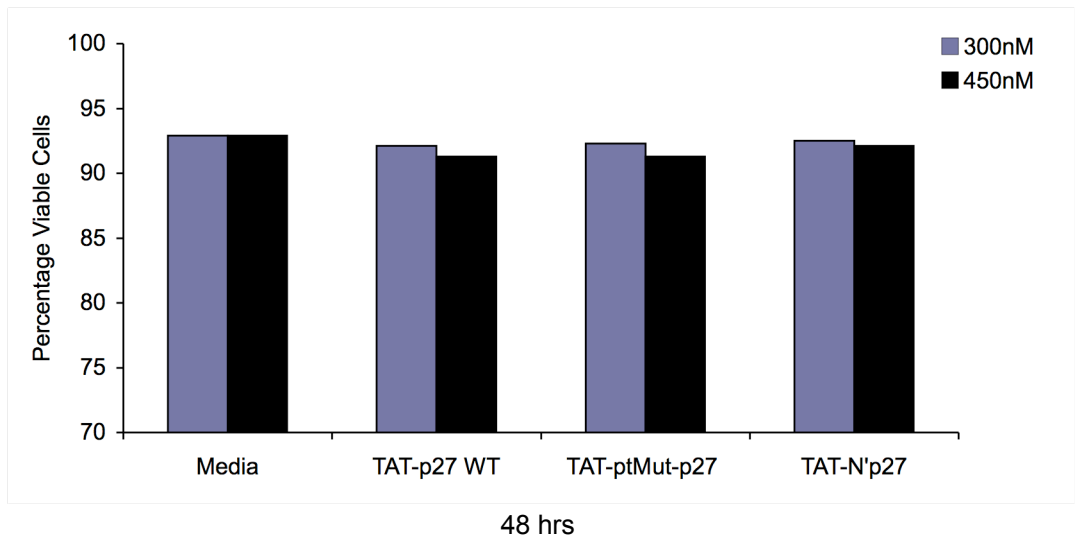


Figure 23. Incubation of LY18 cells with TAT-p27 fusion proteins does not measurably alter the percentage of cells in G₁-phase or S+G₂/M-phase of the cell cycle. LY18 cells were cultured in media alone, or where indicated with 150 nM TAT-p27 wild-type (WT), 150 nM TAT-ptMut-p27, or 150 nM TAT-N'p27 fusion proteins. *A*, At the indicated times, LY18 cells were stained with propidium iodide and cell cycle analyzed by flow cytometry as described in *Materials and Methods*. The data are represented as the percentage of LY18 cells in the G₁-phase of the cell cycle. *B*, At the indicated times, LY18 cells were stained with propidium iodide and cell cycle analyzed by flow cytometry as described in *Materials and Methods*. The data are represented as the percentage of LY18 cells in the S+G₂/M-phase of the cell cycle. The data are representative of 10,000 events.

Figure 23

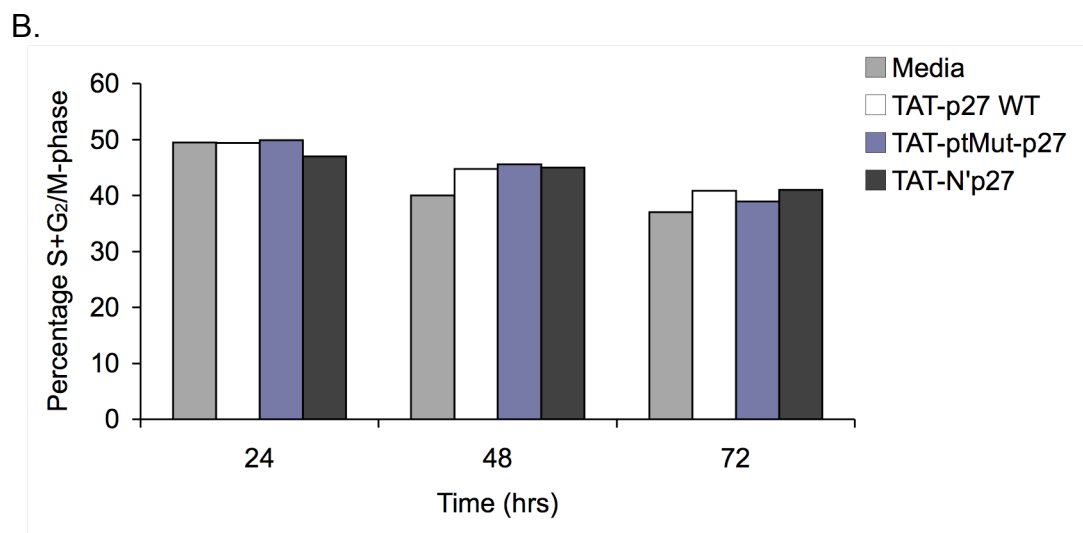
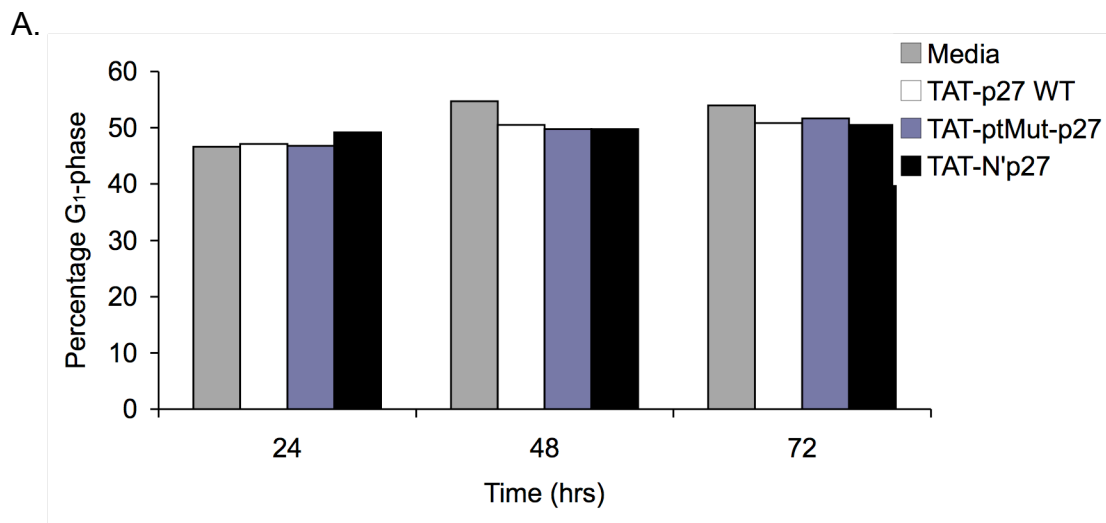


Figure 24. siRNA-mediated knockdown of endogenous p27 has no measurable effect on the viability of cyclin dependent kinase 4 inhibitor (cdk4i) treated LY18 cells. LY18 cells were nucleofected in the presence of media alone (M), 200 pmol control siRNA, or 200 pmol p27 siRNA and then allowed to incubate for 2 hrs before the addition of 5 μ M cdk4i. *A*, At 24 and 72 hrs, whole cell extracts were prepared and Western blotting performed with anti-p27 Ab. The blot was stripped and reprobed with anti-hsp90 Ab to verify equal loading of each lane. *B*, At 24, 48, and 72 hrs, LY18 cells were collected and cell viability was determined by propidium iodide staining. Samples were analyzed by flow cytometry as described in *Material and Methods*. The data are represented as the percentage of LY18 cells that are negative for propidium iodide staining. The data are representative of 10,000 cells.

Figure 24

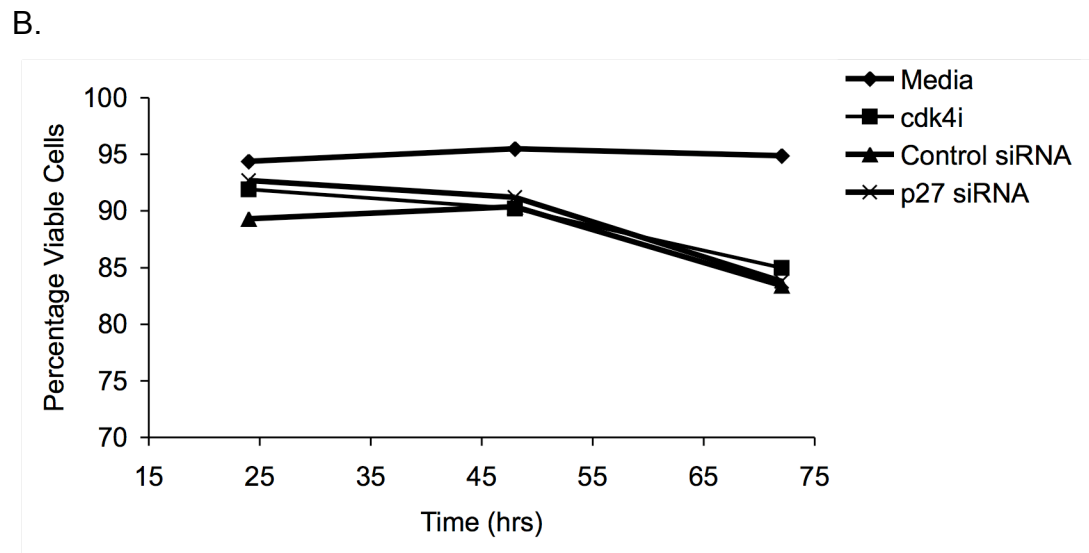
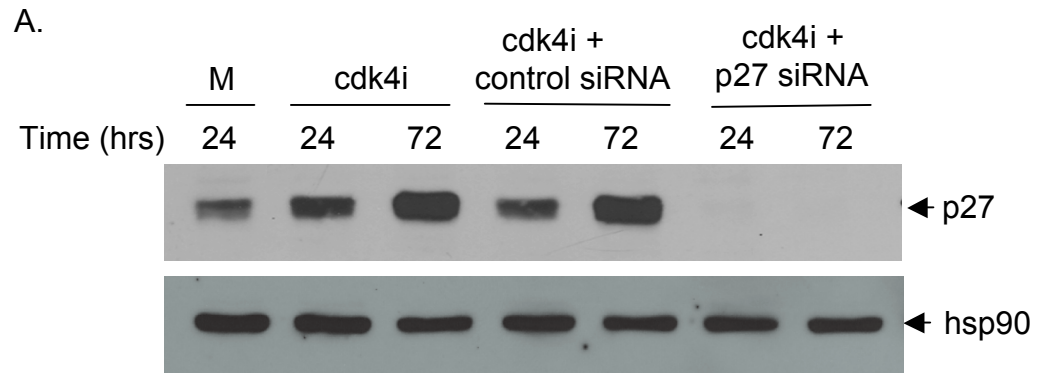


Figure 25. siRNA-mediated knockdown of endogenous p27 has no measurable effect on G₁-phase or S+G₂/M-phase of the cell cycle, in cyclin dependent kinase 4 inhibitor (cdk4i) treated LY18 cells. LY18 cells were nucleofected in the presence of media alone, 200 pmol control siRNA, or 200 pmol p27 siRNA and then allowed to incubate for 2 hours before the addition of 5 μ M cdk4i. *A*, At the indicated times, LY18 cells were stained propidium iodide and cell cycle analyzed by flow cytometry as described in *Materials and Methods*. The data are represented as the percentage of LY18 cells in the G₁-phase of the cell cycle. *B*, At the indicated times, LY18 cells were stained with propidium iodide and cell cycle analyzed by flow cytometry as described in *Materials and Methods*. The data are represented as the percentage of LY18 cells in the S+G₂/M-phase of the cell cycle. The data are representative of 10,000 events.

Figure 25

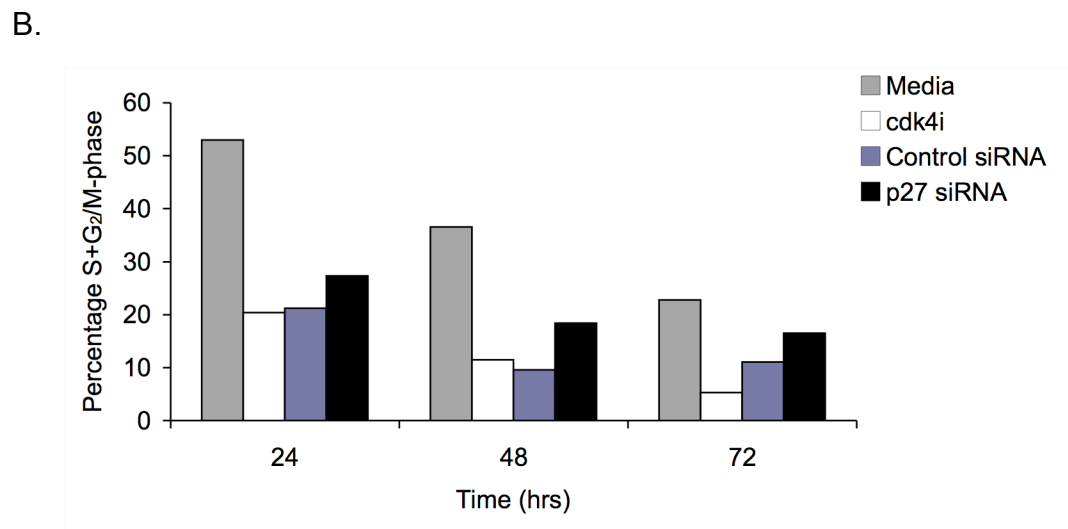
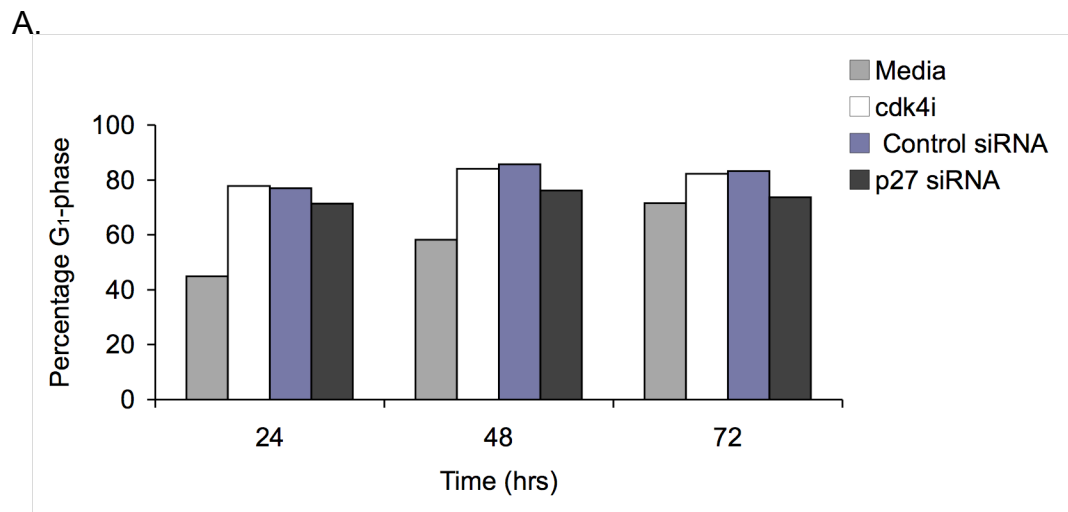
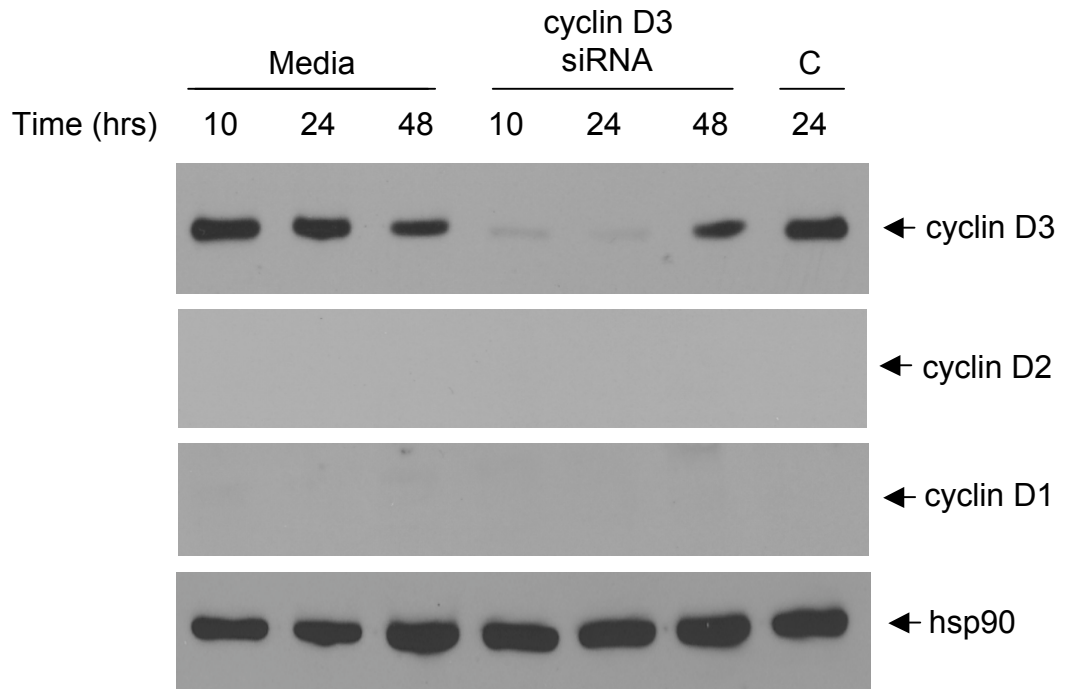


Figure 26. siRNA-mediated knockdown of endogenous cyclin D3 has no measurable effect on LY18 cell viability. LY18 cells were nucleofected in the presence of media alone or 300 pmol cyclin D3 siRNA for various lengths of time. LY18 cells were nucleofected with 300 pmol control siRNA (C) for only 24 hrs. *A*, At 10, 24, and 48 hrs, whole cell extracts were prepared and Western blotting performed with anti-cyclin D3, D2, or D1 Abs. The blot was stripped and reprobed with anti-hsp90 Ab to verify equal loading of each lane. *B*, At 10, 24, and 48 hrs, LY18 cells were collected and cell viability was determined by propidium iodide staining. Samples were analyzed by flow cytometry as described in *Material and Methods*. The data are represented as the percentage of LY18 cells that are negative for propidium iodide staining. The data are representative of 10,000 cells.

Figure 26

A.



B.

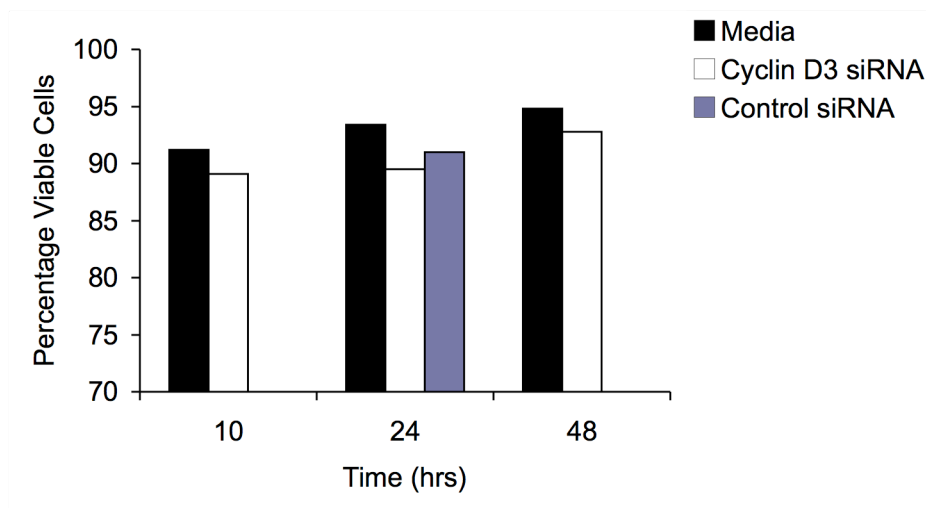


Figure 27. siRNA-mediated knock down of endogenous cyclin D3 does not measurably alter the cell cycle in LY18 cells. LY18 cells were nucleofected in the presence of media alone or 300 pmol cyclin D3 siRNA for various lengths of time. LY18 cells were nucleofected with 300 pmol control siRNA for only 24 hrs. At 10, 24, and 48 hrs, LY18 cells were collected and stained with propidium iodide and cell cycle analyzed by flow cytometry as described in *Materials and Methods*. The data are presented as the number of cells (counts) versus propidium iodide (PI-A), with percentages represented by black bars, indicating LY18 cells in G₁ or S+G₂/M-phase of the cell cycle, respectively. The data are representative of 10,000 cells.

Figure 27

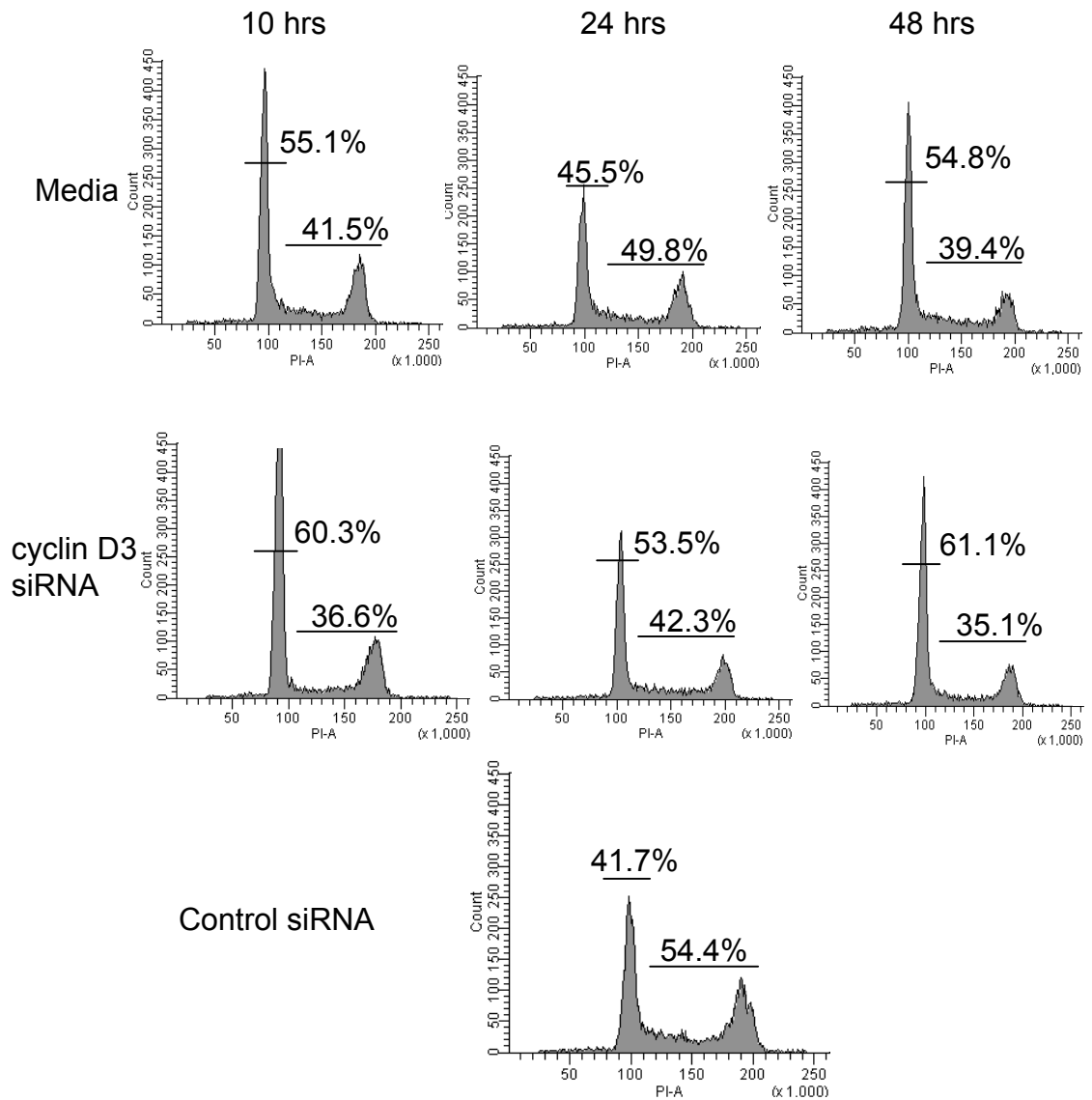


Figure 28. siRNA-mediated knock down of endogenous cyclin D3 does not measurably affect DNA synthesis in LY18 cells. LY18 cells were nucleofected in the presence of media alone or 300 pmol cyclin D3 siRNA for various lengths of time. LY18 cells were nucleofected with 300 pmol control siRNA for only 48 hrs. At the indicated times, LY18 cells were collected and DNA synthesis was monitored by BrdU incorporation and analyzed by flow cytometry as described in *Materials and Methods*. The data are representative of 10,000 events.

Figure 28

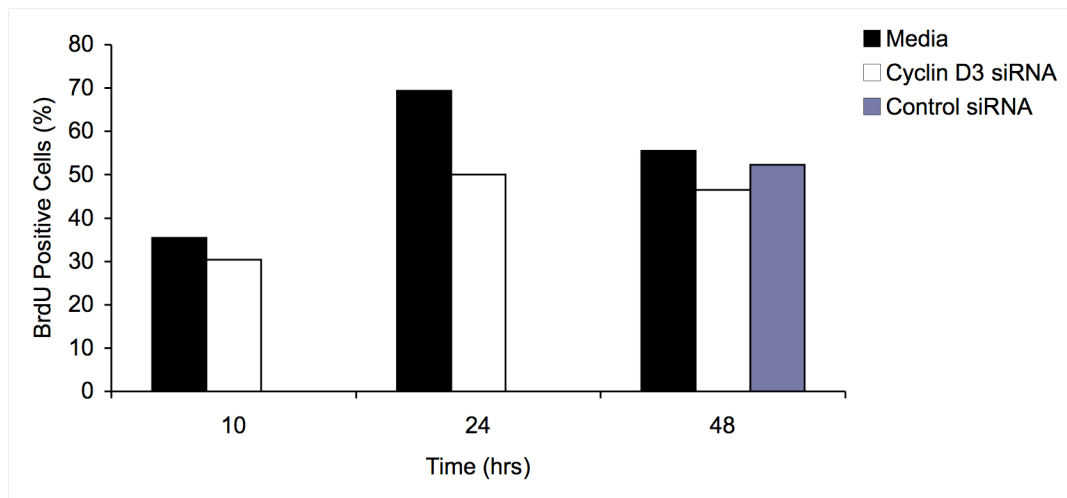


Figure 29. siRNA-mediated knockdown of both cyclin D3 and cyclin E and of cdk4, cdk6, and cdk2 reduces constitutive pRb^{Ser807/811} and pRb^{Thr821} phosphorylation in LY18 cells. LY18 cells were nucleofected in the presence of 200 pmol cdk4, cdk6, cdk2, cyclin D3, or cyclin E siRNA individually, or both cyclin D3 and cyclin E siRNA combined, or cdk4, cdk6, and cdk2 siRNA combined. At 48 hrs, whole cell extracts were prepared and western blotting performed with anti-phospho-pRb^{Ser807/811} and anti-phospho-pRb^{Thr821} Abs.

Figure 29

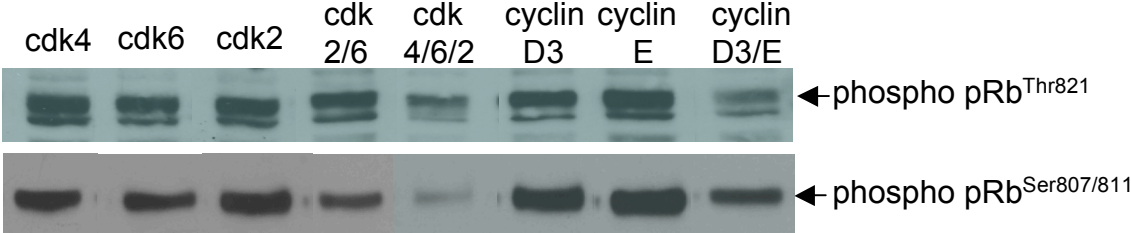


Table 1. Target sequences of siRNAs used to knockdown endogenous proteins in LY18 cells. LY18 cells were nucleofected with varying concentrations over time with individual siRNA or combinations of siRNAs. p27 and cyclin D3 siRNA are siGENOME target sequences, and cdk4, cdk6, cdk2, and cyclin E are siGENOME SMARTpool sequences.

Table 1

Target Sequences	
Control siRNA	Non-Targeting siRNA #3
p27 siRNA	CGACGAUUCUUCUACUCAA
cdk4 siRNA	GCAGCACUCUUAUCUACAU GGAGGAGGCCUUCCCAUCA UCGAAAGCCUCUCUUCUGU GUACCGAGCUCCCGAAGUU
cdk6 siRNA	GCAAAGACCUACUUCUGAA GAAGAAGACUGGCCUAGAG UAACAGAUUCGAUGAACU GGCCUUGCCCGCAUCUAUA
cdk2 siRNA	GAGCUUAACCAUCCUAAUA GAGAGGUGGUGGCGCUUAA GCACCAAGAUCUCAAGAAA GGACGGAGCUUGUUAUCGC
cyclin E siRNA	GGAAAUCUAUCCUCCAAAG GGAGGUGUGUGAAGUCUAU CUAAAUGACUUACAUGAAG GUAUAUGGCGACACAAGAA
cyclin D3 siRNA	GAUCGAAGCUGCACUCAGG

Figure 30. siRNA-mediated knock down of endogenous cdk4 has no measurable effect on LY18 cell viability. LY18 cells were nucleofected in the presence of media alone or 200 or 400 pmol cdk4 siRNA for various lengths of time. LY18 cells were nucleofected with 400 pmol control siRNA (C) for only 48 hrs. *A*, At 24 and 48 hrs, whole cell extracts were prepared and Western blotting performed with anti-cdk4, anti-cdk6, or anti-cdk2 Abs. The blot was stripped and reprobed with anti-hsp90 Ab to verify equal loading of each lane. *B*, At 24 and 48 hrs, LY18 cells were collected and cell viability was determined by propidium iodide staining. Samples were analyzed by flow cytometry as described in *Material and Methods*. The data are represented as the percentage of LY18 cells that are negative for propidium iodide staining. The data are representative of 10,000 cells.

Figure 30

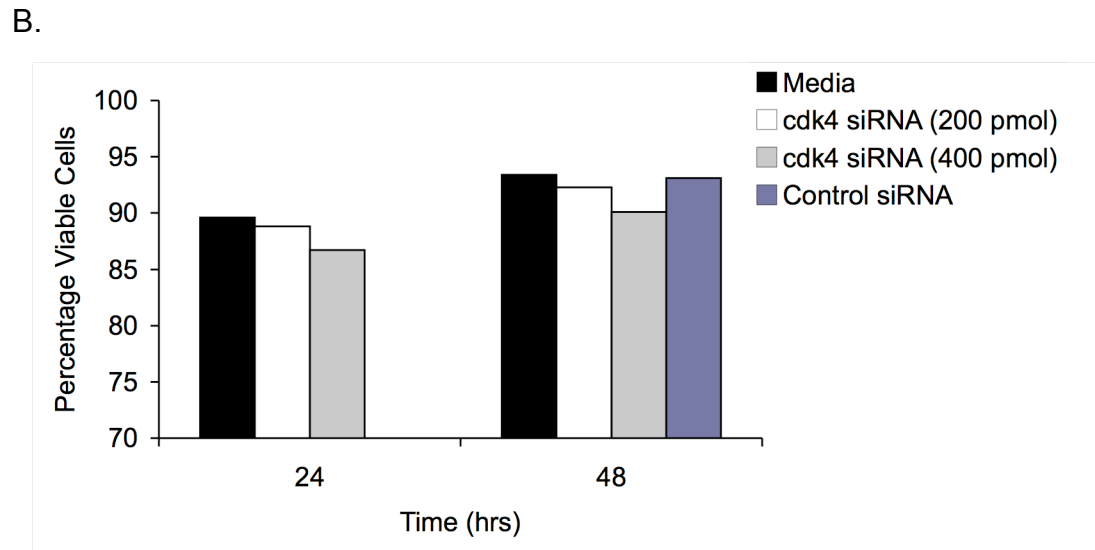
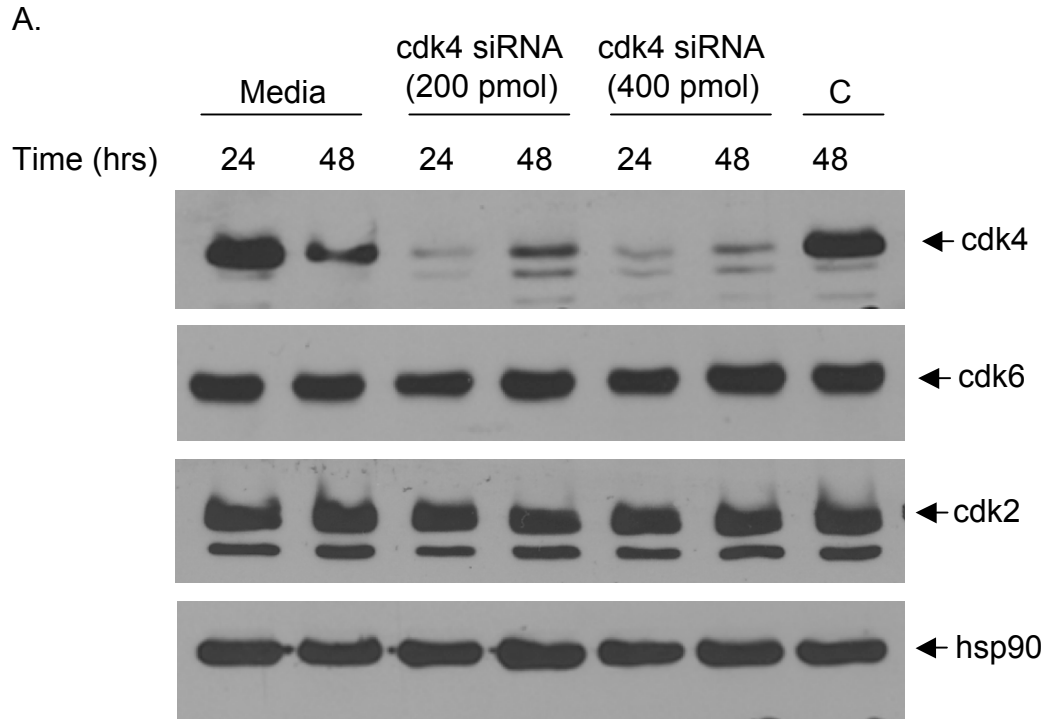


Figure 31. Knockdown of endogenous cdk6 following incubation of LY18 cells with cdk6 siRNA has no measurable effect on the viability. LY18 cells were nucleofected in the presence of media alone (M) or 200 or 400 pmol cdk6 siRNA for various lengths of time. LY18 cells were nucleofected with 400 pmol control siRNA (C) for only 24 hrs. *A*, At 24 and 48 hrs, whole cell extracts were prepared and Western blotting performed with anti-cdk6, or anti-cdk4 Abs. The blot was stripped and reprobed with anti-hsp90 Ab to verify equal loading of each lane. *B*, At 24 and 48 hrs, LY18 cells were collected and cell viability was determined by propidium iodide staining. Samples were analyzed by flow cytometry as described in *Material and Methods*. The data are represented as the percentage of LY18 cells that are negative for propidium iodide staining. The data are representative of 10,000 cells.

Figure 31

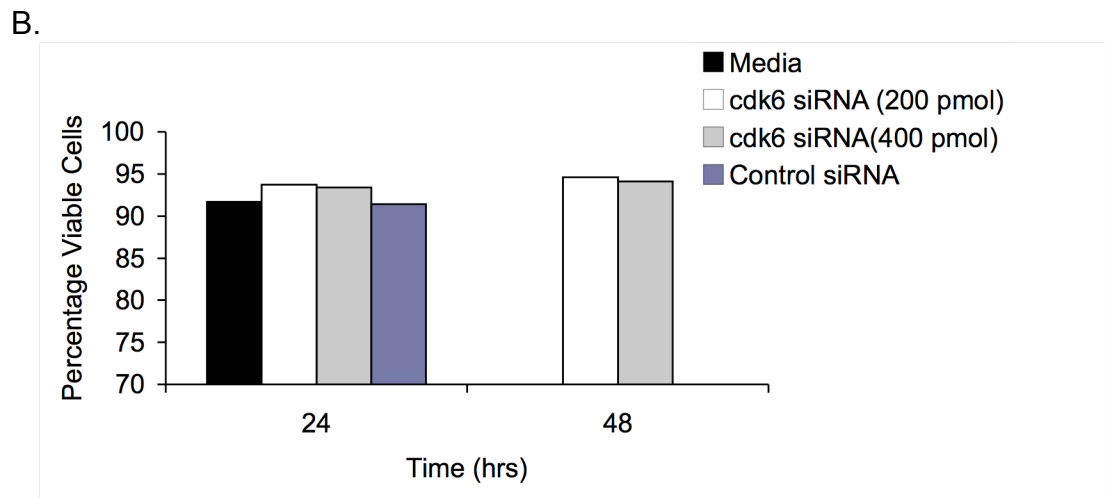
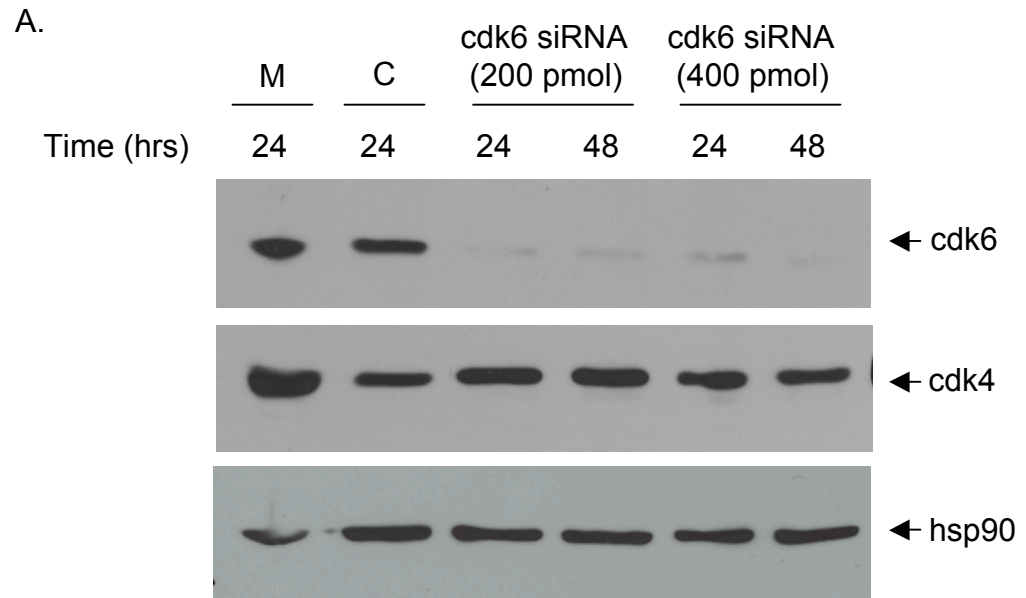


Figure 32. siRNA-mediated knock down of endogenous cdk4 does not measurably alter the cell cycle in LY18 cells. LY18 cells were nucleofected in the presence of media alone or 200 pmol cdk4 siRNA for various lengths of time. LY18 cells were nucleofected with 200 pmol control siRNA (C) for only 48 hrs. At 24 and 48 hrs, LY18 cells were collected and stained with propidium iodide and cell cycle analyzed by flow cytometry as described in *Materials and Methods*. The data are presented as the number of cells (counts) versus propidium iodide (PI-A), with percentages represented by black bars, indicating LY18 cells in G₁ or S+G₂/M-phase of the cell cycle, respectively. The data are representative of 10,000 cells.

Figure 32

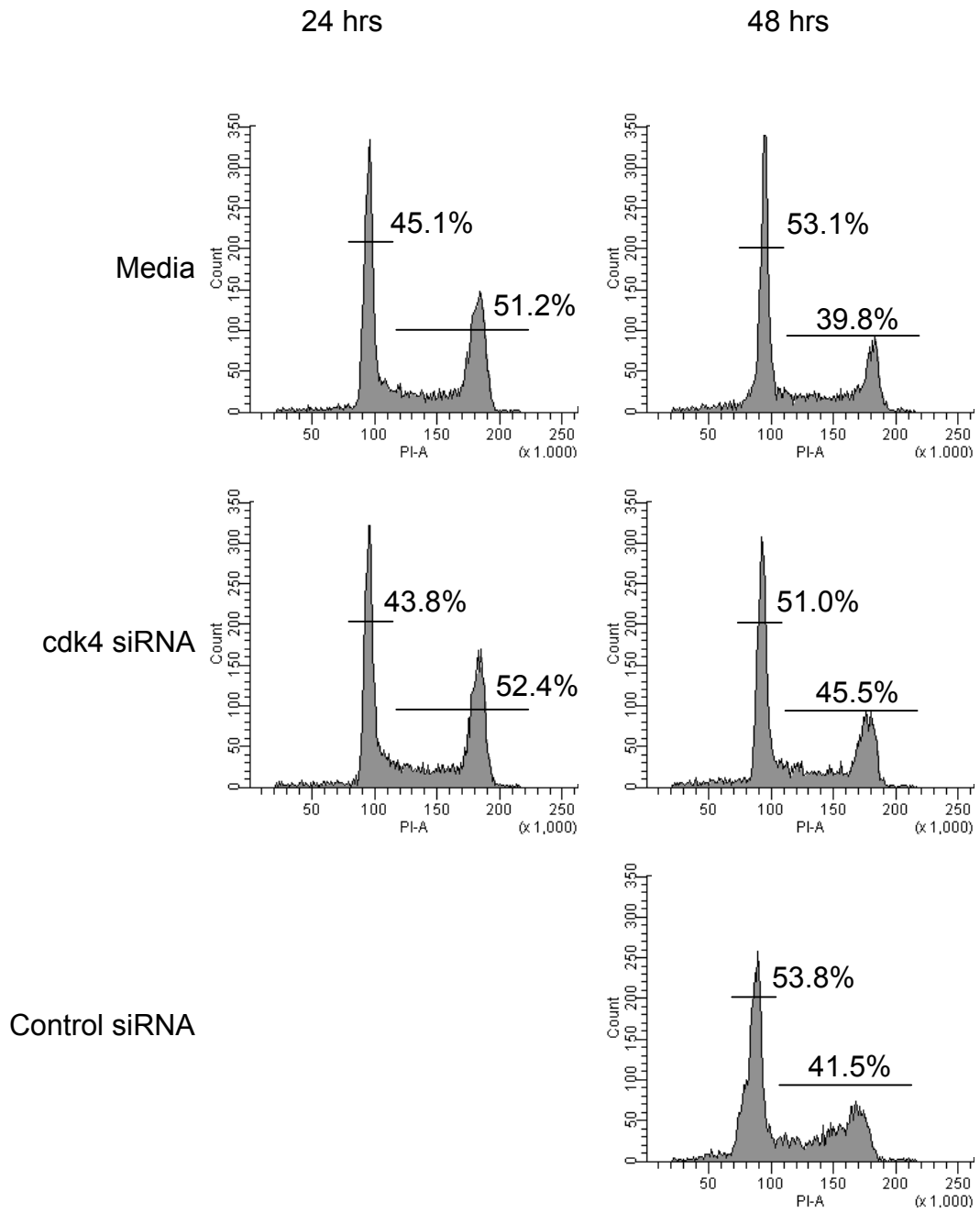


Figure 33. Knockdown of endogenous cdk6 following incubation of LY18 cells with cdk6 siRNA does not measurably alter the cell cycle. LY18 cells were nucleofected in the presence of media alone or 300 pmol cdk6 siRNA for various lengths of time. LY18 cells were nucleofected with 300 pmol control siRNA for only 24 hrs. At 24 and 48 hrs, LY18 cells were collected and stained with propidium iodide and cell cycle analyzed by flow cytometry as described in *Materials and Methods*. The data are presented as the number of cells (counts) versus propidium iodide (PI-A), with percentages represented by black bars, indicating LY18 cells in G₁ or S+G₂/M-phase of the cell cycle, respectively. The data are representative of 10,000 cells.

Figure 33

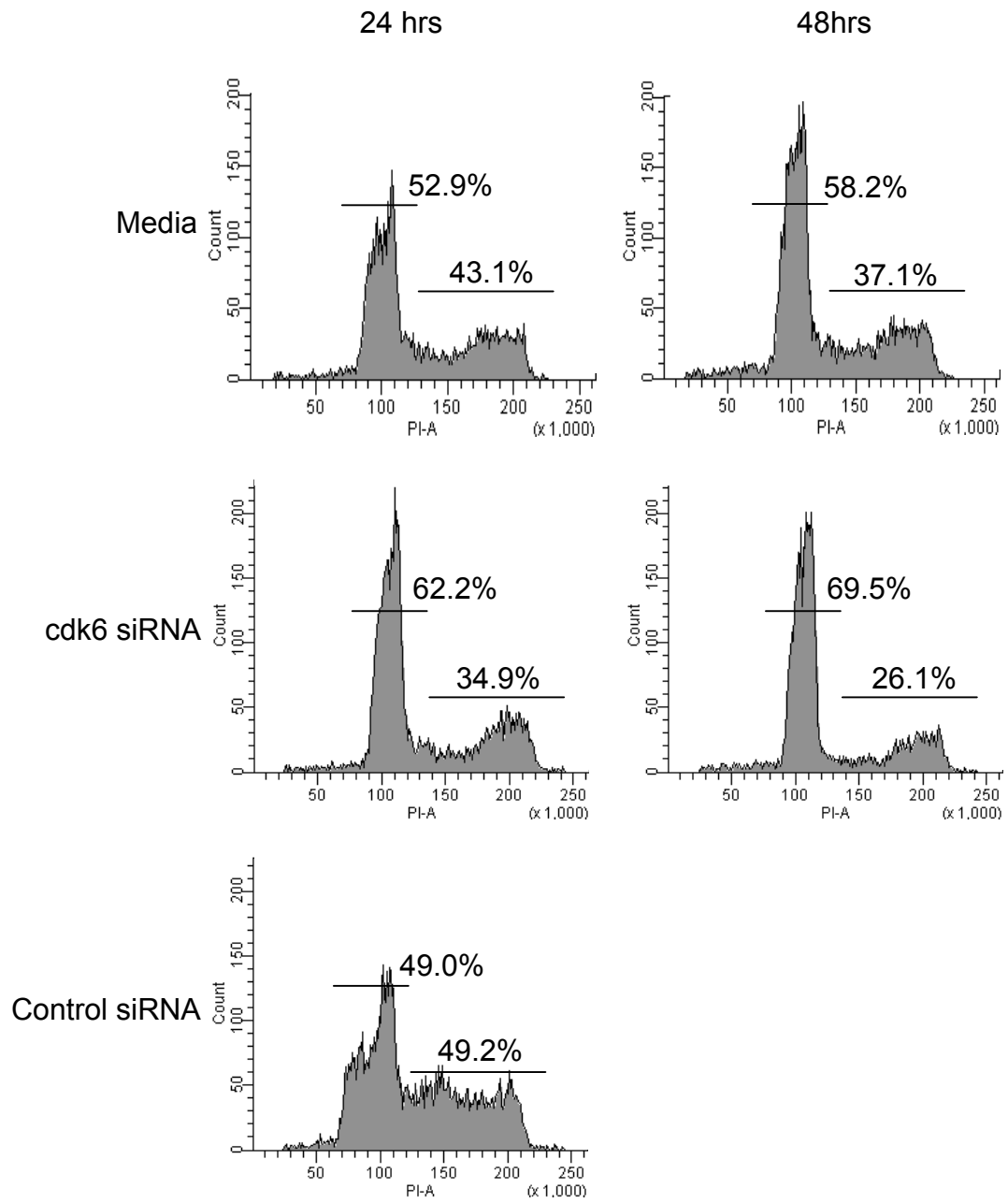
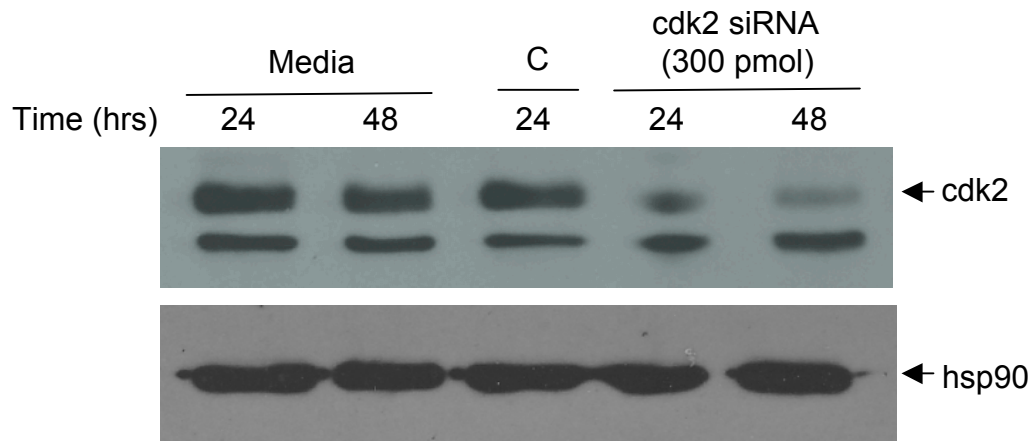


Figure 34. Knockdown of endogenous cdk2 following incubation with cdk2 siRNA has no measurable effect on LY18 cell viability. LY18 cells were nucleofected in the presence of media alone or 300 pmol cdk2 siRNA for various lengths of time. LY18 cells were nucleofected with 300 pmol control siRNA (C) for only 24 hrs. *A*, At 24 and 48 hrs, whole cell extracts were prepared and Western blotting performed with anti-cdk2 Ab. The blot was stripped and reprobed with anti-hsp90 Ab to verify equal loading of each lane. *B*, At 24 and 48 hrs, LY18 cells were collected and cell viability was determined by propidium iodide staining. Samples were analyzed by flow cytometry as described in *Material and Methods*. The data are represented as the percentage of LY18 cells that are negative for propidium iodide staining. The data are representative of 10,000 cells.

Figure 34

A.



B.

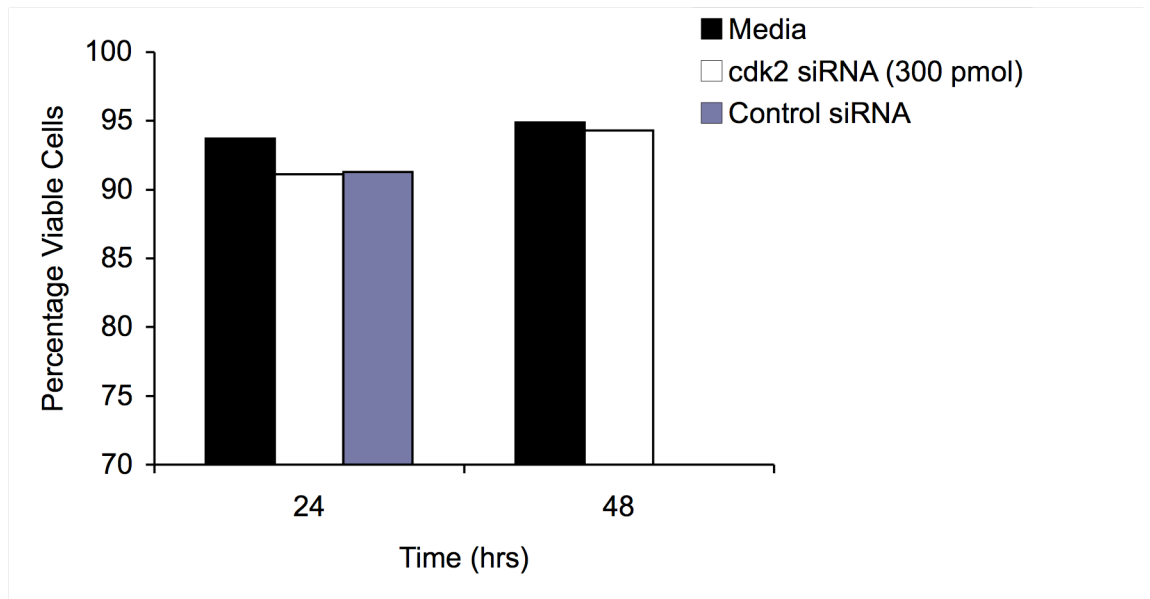


Figure 35. siRNA-mediated knockdown of endogenous cyclin E has no measurable effect on LY18 cell viability. LY18 cells were nucleofected in the presence of media alone or 300 pmol cyclin E siRNA for various lengths of time. LY18 cells were nucleofected with 300 pmol control siRNA for only 24 hrs. At 24 and 48 hrs, LY18 cells were collected and cell viability was determined by propidium iodide staining. Samples were analyzed by flow cytometry as described in *Material and Methods*. The data are represented as the percentage of LY18 cells that are negative for propidium iodide staining. The data are representative of 10,000 cells.

Figure 35

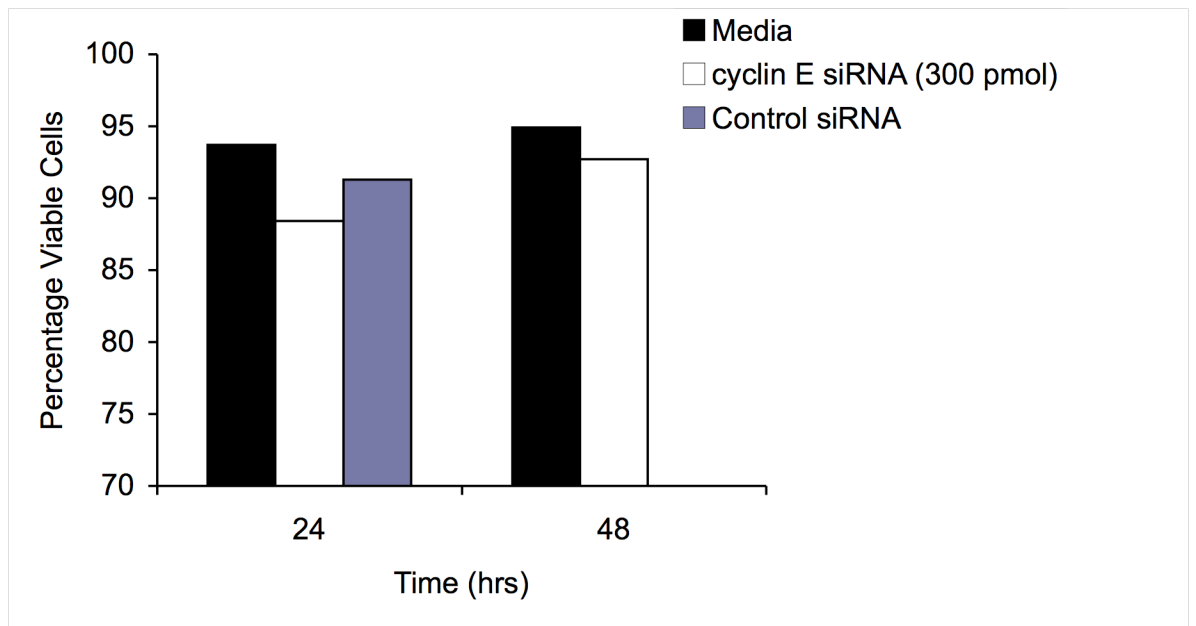


Figure 36. siRNA-mediated knockdown of endogenous cyclin E has no measurable effect on the cell cycle in LY18 cells. LY18 cells were nucleofected in the presence of media alone or 300 pmol cyclin E siRNA for various lengths of time. LY18 cells were nucleofected with 300 pmol control siRNA for only 24 hrs. At 24 and 48 hrs, LY18 cells were collected and stained with propidium iodide and cell cycle analyzed by flow cytometry as described in *Materials and Methods*. The data are presented as the number of cells (counts) versus propidium iodide (PI-A), with percentages represented by black bars, indicating LY18 cells in G₁ or S+G₂/M-phase of the cell cycle, respectively. The data are representative of 10,000 cells.

Figure 36

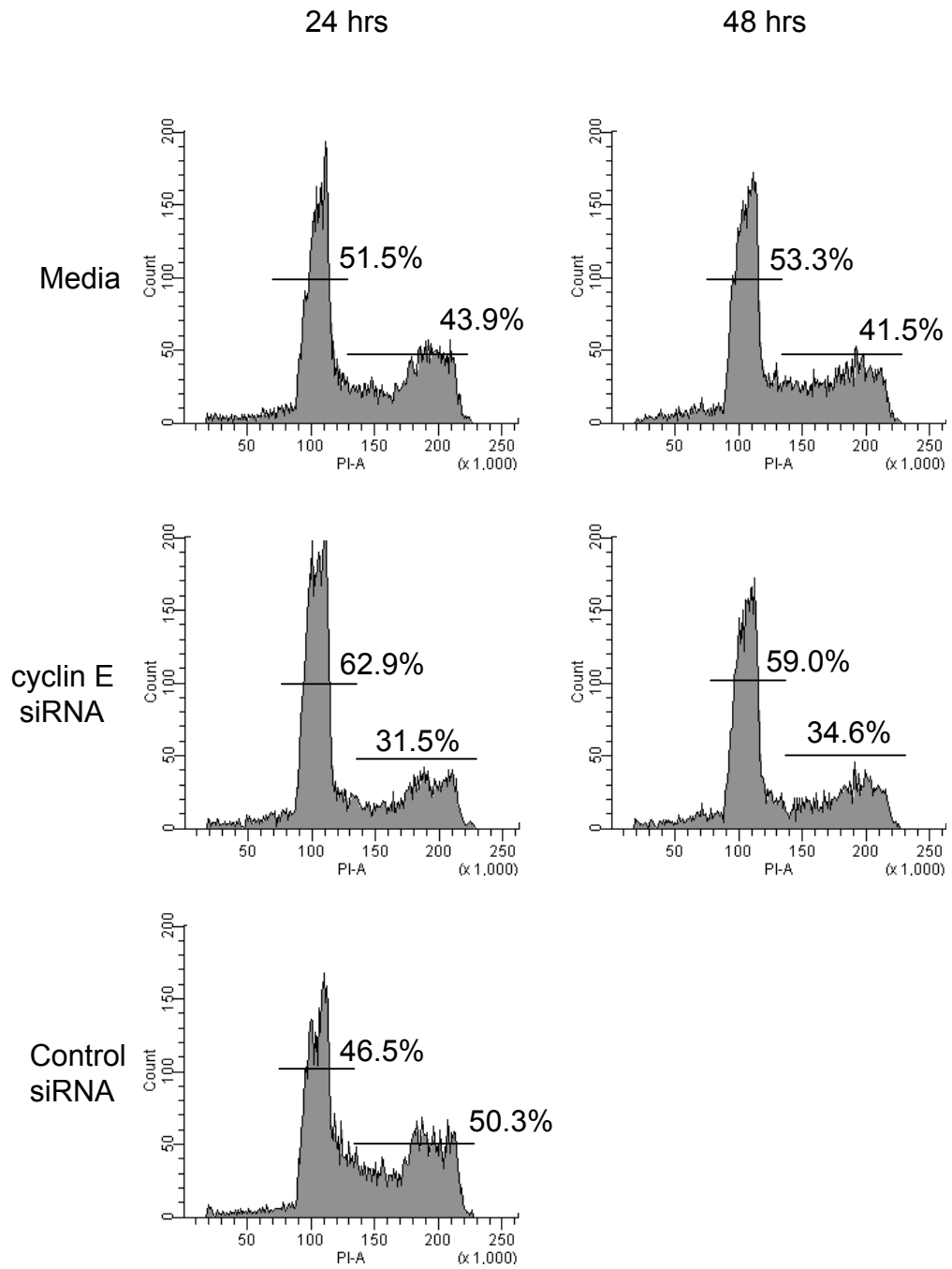


Figure 37. Knockdown of endogenous cdk2 following incubation of LY18 cells with cdk2 siRNA does not measurably alter the cell cycle. LY18 cells were nucleofected in the presence of media alone or 300 pmol cdk2 siRNA for various lengths of time. LY18 cells were nucleofected with 300 pmol control siRNA for only 24 hrs. At 24 and 48 hrs, LY18 cells were collected and stained with propidium iodide and cell cycle analyzed by flow cytometry as described in *Materials and Methods*. The data are presented as the number of cells (counts) versus propidium iodide (PI-A), with percentages represented by black bars, indicating LY18 cells in G₁ or S+G₂/M-phase of the cell cycle, respectively. The data are representative of 10,000 cells.

Figure 37

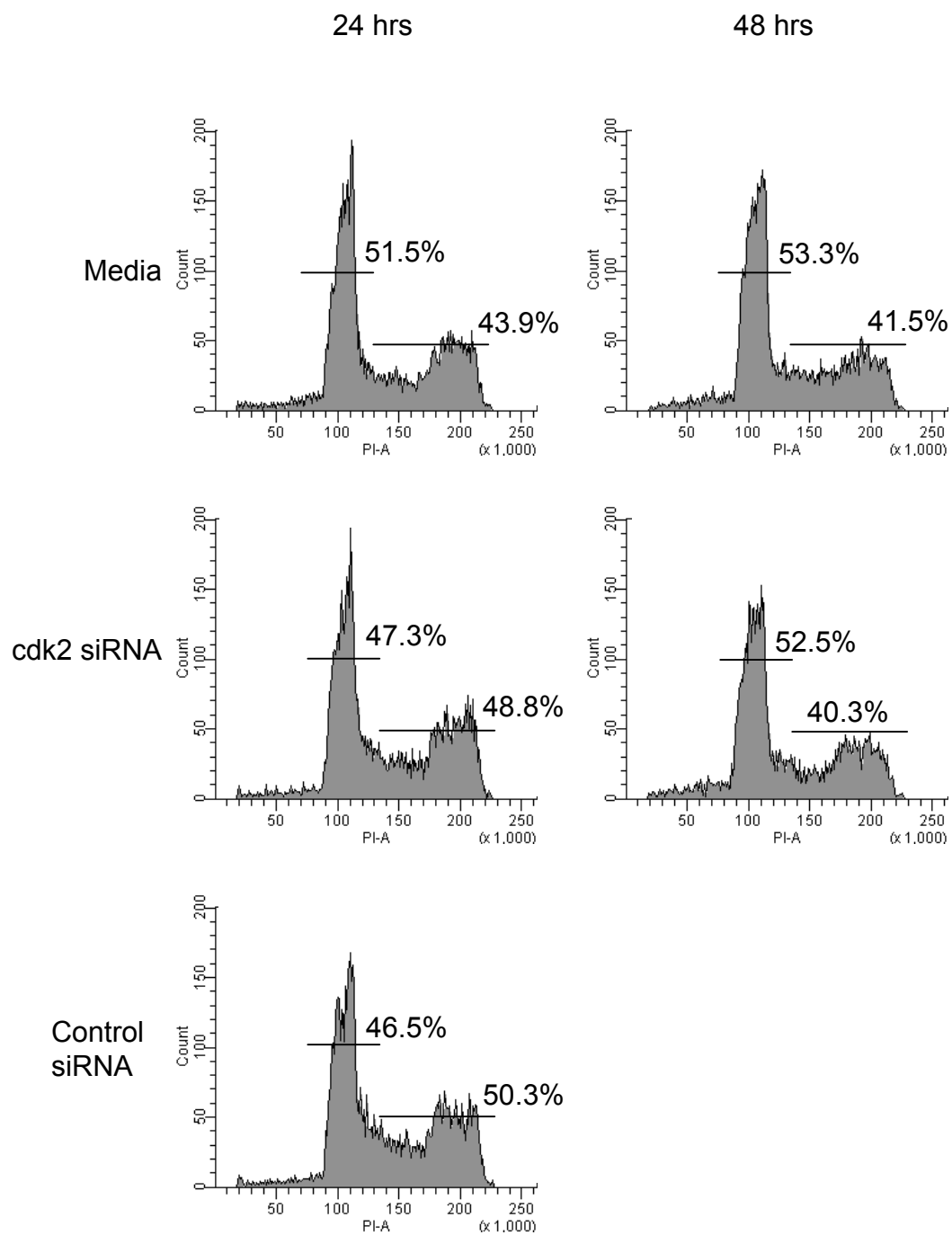


Figure 38. siRNA-mediated knockdown of endogenous cdk4 and cdk6 has no detectable effect on LY18 cell viability. LY18 cells were nucleofected in the presence of media alone or 200 pmol of both cdk4 and cdk6 siRNA for various lengths of time. LY18 cells were nucleofected with 200 pmol control siRNA for only 24 hrs. At 24 and 48 hrs, LY18 cells were collected and cell viability was determined by propidium iodide staining. Samples were analyzed by flow cytometry as described in *Material and Methods*. The data are represented as the percentage of LY18 cells that are negative for propidium iodide staining. The data are representative of 10,000 cells.

Figure 38

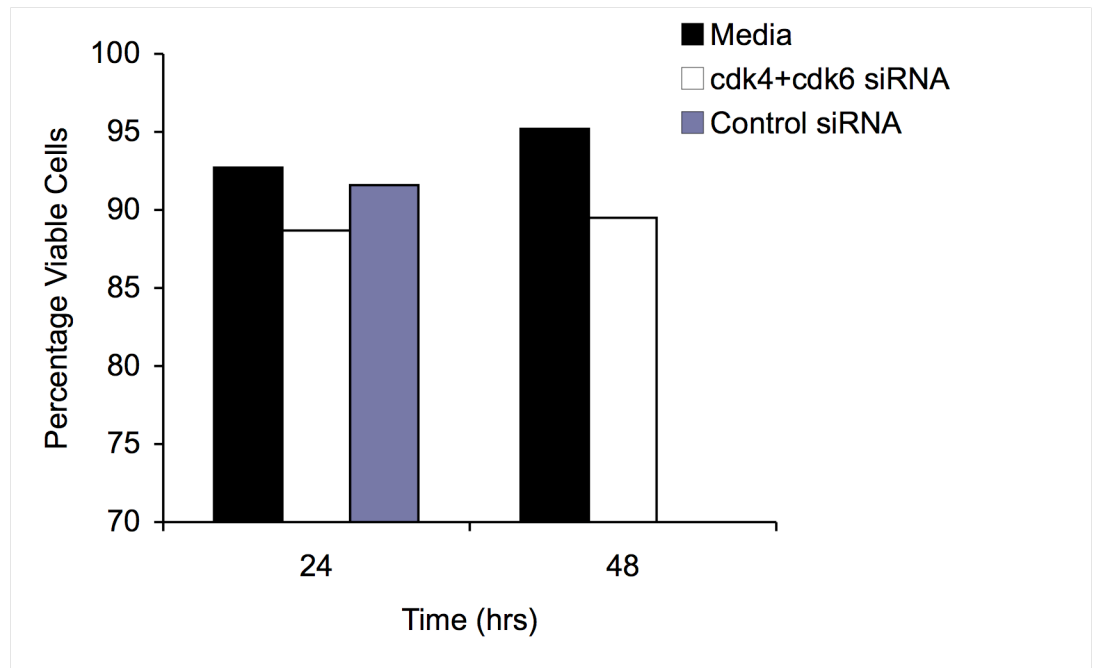


Figure 39. siRNA-mediated knockdown of endogenous cdk4 and cdk6 results in an increase in the percentage of LY18 cells in G₁-phase of cell cycle and a decrease in the percentage of LY18 cells in S+G₂/M-phase of the cell cycle. LY18 cells were nucleofected in the presence of media alone or 200 pmol of both cdk4 and cdk6 siRNA for various lengths of time. LY18 cells were nucleofected with 200 pmol control siRNA for only 24 hrs. At 24 and 48 hrs, LY18 cells were collected and stained with propidium iodide and cell cycle analyzed by flow cytometry as described in *Materials and Methods*. The data are presented as the number of cells (counts) versus propidium iodide (PI-A), with percentages represented by black bars, indicating LY18 cells in G₁ or S+G₂/M-phase of the cell cycle, respectively. The data are representative of 10,000 cells.

Figure 39

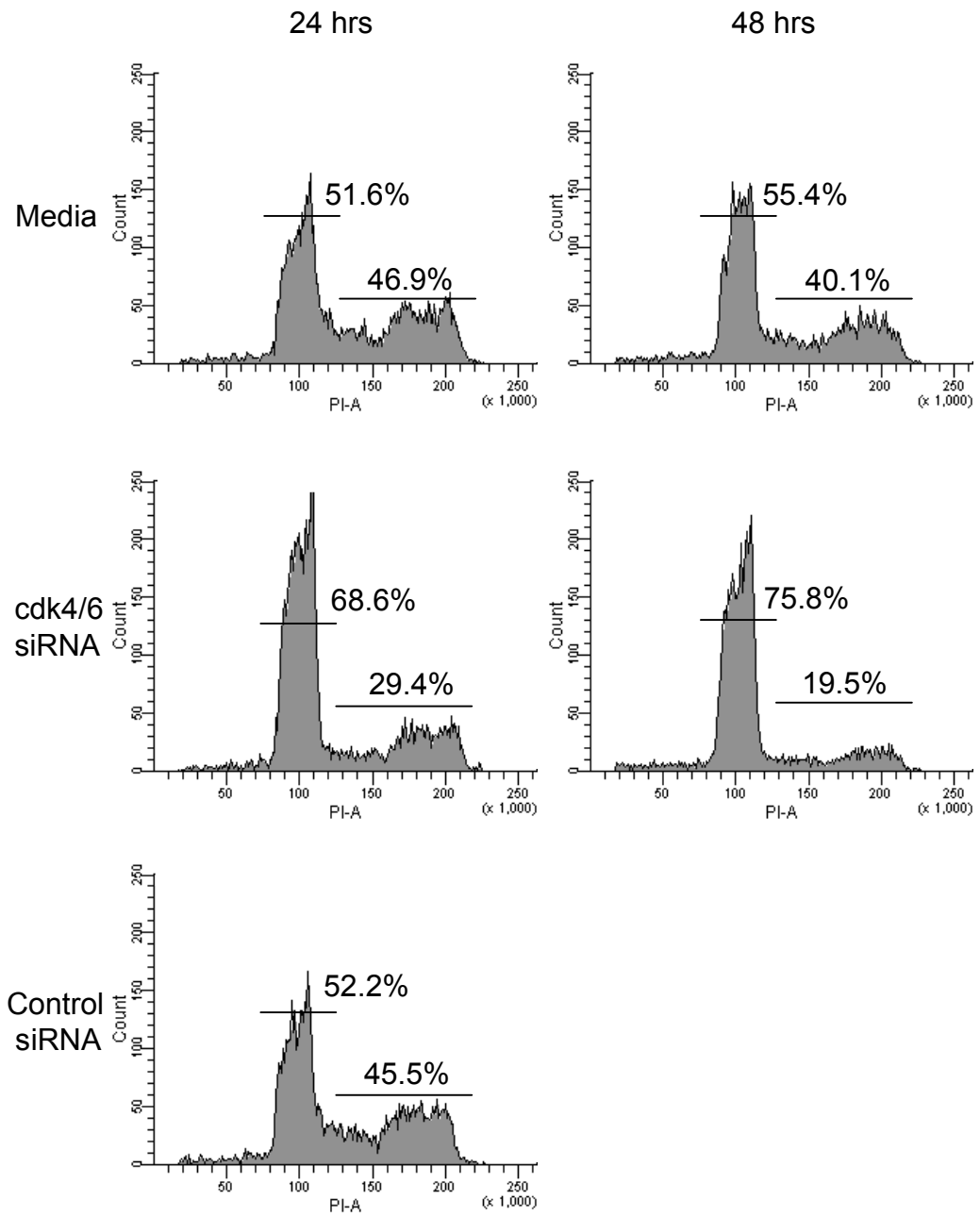
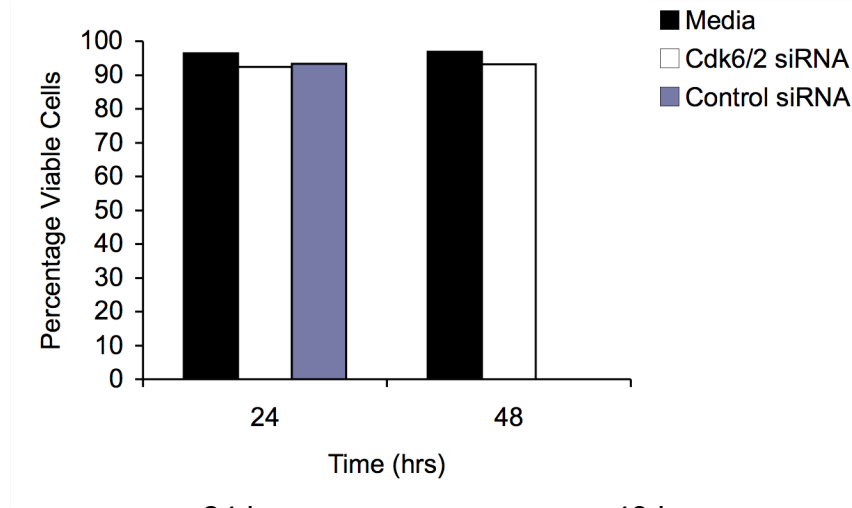


Figure 40. siRNA-mediated knockdown of endogenous cdk6 and cdk2 has no detectable effect on LY18 cell viability, however, it results in an increase in the percentage of LY18 cells in G₁-phase of cell cycle and a decrease in the percentage of LY18 cells in S+G₂/M-phase of the cell cycle. LY18 cells were nucleofected in the presence of media alone or 200 pmol of both cdk6 and cdk2 siRNA for various lengths of time. LY18 cells were nucleofected with 200 pmol control siRNA for only 24 hrs. *A*, At 24 and 48 hrs, LY18 cells were collected and cell viability was determined by propidium iodide staining. Samples were analyzed by flow cytometry as described in *Material and Methods*. The data are represented as the percentage of LY18 cells that are negative for propidium iodide staining. The data are representative of 10,000 cells. *B*, At 24 and 48 hrs, LY18 cells were collected and stained with propidium iodide and cell cycle analyzed by flow cytometry as described in *Materials and Methods*. The data are presented as the number of cells (counts) versus propidium iodide (PI-A), with percentages represented by black bars, indicating LY18 cells in G₁ or S+G₂/M-phase of the cell cycle, respectively. The data are representative of 10,000 cells.

Figure 40

A.



B.

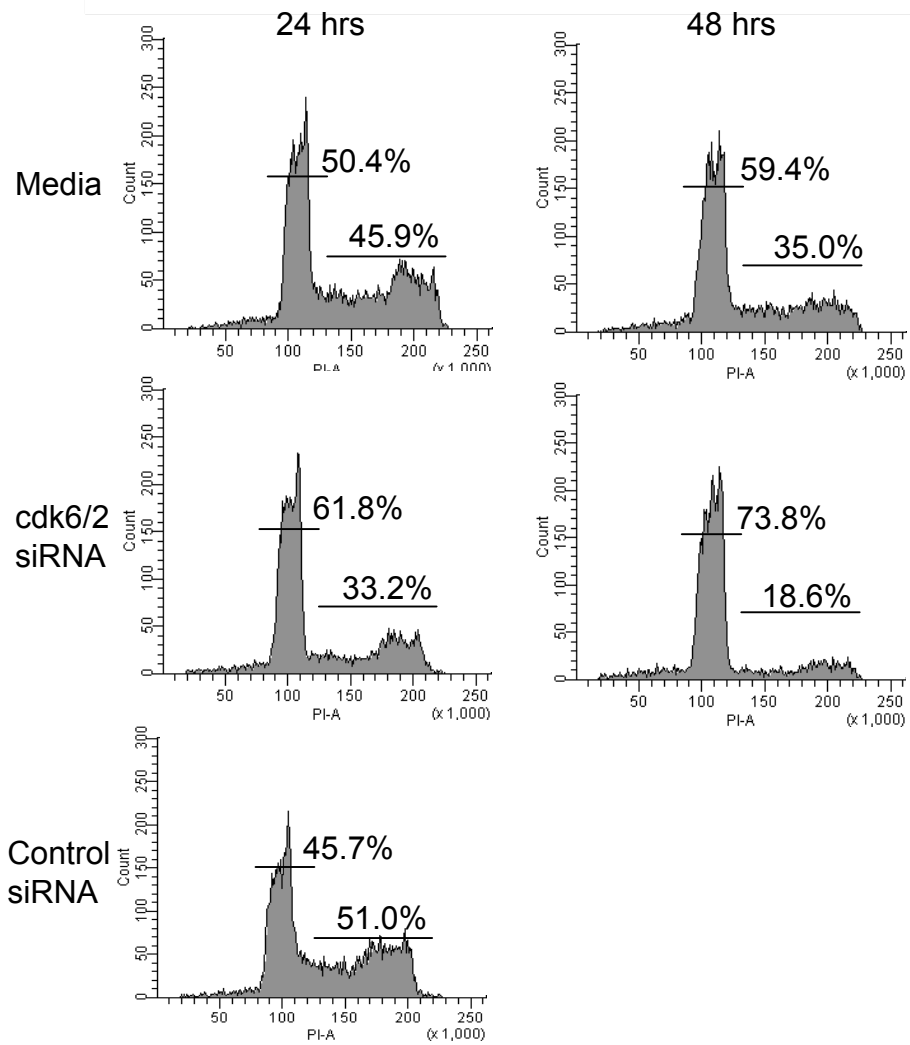
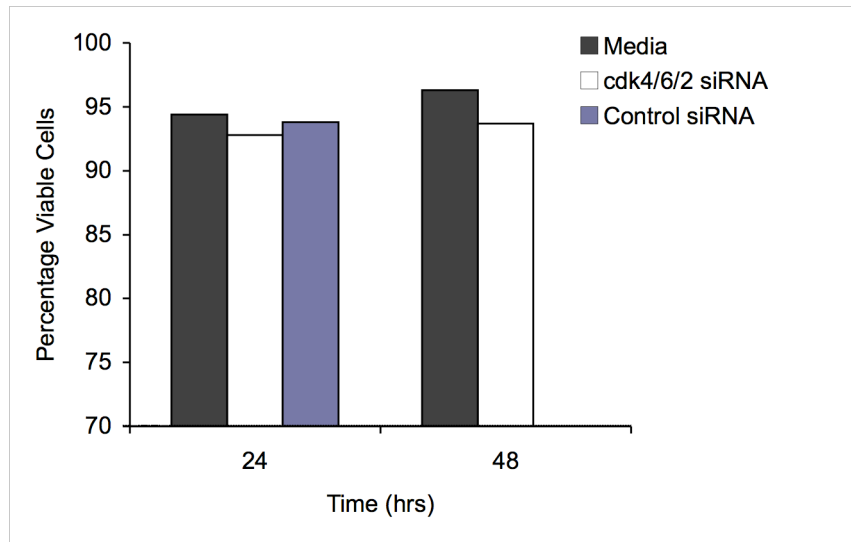


Figure 41. siRNA-mediated knockdown of endogenous cdk4, cdk6, and cdk2 has no measurable effect on LY18 cell viability, however, it results in an increase in the percentage of LY18 cells in G₁-phase of cell cycle and a decrease in the percentage of cells in S+G₂/M-phase of the cell cycle. LY18 cells were nucleofected in the presence of media alone or 200 pmol of cdk4, cdk6, and cdk2 siRNA for various lengths of time. LY18 cells were nucleofected with 200 pmol control siRNA for only 24 hrs. *A*, At 24 and 48 hrs, LY18 cells were collected and cell viability was determined by propidium iodide staining. Samples were analyzed by flow cytometry as described in *Material and Methods*. The data are represented as the percentage of LY18 cells that are negative for propidium iodide staining. The data are representative of 10,000 cells. *B*, At 24 and 48 hrs, LY18 cells were collected and stained with propidium iodide and cell cycle analyzed by flow cytometry as described in *Materials and Methods*. The data are presented as the number of cells (counts) versus propidium iodide (PI-A), with percentages represented by black bars, indicating LY18 cells in G₁ or S+G₂/M-phase of the cell cycle, respectively. The data are representative of 10,000 cells.

Figure 41

A.



B.

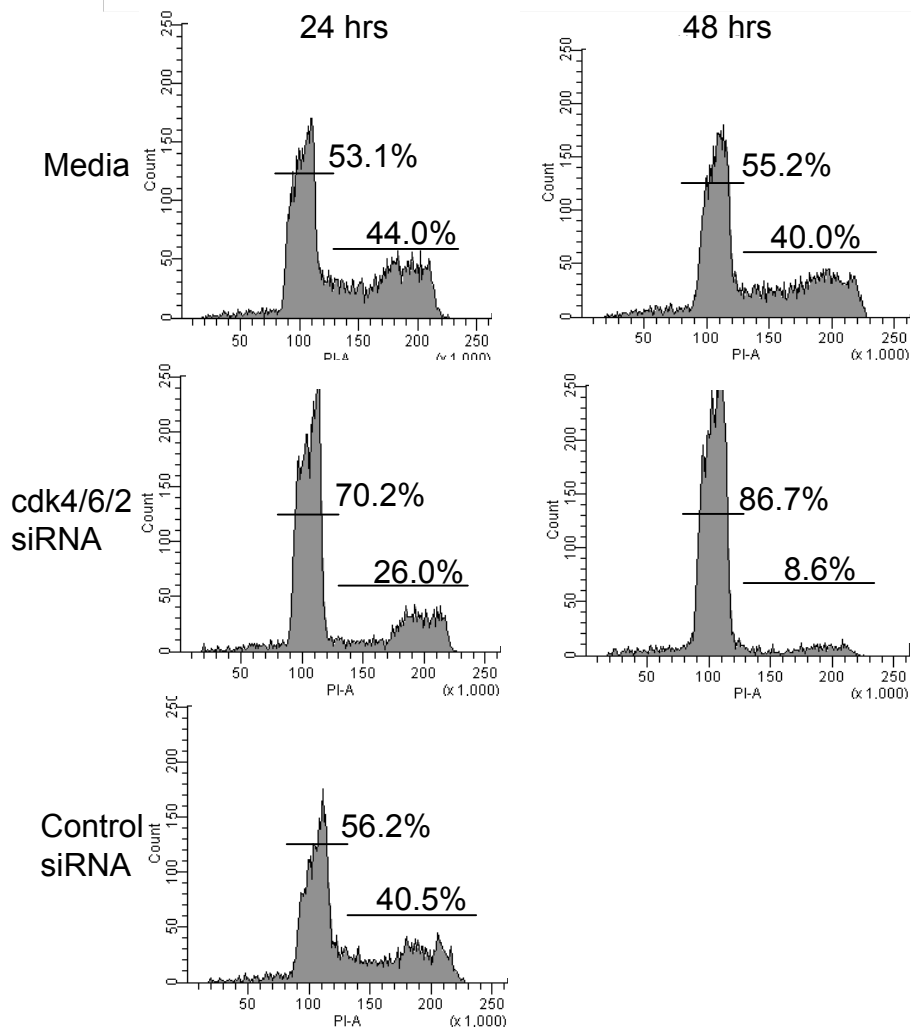


Figure 42. siRNA-mediated knockdown of endogenous cyclin D3 and cyclin E has no measurable effect on the viability in LY18 cells. LY18 cells were nucleofected in the presence of media alone or 200 pmol of both cyclin D3 and cyclin E siRNA for various lengths of time. LY18 cells were nucleofected with 200 pmol control siRNA for only 24 hrs. At 24 and 48 hrs, LY18 cells were collected and cell viability was determined by propidium iodide staining. Samples were analyzed by flow cytometry as described in *Material and Methods*. The data are represented as the percentage of LY18 cells that are negative for propidium iodide staining. The data are representative of 10,000 cells.

Figure 42

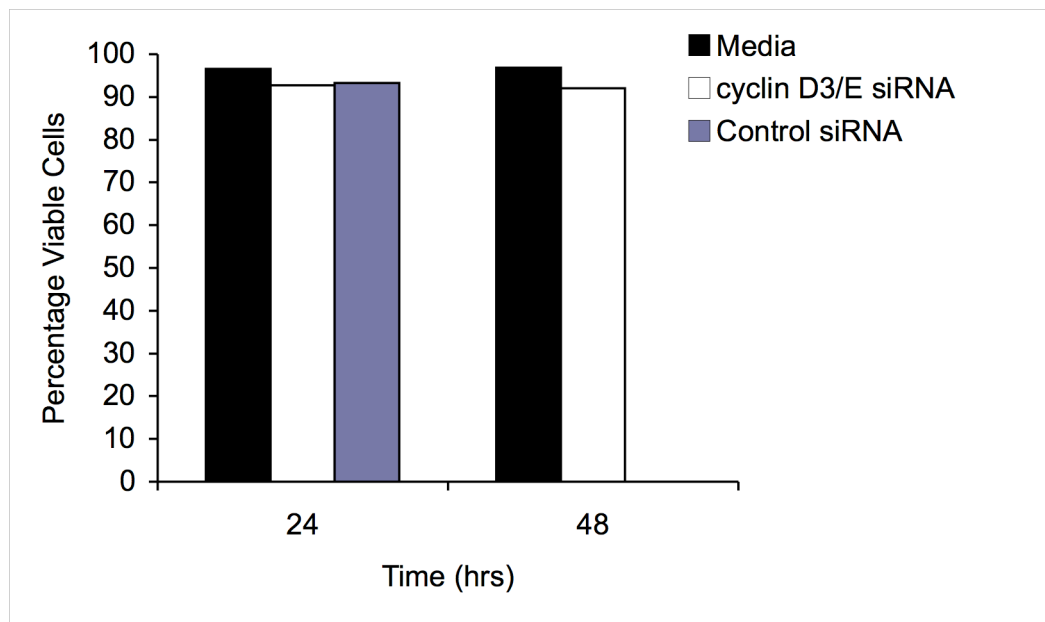
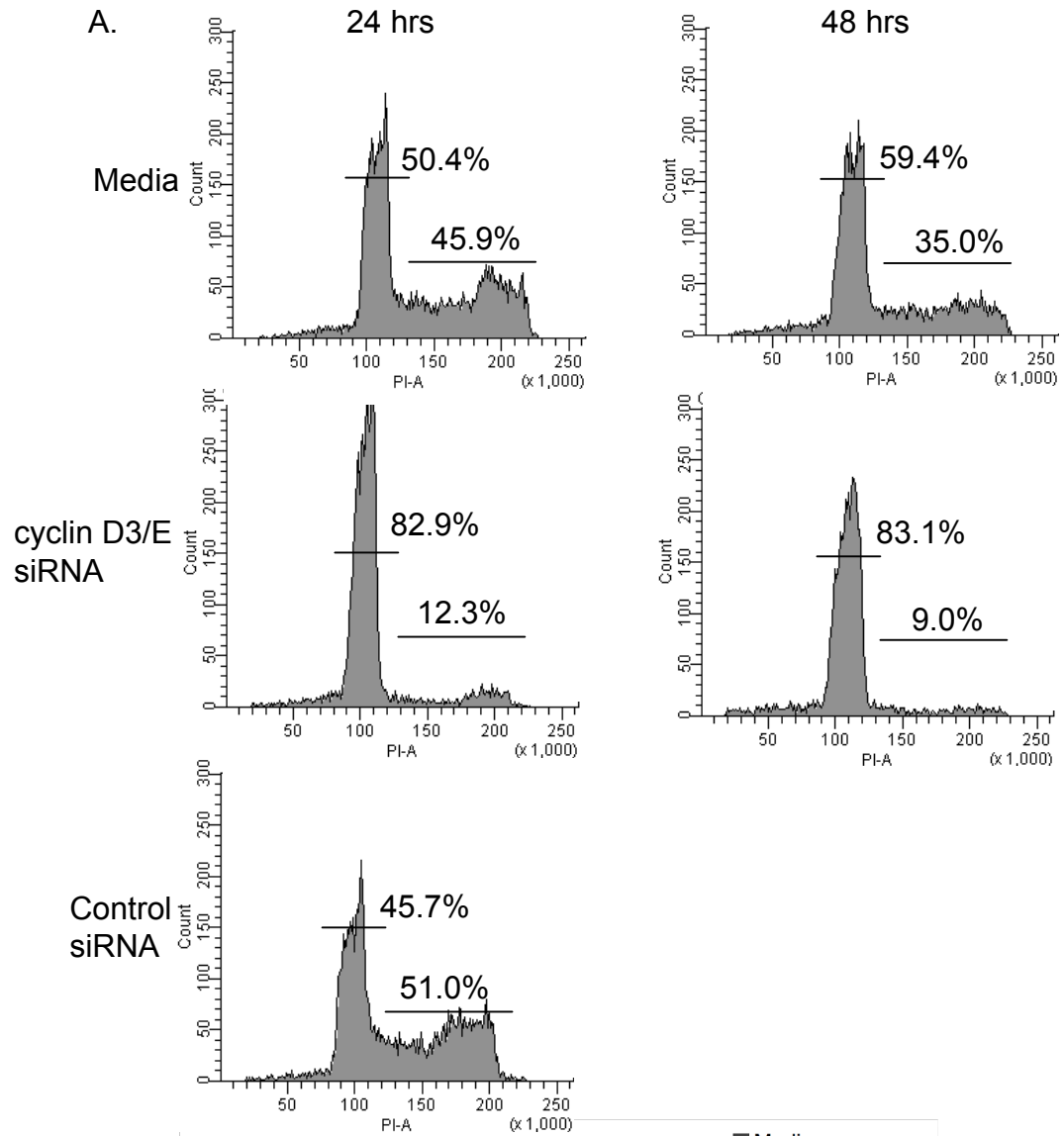


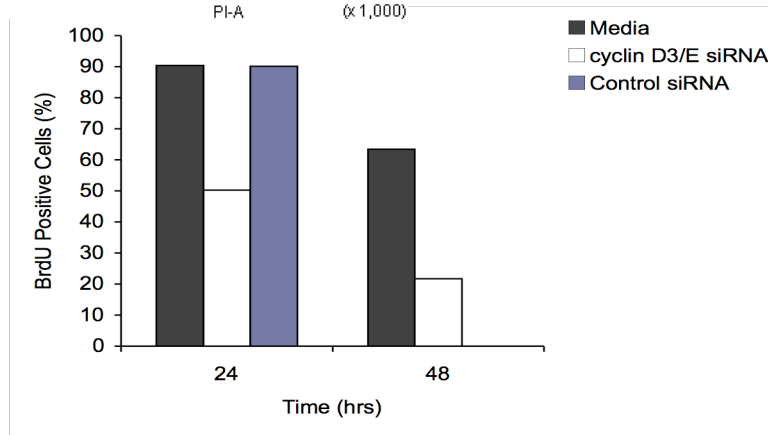
Figure 43. siRNA-mediated knockdown of endogenous cyclin D3 and cyclin E results in an increase in the percentage of LY18 cells in G₁-phase of the cell cycle and inhibits DNA synthesis. LY18 cells were nucleofected in the presence of media alone or 200 pmol of both cyclin D3 and cyclin E siRNA for various lengths of time. LY18 cells were nucleofected with 200 pmol control siRNA for only 24 hrs. *A*, At 24 and 48 hrs, LY18 cells were collected and stained with propidium iodide and cell cycle analyzed by flow cytometry as described in *Materials and Methods*. The data are presented as the number of cells (counts) versus propidium iodide (PI-A), with percentages represented by black bars, indicating LY18 cells in G₁ or S+G₂/M-phase of the cell cycle, respectively. The data are representative of 10,000 cells. *B*, At the indicated times, LY18 cells were collected and DNA synthesis was monitored by BrdU incorporation and analyzed by flow cytometry as described in *Materials and Methods*. The data are representative of 10,000 events.

Figure 43

A.



B.



**Chapter 3: Function and regulation of ATP citrate lyase (ACL)
in B-Lymphocyte growth**

RESULTS

Glucose-derived carbon is incorporated into de novo lipid synthetic pathways prior to the onset of blastogenesis in splenic B cell stimulated through the B cell receptor (BCR)

One of the biosynthetic fates of glucose is the conversion to lipids during *de novo* lipogenesis. Bauer et al. has reported that glucose supports *de novo* lipid synthesis in growing hematopoietic cells in a manner that is regulated by cytokine availability [45]. Lymphocytes undergoing growth and proliferation require a constant supply of lipids to fuel membrane biogenesis and protein modifications that are essential for membrane integrity, permeability, and signal transduction. For our study, we analyzed whether glucose-derived carbons were incorporated into *de novo* lipid synthesis in B cells stimulated through the BCR. To determine if glucose was utilized to synthesize *de novo* lipids in growing cells, B cells cultured with anti-IgM and IL-4 were incubated in the presence of radiolabeled glucose, cellular lipids extracted, and radioactive counts determined. A significant incorporation of glucose into lipids was observed in anti-IgM/IL-4 stimulated B cells (Figure 44A). We then analyzed the content and distribution of neutral lipids by means of high-performance thin-layer chromatography (HPTLC) and quantitatively analyzed radiolabeled lipids using a Bioscan imaging system. When evaluated at 48 hours, cholesterol (C) and phosphatidylcholine (PC) accounted for the bulk of total lipid synthesis, 22.98% and 44.3%, respectively (Figure 44B). Results obtained at 72 hours demonstrated similar levels of cholesterol (C) (14.95%) and

phosphatidylcholine (PC) (46.33%), and an increase in triglycerides (TG) (5.45%-12.94%) (Figure 44B). Other classes of lipids synthesized included: cholesterol esters (CE), triglycerides (TG), ceramide (CM), phosphatidylethanolamine (PE), and at lower levels sphingomyelin (SPM) (Figure 44). Collectively, these results suggest that glucose derived carbon is incorporated into *de novo* lipid synthesis in B cell stimulated through the BCR. Interestingly, the major lipids synthesized were phosphatidylcholine and cholesterol, which make up the major components of biological cell membranes.

ATP citrate lyase (ACL) phosphorylation and ACL enzyme activity is regulated by BCR- and IL-4-stimulated splenic B cells

ACL is a key enzyme linking glucose metabolism to lipid synthesis. As discussed in the *Introduction* section, ACL cleaves citrate to generate cytosolic acetyl CoA, a lipogenic building block [42,43]. Studies have demonstrated that Akt phosphorylates ACL on Ser⁴⁵⁴ and this phosphorylation stimulates the enzymatic activity of ACL [47-49]. To determine if ACL is regulated in response to BCR and IL-4 signaling, phosphorylation on Ser⁴⁵⁴ was monitored. Anti-IgM in addition to IL-4 stimulation led to an increase in phospho-ACL^{Ser454} over the 24 hours observed in comparison to untreated (M) B cells, while ACL levels remained the same (Figure 45A). It is important to note that we observed two bands in the Western blots probed with anti-ACL^{Ser454} Ab and anti-ACL Ab. Currently, we do not know if the second band reflects a non-specific interaction of the Ab with an unrelated protein or phosphorylation of ACL on another phospho-specific site. There has been no further analysis at this time. To test the

regulation of ACL in response to cytokine signaling alone, ACL phosphorylation was determined in IL-4 stimulated B cells. Similar results were observed, in that IL-4-stimulated B cells led to an increase in the phosphorylation of ACL on Ser⁴⁵⁴ beginning at 30 minutes and remained elevated through 24 hours (Figure 46A). In contrast, untreated (M) B cells did not express measurable levels of phospho ACL^{Ser454} (Figure 46A); total ACL expression levels remained constant over 24 hours (Figure 46A). To assess whether BCR- and IL-4-stimulated phosphorylation of ACL on Ser⁴⁵⁴ corresponded to an increase in the ACL enzyme activity we measured enzyme activity by the malate dehydrogenase-coupled assay (see *Materials and Methods* section). ACL enzyme activity is expressed as the oxidation of NADH, to NAD⁺ + H⁺, over time as measured by the change in absorbance (OD₃₄₀/mins). Anti-IgM/IL-4 stimulated B cells resulted in a time dependent increase in ACL enzymatic activity (Figure 45B). Specifically, an 82.6% increase in ACL enzyme activity was observed from 0-48 hours in anti-IgM/IL-4 stimulated splenic B cells (Figure 45B). Similar results were obtained in IL-4 treated B cells in comparison to untreated (0 hrs) cells (Figure 46B). ACL enzyme activity increased by 63.8% in IL-4 stimulated splenic B cells, as measured from 0-30 hours (Figure 46B). Of note, the percentage increase in ACL enzyme activity is more pronounced in anti-IgM/IL-4 stimulated B cells in comparison to IL-4 alone, because of the nature of the stimulation and the time interval observed. Anti-IgM/IL-4 stimulation is a more robust signal, which allows B cells to enter the cell cycle and proliferate. In contrast, IL-4 alone supports B cell growth and survival, but not proliferation. These

results demonstrated that signaling through the BCR and IL-4-stimulated B cells phosphorylates ACL on Ser⁴⁵⁴, thereby increasing ACL enzyme activity over time.

PI-3K activity is required for BCR- and IL-4-induced ACL phosphorylation on Ser⁴⁵⁴ and ACL enzyme activity in splenic B cells

The PI-3K pathway is activated and plays a role in modulating glycolysis in response to BCR cross-linking [24]. We wanted to examine the role of PI-3K activity in the regulation of ACL enzyme activity. To begin, we analyzed *ex vivo* splenic B cells isolated from mice deficient in the p85 α subunit of PI-3K, to evaluate the role of PI-3K on phospho-ACL^{Ser454} and on ACL enzyme activity. Specifically, p85 α is a regulatory subunit of PI-3K, and p85 α -deficient mice display a *Xid*-like immunodeficiency, resulting in a shortened life span of ~3 months [173]. The total number of splenic B cells isolated from p85 α -deficient mice are less than half the number isolated from a wild-type littermate [173]. Germane to our studies, p85 α deficient B cells treated with LPS, anti-IgM, or anti-CD40 display impaired proliferative responses as a direct result of impaired BCR-induced PI-3K activation [173]. Notably, impairment of BCR-induced glycolysis in response to BCR cross-linking was observed in p85 α deficient B cells [24]. B cells isolated from wild-type mice (PI-3K^{+/+}) that were treated with anti-IgM/IL4 display increased levels of phospho-ACL^{Ser454} (Figure 47). In contrast, anti-IgM/IL4-stimulated B cells isolated from p85 α subunit deficient mice (PI-3K^{-/-}) did not express measurable levels of phospho-ACL^{Ser454} (Figure 47). Furthermore, ACL enzymatic activity was decreased by 52% in p85 α deficient mice (KO) and by 51% in p85 α heterozygous mice

(HT) in comparison to wild-type littermate control mice (WT) at 18 hours (Figure 47 B). It is of importance to note that p85 α heterozygous mice (HT) display a ~50% decrease of p85 α subunit expression, in comparison to the KO mice, which display a ~100% decrease of the p85 α subunit [174]. In summary, these results demonstrate that p85 α deficient splenic B cells, stimulated through the BCR in addition to IL-4, cannot phosphorylate ACL on Ser⁴⁵⁴, resulting in a decrease in ACL enzyme activity, in comparison to wild-type control B cells.

As a second, independent means to investigate the significance of the PI-3K pathway in regulating phosphorylation of ACL on Ser⁴⁵⁴ and on ACL enzyme activity, B cells were stimulated with IL-4 in the presence or absence of the PI-3K inhibitors LY294002 (LY) or Wortmannin (WT). Wortmannin is a fungal metabolite obtained from *Penicillium fumiculosum*, which specifically inhibits PI-3K (IC₅₀ of 2-4 nM) through a direct interaction with its catalytic subunit, p110 [174]. LY294002 is also a highly selective inhibitor of PI-3K (IC₅₀ of 1.40 μ M), which inhibits PI-3K competitively with respect to ATP [175]. At 24 hours, treatment with LY, and to a lesser extent WT, reduced phospho-ACL^{Ser454} protein expression levels in comparison to IL-4 treated B cells (Figure 48A). ACL levels remained constant (Figure 48A). Enzymatic activity of ACL measured by the malate dehydrogenase-coupled ACL assay revealed that treatment with LY and WT significantly reduced ACL catalytic activity (Figure 48B). At 15 and 24 hours, IL-4 stimulated B cells that were pretreated with LY displayed a 52.8% and 54.5% decrease in ACL activity, respectively, compared to control (IL4) B cells (Figure 48B). IL-4 stimulated B cells that were pretreated with WT displayed a 29.8% and 29.6%

decrease in ACL activity at 15 and 24 hours, respectively, in comparison to control (IL4) B cells (Figure 48B). Collectively these data suggest that PI-3K activity is required for BCR- and IL-4-induced ACL phosphorylation on Ser⁴⁵⁴ and ACL enzyme activity.

Inhibition of ACL with hydroxycitrate (HC) results in a decrease in BCR-stimulated splenic B-lymphocytes

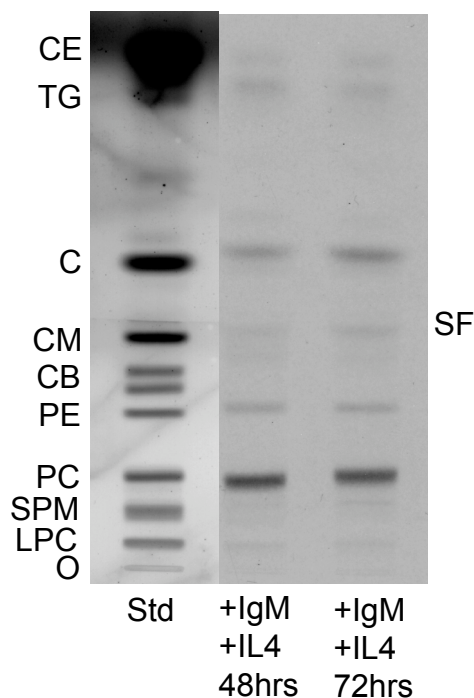
Knockdown of ACL results in a decrease in cytokine stimulated cell growth and proliferation in normal and malignant cells [45,46]. We sought to begin to understand the function of ACL in BCR-induced glucose directed lipogenesis and growth in B cells. First, we inhibited ACL activity with hydroxycitrate (HC), which is the main compound of *Garcinia cambogia* extract [176,177]. HC is a competitive blocker of ACL, therefore a potential inhibitor of lipid biosynthesis [176,177]. We analyzed the affect of HC on cell viability in B cells stimulated through the BCR. In contrast to anti-IgM/IL4 treated B cells, anti-IgM/IL4 incubated cells treated with HC resulted in 15.6% decrease in viable B cells at 40 hours (Figure 49). In summary, these preliminary findings suggest that specific inhibition of ACL affects B cell growth and proliferation.

FIGURES AND LEGENDS

Figure 44. Glucose-derived carbon is incorporated into *de novo* lipid synthetic pathways in splenic B cells stimulated via the BCR. B cells were cultured in 4 ng/ml IL-4 (IL4) and 10 µg/mL anti-mouse IgM (IgM) for 48 and 72 hrs. At several time points the cultures were pulsed for 3 hrs with 4 µCi/ml D-[6-¹⁴C]glucose to monitor glucose-dependent lipid synthesis. *A*, HPTLC of neutral lipids from anti-IgM/IL4 stimulated B cells. Neutral lipids were isolated, purified, and analyzed by high-performance thin-layer chromatography (HPTLC) described in *Materials and Methods*. 4000 dpm of neutral lipids were spotted per lane. The plate was developed to a height of 4.5 cm with chloroform : methanol : acetic acid : formic acid : water (35 : 15 : 6 : 2 : 1 by vol), then developed to the top with hexanes : diisopropyl ether : acetic acid (65 : 35 : 2 by vol). The bands were visualized by charring with 3% cupric acetate in 8% phosphoric acid solution. CE, cholesterol esters; TG, triglycerides; C, cholesterol; CM, ceramide; CB, cerebroside (doublet); PE, phosphatidylethanolamine; PC, phosphatidylcholine; SPM, sphingomyelin; LPC, lysophosphatidylcholine; O, origin; SF, solvent front; Std, neutral lipid standard. The concentration of radiolabeled neutral lipids was determined by scintillation counting. *B*, Neutral lipid distribution in anti-IgM/IL4 stimulated B cells. The percentage distribution of the individual radiolabeled lipid bands were determined by densitometric scanning of HPTLC plates on a Bioscan imaging system as previously described [166]. Values represent percentages of individual lipids.

Figure 44

A.



B.

	IgM+IL-4 48 hours	IgM+IL-4 72 hours
Neutral Lipids^a		
Cholesterol Esters (CE)	10.71	5.71
Triglycerides (TG)	5.45	12.94
Cholesterol (C)	22.98	14.95
Ceramide (CM)	8.88	8.78
Cerebrosides (CB)	ND ^b	ND
Phosphatidylethanolamine (PE)	5.75	8.07
Phosphatidylcholine (PC)	44.3	46.33
Sphingomyelin (SPM)	1.93	3.21
Lysophosphatidylcholine (LPC)	ND	ND

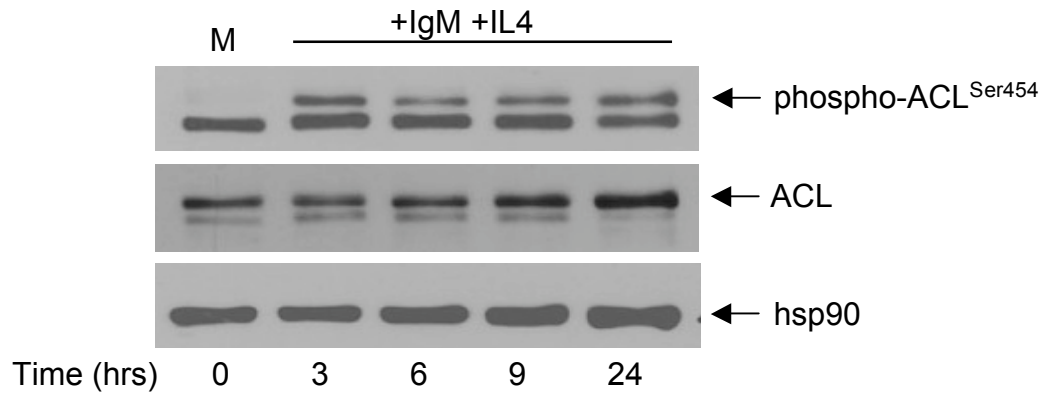
^aValues represent percentages of individual lipids. The percentage distributions for neutral lipids were generated from the densitometric scanning of HPTLC plates.

^bND=not detectable.

Figure 45. Phosphorylation of ATP citrate lyase (ACL) on Ser⁴⁵⁴ and ACL enzyme activity increases in splenic B-lymphocytes stimulated through the BCR. B cells were cultured in the absence (M) or presence of 4 ng/ml IL-4 (IL4) and 10 µg/mL anti-mouse IgM (IgM). *A*, At the indicated times, whole cell extracts were prepared and Western blotting was performed with an anti-phospho-ACL^{Ser454} Ab. The blot was stripped and reprobed with an anti-ACL Ab or an anti-hsp90 Ab to ensure equal loading. *B*, At the indicated times, whole cell extracts were prepared and ACL enzyme activity was measured via the malate dehydrogenase-coupled method as described in *Materials and Methods*. ACL enzyme activity is expressed as the oxidation of NADH over time as measured by the change in absorbance (OD₃₄₀/mins).

Figure 45

A.



B.

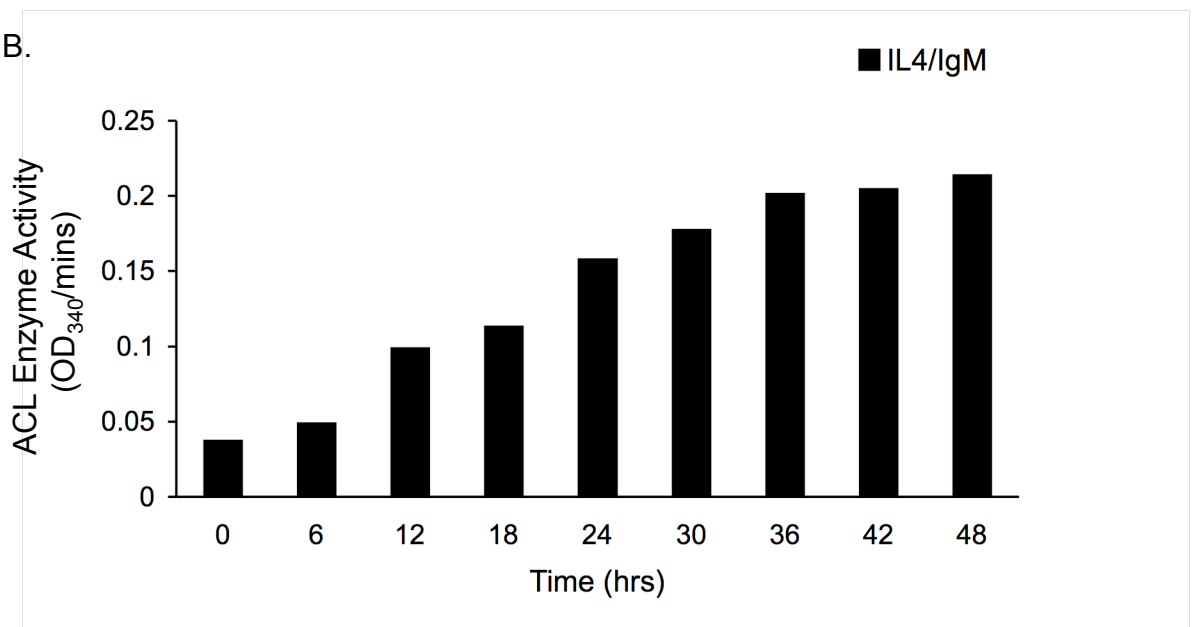
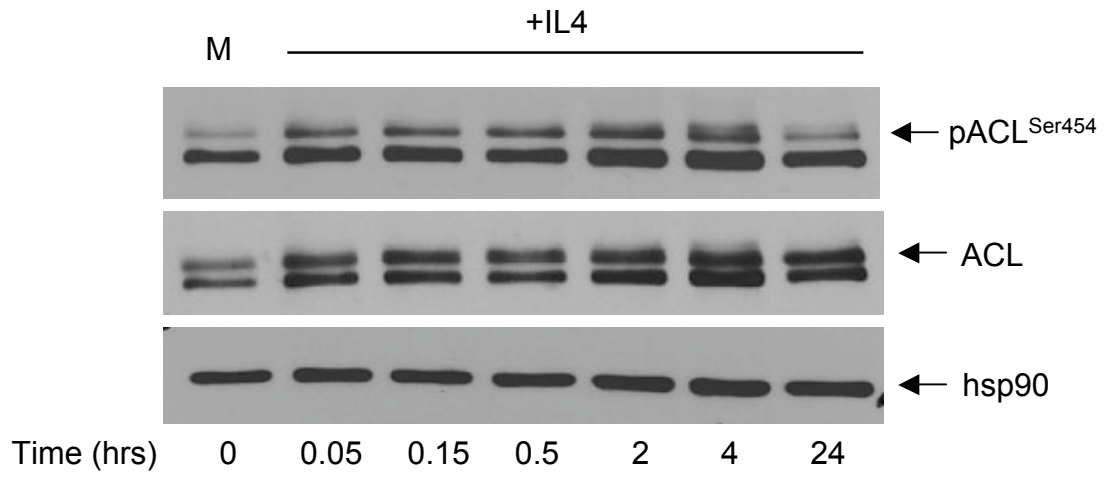


Figure 46. ATP citrate lyase (ACL) phosphorylation on Ser⁴⁵⁴ and ACL enzyme activity increases in IL-4-stimulated splenic B-lymphocytes. B cells were either untreated (M) or cultured in 4 ng/ml IL-4 (IL4). *A*, At the indicated times, whole cell extracts were prepared, and Western blotting was performed with an anti-phospho-ACL^{Ser454} Ab (pACL^{Ser454}). The blot was stripped and reprobed with an anti-ACL Ab or anti-hsp90 Ab to ensure equal loading. *B*, At the indicated time, whole cell extracts were prepared and ACL enzyme activity was measured via the malate dehydrogenase-coupled method as described in *Materials and Methods*. ACL enzyme activity is expressed as the oxidation of NADH over time as measured by the change in absorbance (OD₃₄₀/mins). Results represent mean values of triplicate cultures with lines indicating standard errors of the means. The data are representative of three independent experiments.

Figure 46

A.



B.

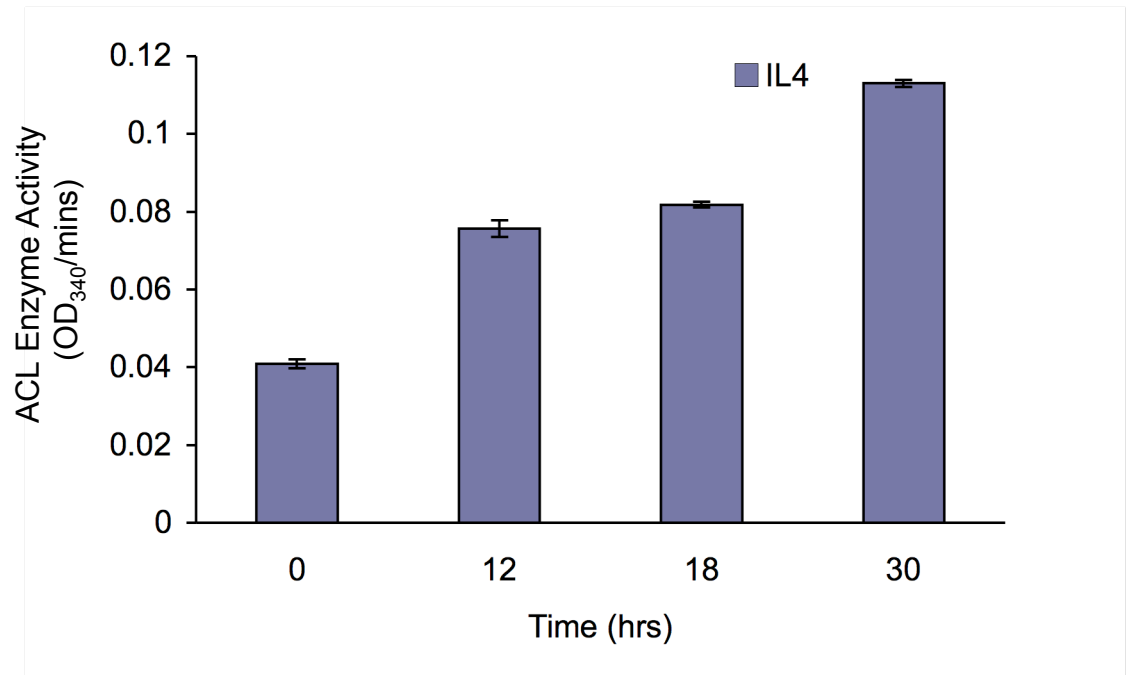
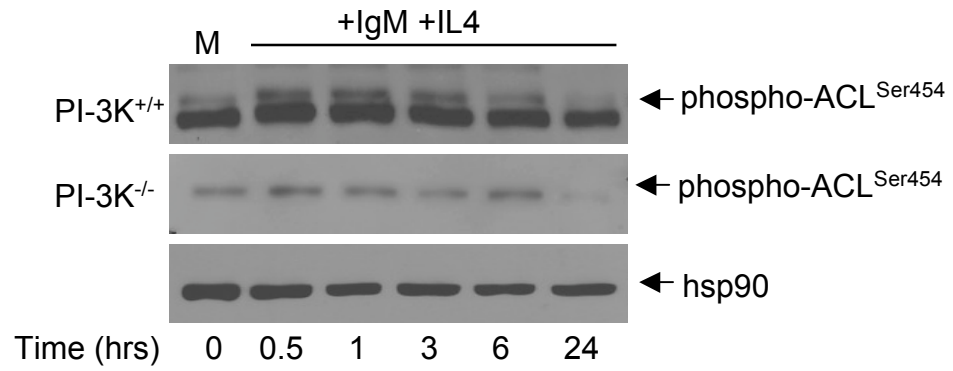


Figure 47. Increased phospho-ATP citrate lyase (ACL)^{Ser454} and ACL enzyme activity in response to BCR cross-linking is impaired in PI-3K-deficient B-lymphocytes. *A*, B-lymphocytes were isolated from PI-3K wild-type mice (PI-3K^{+/+}) and PI-3K-deficient mice (PI-3K^{-/-}) and were either untreated (M) or stimulated with 4 ng/ml IL-4 (IL4) and 10 µg/mL anti-mouse IgM (IgM). At the indicated times, whole cell extracts were prepared and Western blotting was performed with an anti-phospho-ACL^{Ser454} Ab. The blot was stripped and reprobed with an anti-ACL Ab or anti-hsp90 Ab to ensure equal loading. *B*, B cells were isolated from PI-3K wild-type mice (WT), PI-3K heterozygous mice (HT), and PI-3K-deficient mice (KO), and were stimulated with 4 ng/ml IL-4 (IL4) and 10 µg/mL anti-mouse IgM (IgM) for 0 and 18 hrs. At the indicated time, whole cell extracts were prepared and ACL enzyme activity was measured via the malate dehydrogenase-coupled method as described in *Materials and Methods*. ACL enzyme activity is expressed as the oxidation of NADH over time as measured by the change in absorbance (OD₃₄₀/mins).

Figure 47

A.



B.

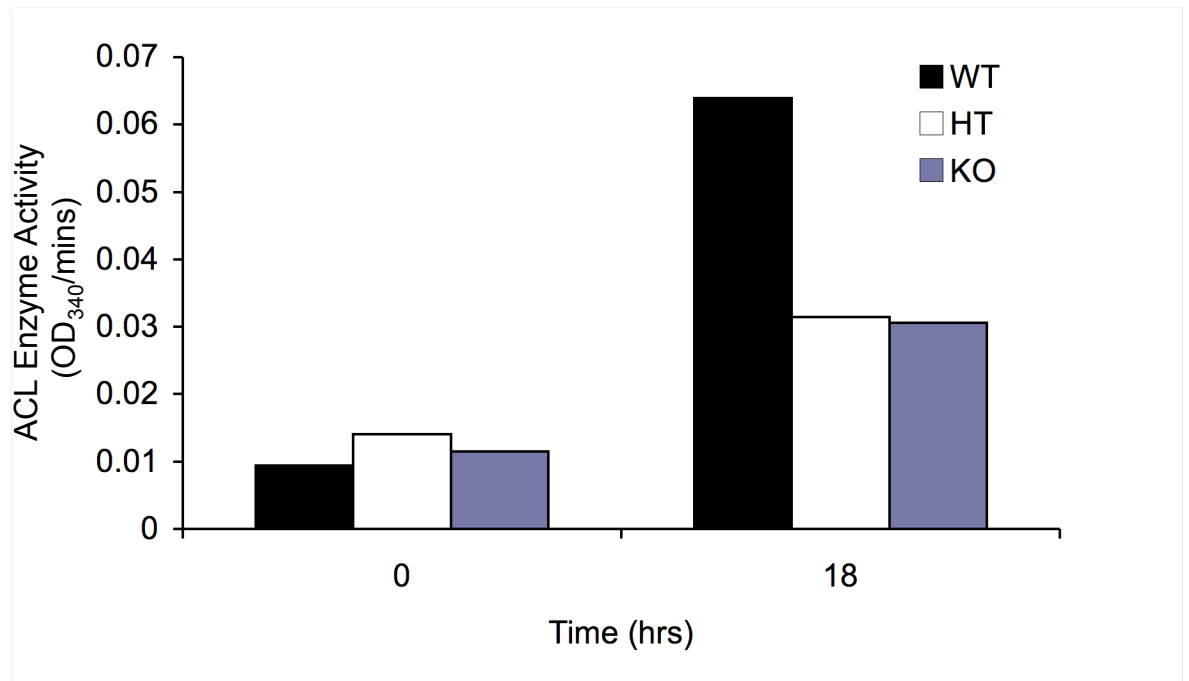


Figure 48. Phosphorylation of ATP citrate lyase (ACL) on Ser⁴⁵⁴ and ACL enzyme activity in IL-4 stimulated B-lymphocytes requires PI-3K activity. B cells were either untreated (IL4, -) or cultured in 4 ng/ml IL-4 (IL4, +) containing a DMSO vehicle for 24 hrs; parallel B cells were pretreated (30 mins) in the absence (-) or presence (+) of 10 μ M LY294002 (LY) or 20 nM Wortmannin (WT) and then stimulated with IL-4. *A*, At the indicated times, whole cell extracts were prepared, and Western blotting was performed with an anti-phospho-ACL^{Ser454} Ab. The blot was stripped and reprobed with an anti-ACL Ab or anti-hsp90 Ab to ensure equal loading. *B*, At the indicated time, whole cell extracts were prepared and ACL enzyme activity was measured via the malate dehydrogenase-coupled method as described in *Materials and Methods*. ACL enzyme activity is expressed as the oxidation of NADH over time as measured by the change in absorbance (OD₃₄₀/mins).

Figure 48

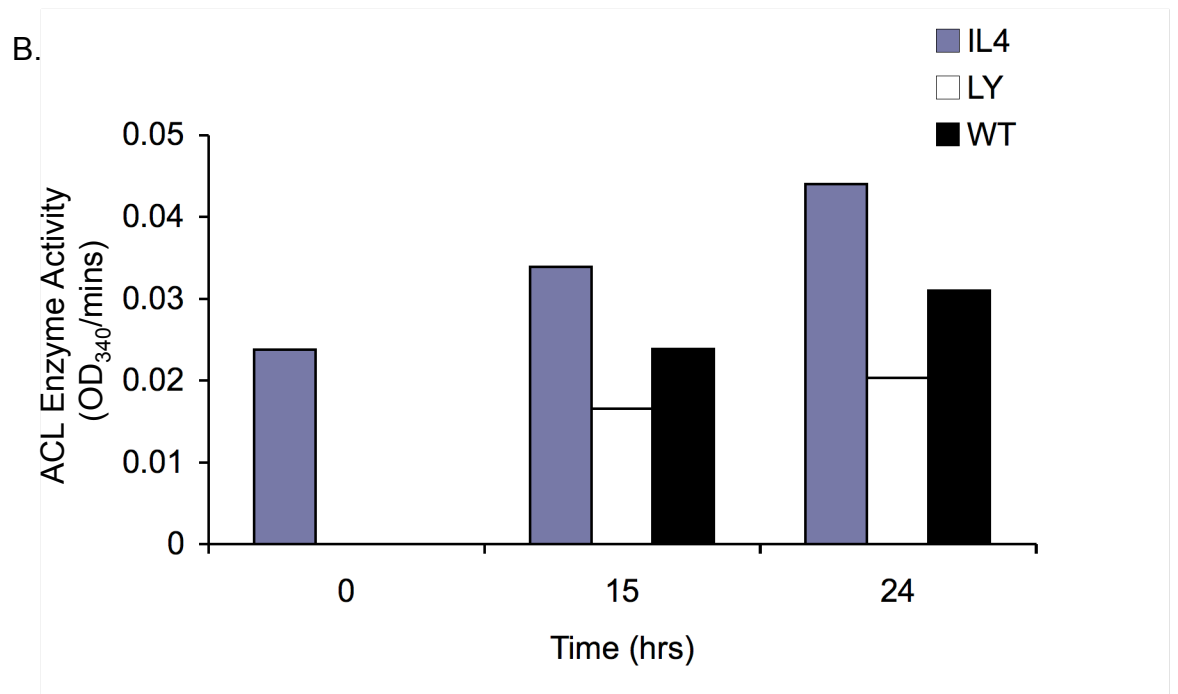
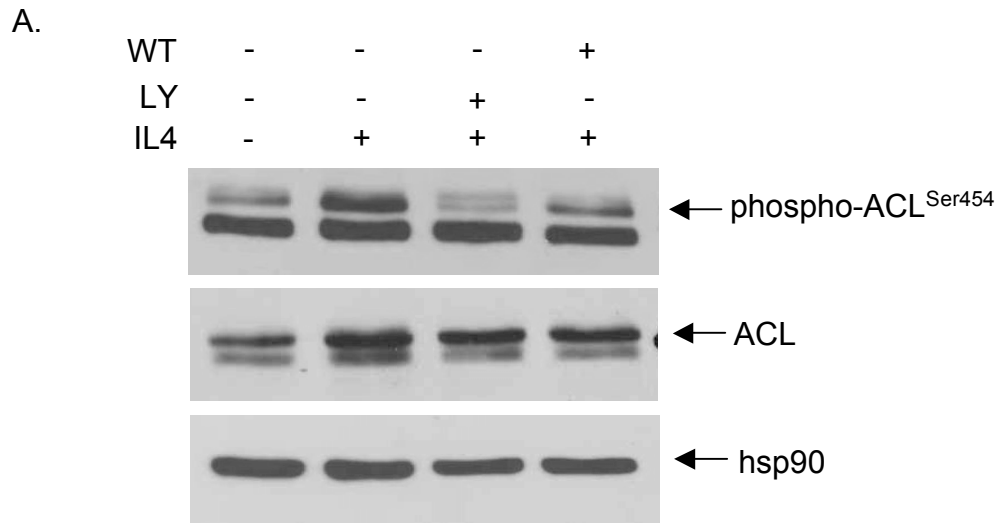
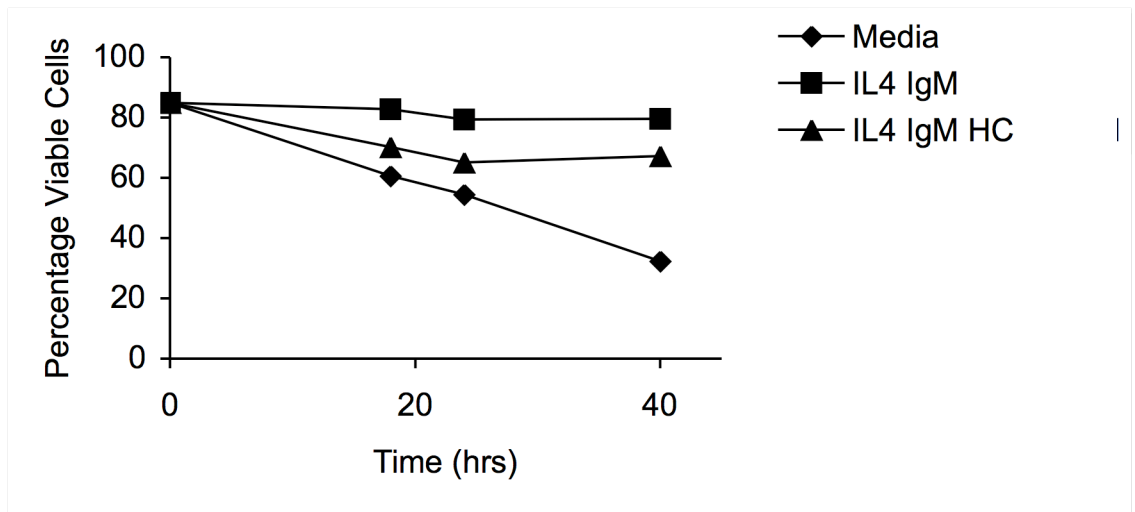


Figure 49. Treatment of splenic B-lymphocytes stimulated via the BCR with hydroxycitrate (HC) causes a decrease in viable cells. B cells were cultured in the absence (Media) or presence of 4 ng/ml IL-4 (IL4) and 10 µg/mL anti-mouse IgM (IgM) for 40 hrs; parallel anti-IgM/IL-4 stimulated B cells were cultured with 100 µM hydroxycitrate (HC). At the indicated times, B cells were collected and cell viability was determined by propidium iodide staining. Samples were analyzed by flow cytometry as described in *Material and Methods*. The data are represented as the percentage of B cells that were negative for propidium iodide staining. The data are representative of 10,000 cells.

Figure 49



DISCUSSION

I. Chapter 1

In summary, the non-overlapping expression between cyclin D2 and cyclin D3 in B-1a cells allowed us to examine the role of cyclin D3 in late G₁-phase. The early and transient up-regulation of cyclin D2 is not enough to drive stimulated B-1a cells into S-phase of the cell cycle. This is supported by our data, which indicated that inhibition of cyclin D3-cdk4/6 complexes with TAT-p16 wild-type peptide blocked normal B-1a cell proliferation in response to PMA, LPS, and CD40L. However, studies in PMA-stimulated B-1a cells deficient in cyclin D3 (cyclin D3-deficient mice) did not demonstrate a decrease in proliferation. Our studies demonstrated that a compensatory increase in cyclin D2 mRNA (data not shown) and continuous expression of functional cyclin D2 protein was able to overcome the cyclin D3 deficiency and drive cells into S-phase. Therefore, dysregulated cyclin D2 expression can compensate in PMA-stimulated B-1a cells deficient in cyclin D3 and drive cell cycle progression. It is important to note that compensation by cyclin D2 in cyclin D3-deficient mice can mask the normal function that cyclin D3 provides in the mitogenesis of B-1a cells.

Previous findings from the Chiles' Lab demonstrate that cyclin D3 is uniquely positioned to progress B-1a cells from G₁-S-phase [65,134]. Specifically, cyclin D2 expression increases rapidly and transiently in PMA-stimulated B-1a cells and forms active complexes with cdk4/6, which accounts for a minor amount of pRb phosphorylation [65]. However, in late G₁-phase, phosphorylation of pRb on cdk4/6

specific sites dramatically increases (during the time when cyclin D2 protein level were not detectable), which corresponded with an increase in cyclin D3 expression levels and active cyclin D3-cdk4/6 complexes [134]. We were able to transduce TAT-p16 peptides into ~100% of primary B-1a cells [124]. This technology is very specific and efficient as it allowed us to avoid any of the associated problems with plasmids, such as artifacts induced by the unregulated expression of recombinant proteins [157]. TAT-p16 peptide (a p16^{INK4a} mimetic) was able to bind cdk4 and cdk6, however the charge-matched mutant control TAT-p16 was not. TAT-p16 wild-type peptide blocked cyclin D3-cdk4/6 assembly and resulted in a loss of PMA-stimulated phospho-pRb on the specific cdk4/6 phosphorylation site. Induction of TAT-p16 peptides into PMA-stimulated B-1a cells produced an inhibition in B-1a cell proliferation, as evidence by reduced PMA-stimulated tritiated thymidine incorporation and reduced percentage of B-1a cells in S+G₂/M-phases of the cell cycle. Comparable results were observed in B-1a cells stimulated with LPS or CD40L.

Mice have been generated that are deficient in individual D-type cyclins. Interestingly, although D-type cyclin expression is widespread, mice with an individual D-type cyclin deficiency display very narrow, tissue specific phenotypes [89]. Specifically, cyclin D1-deficient mice are viable and display neurological abnormalities and cyclin D2-deficient mice are viable and display cerebellar development abnormalities, B-lymphocyte proliferation abnormalities, and pancreatic β -cell proliferation abnormalities [89]. Finally, cyclin D3-deficient mice are viable and display defects in the development of T-Lymphocytes [89]. Mice lacking combinations of the D-

type cyclins have also been generated. Double knockout mice display the sum of the abnormalities observed in the individual deletions and mice deficient in cyclin D1, D2, and D3, die at embryonic day 17.5 [89]. Specifically, mice deficient in all D-type cyclins are lethal because of the failure of HSCs to proliferate, demonstrating that specific lineages of cells (i.e., lymphocytes) critically require D-type cyclins [72]. These observations suggest that in D-type cyclin knockout mice the remaining intact D-cyclins allow for relatively normal development.

An interesting finding from our results is that cyclin D2 induction alone is not sufficient to mediate proliferation induced by PMA, LPS, or CD40L, in B-1a cells where cyclin D3-cdk4/6 complex assembly has been selectively disrupted by TAT-p16 peptide. This might reflect the relatively low pRb kinase activity associated with cyclin D2-cdk4/6 complexes and/or the transient nature of cyclin D2 holoenzyme activation in stimulated B-1a cells [65]. Without further phosphorylation on pRb by cyclin D3-cdk4/6 complexes, the duration of active cyclin D2-cdk4/6 complexes may not be strong enough to drive progression through the R point and into S-phase of the cell cycle. It is important to point out that we do not believe that TAT-p16 was able to block cell cycle progression in B-1a cells because of disruption of cyclin D2 that may be below our level of detection. pRb kinase activity of cyclin D2 is relatively low as compared with cyclin D3. Alternatively, in actively proliferating B-1a cells, cyclin D2 function may not be directly involved in cell proliferation, but rather it may be involved and limited to cell growth (i.e., accumulation of cell mass) and survival, occurring early in G₁-phase of the cell cycle. It is well documented that in rapidly proliferating human germinal center B cells

that cyclin D2 complexes fail to mediate significant pRb phosphorylation, suggesting that cyclin D3, is the key D-type cyclin regulating cell cycle progression [92]. Interestingly, studies performed in pro-B cell lines demonstrate a role of cyclin D2 in survival. Specifically, ectopic expression of cyclin D2 is sufficient to prevent apoptosis induced by cytokine withdrawal [178]. These findings provide further evidence for cell type-specific utilization of D-type cyclins. It is also of importance to note that while studies in cyclin D2-deficient mice has revealed significantly decreased numbers of peritoneal B-1a cells, the molecular mechanism(s) underlying this loss remains to be established [81].

The possibility that cyclin D3 may carry out additional roles in B-1a cells separate from regulating pRb phosphorylation and G₁-S-phase progression, can not be ruled out. Although the D-type cyclins show high amino acid homology within the cdk-binding region (75-78%), the extent of homology outside of that region is 39-47% [77,78]. In addition to their cell cycle role, D-type cyclins have cdk-independent functions that act as either positive or negative regulators of transcription factors, such as STAT3 and cyclin D-interacting myb-like protein-1 [72]. Specifically, the cdk-independent role of cyclin D1 as an inhibitor of STAT3 activation, suggests a novel biological role of cyclin D1 in feedback regulation [179]. Furthermore, cyclin D3 was identified as a negative regulator of the hemopoietic transcription factor acute myeloid leukemia 1 (AML1), presumably by a mechanism that involves displacement of core binding factor β from AML1, thereby inhibiting AML1 DNA binding to target gene promoters [180]. The direct association of AML1 with cyclin D3 functions as a potential feedback mechanism to regulate cell cycle progression [180]. Recent reports by Gu and coworkers [181] have served to extend the

list of cyclin D3 partner proteins beyond transcriptional regulators to include the signal transduction protein kinase ERK3. Extracellular signal-related kinase 3 (ERK3) potentially inhibits cell cycle progression [181]. The functional consequences of the interaction between cyclin D3 and ERK3 need to be further investigated to elucidate the involvement in cell cycle regulation [181]. Nonetheless, our results provide the first direct proof that cyclin D3 assembled complexes with cdk4/6 are required for the G₁-S phase progression in stimulated B-1a cells.

We further analyzed the function of cyclin D3 by isolating and then stimulating B-1a cells from cyclin D3-deficient mice. Homozygous mice containing a mutant allele with a targeted deletion of the first two coding exons of cyclin D3 are viable, but suffer defects in thymocyte development characterized by reduced CD4⁺CD8⁺ double-positive T cells [95]. Cyclin D3-deficient mice display a decrease over wild-type littermates in the total splenocytes produced, specifically, by a decrease in the number of splenic B-2 cells. Further studies need to be performed to investigate these findings. Importantly, a cyclin D3 deficiency did not impact the peritoneal B-1 compartment in comparison to wild-type littermate controls. These results suggest that cyclin D3, but not cyclin D2, is dispensable for B-1 cell development, self-renewal, and function. As mentioned, cyclin D2-deficient mice have a significant decrease in peritoneal CD5⁺ B cells [87]. Thus, cyclin D2 provides a nonredundant function in the development and/or self-renewal of peritoneal B-1a cells.

PMA-stimulated peritoneal B-1a cells isolated from cyclin D3-deficient mice, proliferate at a normal rate in comparison to wild-type B-1a cells. Our results with the

use of TAT-p16 peptides in normal cells B-1a cells indicates that cyclin D3 is significant for mediating proliferation in PMA-, LPS-, and CD40L-stimulated cells. Results in cyclin D3-deficient B-1a cells displayed an increase in *cyclin D2* gene expression 4-fold above the levels found in PMA-stimulated wild-type B-1a cells [124]. Furthermore, the elevated levels of cyclin D2 mRNA [124] is associated with an increased and sustained expression of cyclin D2 protein throughout G₁-S-phase in cyclin D3-deficient B-1a cells. The sustained expression of cyclin D2 contrasts with the early and transient expression of cyclin D2 in wild-type, PMA-stimulated B-1a cells. The possibility that cyclin D2 may functionally replace cyclin D3 is strengthened by the observation that the level of endogenous pRb phosphorylation on cdk 4/6-targeted residues in cyclin D3-deficient B-1a cells is comparable to that of wild-type B-1a cells similarly stimulated with PMA for 21 hours. Additional support for the notion that cyclin D2 may be functioning to compensate for cyclin D3 loss in driving B-1a cell proliferation by PMA was obtained in that DNA synthesis was blocked by transduction of TAT-p16 wild-type, but not TAT-p16 mutant peptides into cyclin D3-deficient B-1a cells. It is important to note, that mice with both cyclin D2 and cyclin D3 genes knocked out are not viable and die by E18.5 [182]. While death is due to severe anemia, other hematopoietic lineages were not evaluated [182]. Although we cannot entirely rule out the possibility of a compensatory role by a cyclin D-independent pathway in PMA-induced B-1a cell proliferation, it is noteworthy that no measurable changes in the timing and level of gene expression for the E-type cyclins were observed between wild-type and cyclin D3-deficient B-1a cells stimulated with PMA [124]. Taken together, we interpret these finding as indicating that

although cyclin D3 normally fulfills a critical role in late G₁-phase, in the absence of cyclin D3, PMA can drive B-1a cell proliferation via sustained expression of cyclin D2. Currently, the molecular mechanisms underlying the sustained expression of cyclin D2 in cyclin D3-deficient mice is unknown.

The compensatory accumulation of cyclin D2 raises the possibility of a negative feedback loop, in which cyclin D3 limits the duration of cyclin D2 accumulation in normal B-1a cells. Genetic ablation of cyclin D3 would then be predicted to relieve this restriction, thereby allowing for sustained accumulation of cyclin D2 throughout the G₀-S interval. It remains unclear whether the apparent compensatory mechanism for cyclin D2 up-regulation identified here is present (but not activated) in wild-type B-1a cells, or only comes into play when cyclin D3 is completely absent.

The finding that sustained accumulation of cyclin D2 is functioning in a compensatory manner, with regard to mediating S-phase entry, represents a unique opportunity to understand the molecular mechanisms that control the accumulation of cyclin D2. Importantly, induction of D-type cyclins by mitogens is controlled, in part, through *de novo* transcription and increased translation, whereas D-type cyclin turnover is controlled by ubiquitin-mediated proteasome degradation [60]. Our knowledge of these events is largely limited to studies performed with cyclin D1. To begin to understand the molecular basis for the sustained accumulation of cyclin D2 in cyclin D3-deficient B-1a cells, we examined the stability (half-life of protein turnover) of endogenous cyclin D2 and cyclin D3 proteins in PMA-stimulated B-1a cells. Our data supports that cyclin D2 and D3 are degraded via ubiquitination and the proteasome

pathway. These preliminary data suggest that cyclin D2 is less stable and has an increased turnover rate in comparison to cyclin D3 in B-1a cells isolated from wild-type mice. Should further analysis support these findings, then experiments will be performed to compare these readouts with data from parallel experiments in cyclin D3-deficient B-1a cells. We hypothesize that cyclin D2 protein will exhibit an increase in stability (i.e., half-life) in cyclin D3-null B-1a cells in comparison to wild-type B-1a cells. To note, should there be no differences in protein stability, we will evaluate the potential differences in *de novo* cyclin D2 transcription rates in both wild-type and cyclin D3-deficient B-1a cells. Should our results support our hypothesis, then we will begin to investigate the pathway(s) involved in the turnover of cyclin D2 and whether or not they are altered in cyclin D3 B-1a cells. For example, we will evaluate the contributions of putative phosphorylation events and ubiquitination of cyclin D2. Additional experiments are underway to further elucidate the molecular basis of sustained cyclin D2 accumulation in cyclin D3-deficient mice.

In summary, our findings report that disruption of cyclin D3 blocks proliferation of normal B-1a cells, but loss of cyclin D3 is compensated by cyclin D2 in cyclin D3-deficient mice. The importance of understanding the molecular mechanisms that regulate entry into S-phase in B-1 cells cannot be overstated as proliferation represents a fundamental determinant in the maintenance of the self-replenishing population of peritoneal B-1 cells in the adult. Moreover, the expansion of auto reactive B-1 cells is associated with malignancy and autoimmune disease, a fact that emphasizes the importance of understanding the biology of R point control in this B cell subset.

II. Chapter 2

Diffuse large B cell lymphoma (DLBCL) is a heterogeneous group of lymphomas characterized by a diffuse pattern of growth. DLBCL's commonly display overexpression of the genes *CDK2* in 12q13.3 and *CDK4* in 12q14.1 along the 12q region [146-149]; however, little is known regarding the function of the G₁-cdk-dependent pathways in DLBCL. Our studies herein demonstrate that human LY18 cells express endogenous cyclin D3 protein with no measurable detection of cyclin D1 or D2 proteins by Western blotting. Furthermore, they express endogenous cdk4, cdk6, and cdk2 proteins. Together, these findings suggest that G₁-phase proteins in LY18 tumor cells form constitutively active cyclin-cdk complexes, which phosphorylate pRb and potentially promote deregulated cell cycle progression. In support of the former, we find that cyclin D3 forms active complexes with cdk4 and cdk6, and that cyclin E forms active complexes with cdk2 (data not shown). This is confirmed by our results that demonstrate that endogenous pRb is constitutively phosphorylated on Ser^{807/811} and Thr⁸²¹, the cdk4/6 and cdk2 target sites, respectively. Importantly, no measurable levels of endogenous cdk-inhibitors (i.e., p16, p21, or p27) were observed.

The majority of tumor cells express two or three D-type cyclins [76]. Interestingly, our studies have revealed that LY18 cells express cyclin D3 as the only detectable D-type cyclin. The selective expression of cyclin D3 provides a unique opportunity to investigate its role in DLBCL cell cycle progression and survival. As opposed to cyclin D1 and cyclin D2, cyclin D3 has not been conclusively shown to promote oncogenesis [76]. For example, the cyclin D1 gene is amplified or rearranged

and the protein is overexpressed in several human cancers (e.g., breast carcinomas, mantle cell lymphomas, and MM) [95,135]. The cyclin D2 gene is amplified in human testicular tumors, while the protein is overexpressed in B cell lymphocytic leukemias, lymphoplasmacytic lymphomas, and chronic lymphocytic leukemias [95]. Extensive studies in lymphocytes have shown that endogenous cyclin D3 expression correlates with proliferation [76,92,94]. LY18 cells are classified as GC-like DLBCL, meaning they exhibit a similar gene and protein expression profile [93] of normal GC B cells, which undergo rapid proliferation and clonal expansion. GC B cells actively repress cyclin D2 and growth, in order to rapidly proliferate, which may be mediated by cyclin D3 [181]. Gene expression profiling of distinct types of DLBCL by Staudt and colleagues, note the expression of *BCL-6*, a well-established germinal center marker, in the GC B-like DLBCL signature [93]. Microarray analysis of B cell lines that express *BCL-6* revealed that *cyclin D2* is repressed by *BCL-6* [183]. Collectively, these data suggest that in GC B cells, *BCL-6* actively represses *cyclin D2*, to promote rapid cell proliferation. Being that LY18 cells are GC-like B cells, it is probable that *cyclin D2* is repressed in these cells by *BCL-6*. The mechanism by which cyclin D3 is constitutively expressed in LY18 cells is currently unknown. Interestingly, it is hypothesized that *BCL6* may indirectly induce *c-myc* expression, which promotes progression through the cell cycle by induction of D-type cyclins [135]. As noted in the *Introduction* section, LY18 cells carry a translocation, which leads to an alteration of *myc-IgH* genes and a high transcription rate of *c-myc* [150]. The role of *c-myc* and cyclin D3 in LY18 cells remains to be characterized.

The unique expression of cyclin D3 complexed with cdk4/6 provided the means to dissect the role of cyclin D3 in G₁-to-S-phase progression in LY18 cells. To summarize the findings herein, inhibition of cyclin D3-cdk4/6 complexes with TAT-p16 wild-type peptide resulted in an increased expression of hypodiploid DNA and LY18 cell apoptosis. In untreated LY18 cells and TAT-p16 mutant peptide treated cells, high expression levels of endogenous phospho-pRb^{Ser807/811} were observed, which was expected in these hyper-proliferative tumor cells. However, LY18 cells treated with TAT-p16 wild-type peptide displayed a decrease in endogenous phosphorylation on pRb^{Ser807/811}, supporting the idea that TAT-p16 is disrupting cyclin D3-cdk4/6 complex formation and activity. Our data reveals that disruption of active cyclin D3-cdk4/6 complexes with TAT-p16 peptides results in an inhibition in LY18 cell proliferation and ultimately apoptosis. The molecular mechanism linking cell cycle arrest and apoptosis are currently unknown in LY18 cells and are under investigation.

The use of cyclin dependent kinase inhibitors has recently received attention, because inhibiting cdk function has been shown to induce cell cycle arrest as well as apoptosis in cancer cell types [151,184,185]. Specifically, the cdk inhibitors flavopiridol, seliciclib, and BMS-387032 (SNS-032) have been extensively tested in clinical trials [96]. Flavopiridol is a pan cdk inhibitor, while seliciclib and BMS-387032 are cdk2 specific inhibitors [96]. Currently these cdk inhibitors are undergoing analysis to determine whether promiscuous cdk inhibitors are preferable to selective cdk inhibition [96]. To corroborate the TAT-p16 study, we investigated the contribution of cdk4 inhibition in LY18 cells. In this study cdk4 was inhibited using the small molecular

weight compound, 2-bromo-12,13-dihydro-5H-indolo[2,3-a]pyrrolo[3,4-c]carbazole-5,7(6H)-dione (denoted as cdk4i), which has previously been shown, *in vitro*, to inhibit cdk4 with an IC_{50} of 0.076 μ M for cdk4, 0.52 μ M for cdk2, and 2.1 μ M for cdk1, as determined by inhibition of Rb phosphorylation [169,170]. Cdk4i is a cell permeable compound that has been previously shown to induce G_1 arrest in human colon carcinoma and non-small-cell lung carcinoma cell lines [169,170]. The use of low-molecular-weight compounds to inhibit protein function has the benefit of being more stable with better bioavailability as compared with other biologic and peptide inhibitors [151].

We show for the first time that 5 μ M cdk4i induces G_1 -phase arrest in LY18 cells. Our results also strike a cautionary note by demonstrating that increased concentrations of cdk4i have different effects on cell cycle progression and viability. At 10 and 25 μ M, we observed a significant decrease in cell viability, whereas there is no measurable effect with 5 μ M cdk4i. Notably, treatment of LY18 cells at 25 μ M results in a G_2 /M-phase block in cell cycle progression followed by apoptosis. We believe these results exemplify the fact that at higher concentrations cdk4i targets cdk2 and cdk1. This is not uncommon; as studies demonstrate that the majority of compounds that inhibit cdk2 also inhibit cdk1, resulting in an observed S- G_2 /M arrest [96]. Specifically, this has been observed and is undergoing analysis in the cdk2-specific inhibitors, seliciclib and BMS-387032. To avoid promiscuous cdk4i activity, we used 5 μ M cdk4i in the remaining experiments to examine the G_1 -phase arrest that was observed in LY18 cells. Finally, in corroboration with the cell cycle studies above, cdk4i inhibited DNA synthesis in LY18

cells. These results suggest that cyclin D3-cdk4/6 activity is critical for proliferation of LY18 cells.

To begin to delineate the molecular mechanism(s) underlying the observed results, we evaluated specific G₁-protein expression profiles in LY18 cells treated with cdk4i. Treatment with cdk4i resulted in a decrease in endogenous cdk4 and cyclin D3 protein levels over the observed length of time, but had no effect on cdk6 levels. The turnover of cyclin D3 is not surprising as cyclin D3-cdk4 complex formation was disrupted and the D-type cyclins are only stable when bound to cdk4/6 (data not shown). However, it cannot be ruled out that cdk6 turnover could take longer than 48 hours in LY18 cells. Our results demonstrated that cyclin D3 forms complexes with cdk6, however the extent of their activity in LY18 cells needs to be further evaluated. Additional data revealed that phosphorylation of cdk2 on Thr¹⁶⁰, a step is necessary to activate cdk2 kinase activity, is decreased in cdk4i treated LY18 cells. Total levels of cdk2 were not affected. These data suggest that following inhibition of cyclin D3-cdk4 complexes, downstream inhibition of cyclin E-cdk2 complexes occurs. Further evidence of functional inhibition of active cyclin D3-cdk4/6 and cyclin E-cdk2 complexes was supported by our findings that cdk4- and cdk2-mediated phosphorylation of pRb on Ser^{807/811} and Thr⁸²¹, respectively, were decreased over time.

As the results demonstrate thus far, the disruption of cyclin D3-cdk4 complexes results in a decrease in pRb phosphorylation at the cdk4/6 specific site. Downstream there is inhibition of cyclin E-cdk2 complex activation as evidence by the decrease in pRb phosphorylation on Thr⁸²¹, the cdk2 target residue. Strikingly, our data revealed that

in LY18 cells treated with cdk4i there was a dramatic increase in endogenous p27 protein expression levels over 48 hours. This would provide the molecular link between cyclin D3-cdk4 complexes and cyclin E-cdk2 complexes. It was hypothesized that the observed expression of p27, in LY18 cells treated with cdk4i, functions to bind and inhibit cyclin E-cdk2 complexes. Germane to these findings, the literature reports that in many cell types (although not universal), cell cycle progression is dependent on the balance of sequestered p27 by cyclin D-cdk complexes and free p27, which is able to bind and inhibit cyclin E-cdk2 complex activity [92,106,135,172]. In lymphoid tissues, the expression of p27 is inversely related to proliferation; strong p27 expression is detected in quiescent cells, whereas p27 is down regulated in proliferating cells (i.e. GC-B cells). Recent studies have also identified p27 expression in malignant lymphomas as having independent prognostic significance, in which low p27 and high cyclin E expression are significantly associated with a poor prognosis [186]. Collectively, these studies demonstrate that p27 has the potential to be a major factor in regulating cell growth arrest in certain cell types [92,106].

To test the hypothesis that upregulation of endogenous p27 regulates cell cycle arrest in cdk4i treated LY18 cells, we transduced TAT-p27 fusion proteins into untreated LY18 (*i.e.*, no cdk4i). Introduction of various concentrations of exogenous TAT-p27 did not have any affect on LY18 cell viability or on cell cycle progression. At this time, p27 does not appear to mediate G₁-phase arrest in LY18 cells. TAT-protein signal technology typically displays rapid and efficient uptake into cells, however, it is important to note that we do not know whether TAT-p27 was efficiently transduced into LY18 cells. Nor

is it known whether transduced TAT-p27 was being degraded or sequestered by the abundant amount of cyclin D3. To circumvent these concerns, we adopted a siRNA-based approach to knockdown endogenous p27 protein levels. LY18 cells pretreated with cdk4i, followed by p27 siRNA did not display a decrease in viability or any changes in cell cycle progression in comparison to LY18 cells treated with cdk4i alone. It is of interest to point out that in numerous experiments we were able to significantly knockdown p27 protein expression with siRNA and there was no observed compensatory increase of p21. As the aforementioned data supports, it is likely that increased expression of p27 plays no role in cdk4i mediated LY18 cell cycle arrest. Germane to the findings, it has been reported that a broad range of p27 expression exists in DLBCL, ranging from absence of protein expression to overexpression with no positive or negative correlation between p27 and proliferation in DLBCL [135,140]. Should additional analysis confirm that p27 does not play a role in the cdk4i-mediated cell cycle arrest observed in LY18 cells, then the promiscuity of cdk4i will be investigated. At this time, we cannot rule out that 5 μ M cdk4i is binding cdk4/6, cdk2, and cdk1. While this may represent a potential caveat to our interpretations, the importance of understanding the role of cyclin-cdk complexes and cell cycle progression in LY18 cells remains significant.

Given that there was no observable phenotype in cdk4i treated LY18 cells, depleted of p27, we decided to analyze the role of cyclin D3 by RNA interference. Surprisingly, our results indicated that specific knockdown of cyclin D3 with cyclin D3 siRNA, had no effect on LY18 cell viability, cell cycle progression, or DNA synthesis.

Importantly, these results are not due to compensation via upregulation of cyclin D1 or D2 as our analysis points out. siRNA-mediated knockdown of cyclin E also displayed no significant effect on LY18 cell viability or cell cycle progression. Interestingly, our data revealed that in cells without cyclin D3 the cdk4/6 specific phosphorylation target residue on pRb is phosphorylated, which suggests that cdk4 and/or cdk6 are enzymatically active in the absence of cyclin D3. Similar results were observed in siRNA-mediated knockdown of cyclin E with regards to phosphorylation on pRb^{Thr821}, the cdk2-specific residue.

Given this data and the propensity for G₁-proteins to functionally overlap it is likely that there is a compensatory mechanism in LY18 cells. Our results suggest that cyclin E can compensate where cyclin D3 is depleted and vice versa. This observation has also been reported in breast cancer cells, where cyclin E can compensate for a cyclin D deficiency [139,187]. A built-in redundancy for critical cell cycle regulators seems to exist in LY18 cells. Depletion of cyclin D3 or cyclin E individually, failed to result in cell cycle arrest, whereas combined, the depletion of cyclin D3 and cyclin E was sufficient to induce G₁-phase arrest, which coincided with a decrease in DNA synthesis. Importantly, we also observed with siRNA-mediated knockdown of both cyclin D3 and cyclin E a decrease in phospho-pRb on Ser^{807/811} and Thr⁸²¹. The question remains, when cyclin D3 is depleted does cdk4 and cdk6 bind cyclin E in early G₁, or are cyclin E-cdk2 complexes enough to drive LY18 cell cycle progression? Also, it cannot be ruled out that cdk4, cdk6, or cdk2 are functioning independently of cyclin activation. In studies performed with mice deficient in D-type cyclins, there was an observed decrease in pRb

phosphorylation on Ser^{807/811}, but there was still phosphorylation on pRb^{Thr821}. These results provide evidence that cyclin E-cdk2 can function independently of cyclin D-cdk4/6 complexes [72]. At this time it is unclear how induction of cyclin E occurs without the initial cyclin D-dependent phosphorylation on pRb to induce cyclin E expression. We observed that the cdk4/6 phospho-specific target sites on pRb were phosphorylated in cyclin D3 depleted LY18 cells. Based on these observations, we speculate that cdk4 and cdk6 form active complexes with cyclin E in early G₁-phase, while active cyclin E-cdk2 complexes function in late G₁-phase. In support of our observations, studies performed in cyclin D1-deficient mice, where cyclin E was knocked-in are phenotypically normal [138]. Cyclin E knock-in rescued all phenotypic manifestations of cyclin D1 deficiency and restored normal development in cyclin D1-dependent tissues [138]. Thus, cyclin E can functionally replace D-type cyclins.

Mice depleted of all D-type cyclins die before E17.5 due to severe anemia, cardiac abnormalities, and severely defective hematopoietic lineages [72]. In a parallel study, mice lacking cdk4 and cdk6 were generated, which displayed similar phenotypes to the D-type cyclin knockouts [188]. Cdk4 and cdk6-deficient mice die between E14.5 and the end of gestating due to severe anemia and hematopoietic abnormalities [188]. The hematopoietic abnormalities were less pronounced in the cdk4- and cdk6-deficient mice due to compensation by cdk2 [188]. These results conclude that mice lacking either the D-type cyclins or their catalytic partners display similar phenotypes. With this in mind, we sought to evaluate cell cycle control in LY18 cells by RNA interference targeted against cdk4, cdk6, and cdk2. Depletion of cdk4, cdk6 or cdk2 individually,

failed to result in cell cycle arrest, whereas different combinations of the three were sufficient to induce G₁-phase arrest and a decrease in DNA synthesis. Specifically, we found that knockdown of cdk4 and cdk6 with siRNA resulted in 75% of cells in G₁-phase, siRNA-mediated knockdown of cdk6 and cdk2 resulted in a 70% G₁-phase arrest, and siRNA-mediated knockdown of cdk4, 6, and 2 combined resulted in an 86.7% G₁-phase arrest. We hypothesize that in cdk4, 6, or 2 deficient LY18 cells, the remaining cdks are able to compensate. In support of our hypothesis, the data demonstrated that phosphorylation of pRb on cdk4/6 and cdk2-specific residues were not disrupted where individual cdks were knocked down. For example, LY18 cells that are proliferating without cdk2 show that cdk4 and/or cdk6 can phosphorylate pRb at the cdk2 specific site. It is only with depletion of cdk4 and cdk6, cdk6 and cdk2, or cdk4, 6, and 2 that we observe a decrease in pRb phosphorylation on Ser^{807/811} and Thr⁸²¹.

In summary, our siRNA data supports that cdk4 and cdk6 can form active complexes with cyclin E and phosphorylate pRb on Thr⁸²¹. Also, that cdk2 can form complexes with cyclin D3, which in turn phosphorylates pRb on Ser^{807/811}. In support of this hypothesis the literature demonstrates that cyclin D3 can form active complexes with cdk2 [189]. Also, it is reported that cdk2 activity can be dispensable for cancer cell proliferation due to high levels of cdk4 activity, which compensates for the loss cdk2 that is typically required during cell cycle progression [140]. Currently, the molecular mechanisms underlying these observed results are unknown and present the need for future studies.

In conclusion, we find that cyclin D3 is dispensable for the growth and survival of LY18 cells, as evidence for redundancy by cyclin E.

III. Chapter 3

Maintaining glucose energy metabolism is essential for B-lymphocyte growth and function. B-lymphocytes rapidly increase glucose uptake and hyper-induce glycolytic flux in response to BCR-crosslinking [24]. The fate of glucose-derived carbon in B cells remains unknown. An advantage of catabolizing glucose through glycolysis at a rate that exceeds bioenergetic demand, instead of undergoing complete oxidation of glucose by the TCA cycle, is that the growing cell can redirect excessive pyruvate toward lipid synthesis. Growing cells must be able to double their macromolecular mass and continuously duplicate phospholipids, sphingolipids, cholesterol, and lipid moieties for protein modifications that are essential for signal transduction and cell membrane integrity. Specifically, the differentiation of activated B cells into plasma cells is characterized, in part, by the expansion of the intracellular membrane network (i.e., the endoplasmic reticulum and the Golgi compartments), where immunoglobulins are synthesized and assembled into functional antibodies [190]. We hypothesize that activated B cells process glucose at such high rates to produce biosynthetic substrates. We found that glucose-derived carbons were incorporated into *de novo* lipid synthetic pathways in B cells stimulated through the BCR. Importantly, at 48 hours, IgM- and IL4-stimulated B cells primarily synthesized phosphatidylcholine and cholesterol. Phosphatidylcholine is a phospholipid that makes up the major component of biological cell membranes, thereby supporting our hypothesis that glucose-derived carbons must be shuttled towards new membrane synthesis to support cell growth and division. Germane to our studies, phosphatidylcholine is also the primary phospholipid of the ER membrane,

leading to increased ER membrane surface area, ER volume, and cell size, in order to support copious amounts of Ig production. Furthermore, a compelling body of evidence supports the importance of cholesterol in maintaining plasma membrane heterogeneity and regulating BCR signaling and B cell fate [50]. Additional studies to elucidate the regulation and expansion of ER membranes and the regulation of plasma membrane cholesterol content in B cell subsets will be performed.

ACL is a key enzyme that links glucose metabolism to lipid synthesis. ACL deficiency in mice results in embryonic lethality, suggesting that other enzymes (i.e., acetyl-CoA synthetase 1) cannot compensate to supply cytosolic acetyl CoA [191,192]. Our results indicate that ACL is regulated by extrinsic signals in B cells. Specifically, our studies reveal that BCR-stimulated B cells activated ACL enzymatic activity through a post-translational phosphorylation on Ser⁴⁵⁴. Phosphorylation of ACL on Ser⁴⁵⁴ was able to abolish the homotropic allosteric regulation by citrate and enhance the catalytic activity of the enzyme [47], thereby allowing ACL activity to be modulated by extrinsic growth factors. Previous findings demonstrate that IL-4 increases glucose transport and glycolysis in B cells [27], whether IL-4 modulates additional metabolic pathway is unknown. Our results herein, demonstrated that IL-4 increased ACL enzyme activity through post-translational phosphorylation on Ser⁴⁵⁴ in B cells. These data suggest that IL-4 cytokines and signaling through the BCR, stimulates survival and proliferation of B cells through the upregulation of ACL activity, in part, to support B cell growth and macromolecule synthesis.

BCR cross-linking triggers activation of PI-3K, which plays an essential role in normal and malignant B cell growth and proliferation [38]. Specifically, PI-3K signaling orchestrates glucose carbon flow by regulating key rate-limiting enzymes that control macromolecular synthetic demands imposed by BCR ligation [24]. Mice deficient in the p85 α subunit of PI-3K were used to assess the contribution of PI-3K on the aforementioned glucose-directed *de novo* lipogenesis in BCR-stimulated B cells. Our results indicated that expression of phospho-ACL^{Ser454} and ACL enzyme activity depends on signaling through the PI-3K pathway, as p85 α -deficient mice display undetectable expression of phospho-ACL^{Ser454} and half the ACL enzymatic activity in comparison to wild-type controls. In addition to the aforementioned results, additional studies revealed that PI-3K plays a role in ACL directed *de novo* lipogenesis in that treatment with LY294002 (LY) and Wortmannin (WT) blocked ACL phosphorylation on Ser⁴⁵⁴ and significantly reduced its enzymatic activity. It should be mentioned that LY is a potent PI-3K inhibitor, but it has also been shown to inhibit other signaling molecules [193]. While this may represent a potential caveat to our interpretations we provide similar results with the PI-3K inhibitor, WT.

Interestingly, a growing body of literature demonstrates that knockdown of ACL results in a decrease in cytokine stimulated cell growth and proliferation in normal and malignant cells [45,46]. In future studies, we plan to inhibit endogenous ACL with specific ACL inhibitors and siRNA to establish the functional requirement of ACL in the regulation of glucose-directed lipogenesis in response to BCR engagement. Preliminary studies with hydroxycitrate (HC), a potent ACL inhibitor, are currently underway.

Specifically, anti-IgM- and IL-4-stimulated B cells treated with HC displayed a time dependent decrease in viable cells. These data suggest that ACL is potentially regulating growth and proliferation. These studies are of interest because of the growing body of literature that demonstrates that ACL inhibition can suppress tumor cell growth in highly glycolytic tumors [46]. Cancer cells displaying high rates of glucose metabolism are more severely affected. Cells with a higher flux of glycolytic carbons from the cytosol to the mitochondrial depend on glucose for lipid synthesis to support cell growth, thereby increasing their sensitivity to ACL targeted inhibition. ACL inhibition provides an advantage over strategies targeting other lipogenic enzymes because ACL is located upstream of other enzymes. In future experiments we plan to elucidate the physiological effects of inhibiting endogenous ACL enzyme activity on B-cell growth responses. Specifically, we will use multiple readouts of growth, including increased cell size, increased *de novo* protein and RNA synthesis, and cell cycle progression. Other potent ACL inhibitors will be analyzed to corroborate the data. Finally, ACL studies are on going in CH12.LX B-cells rendered deficient in ACL. CH12.LX cells represent a model to study IgM synthesis and secretion in response to LPS.

Many transformed cells exhibit high rates of glycolysis and activation of PI-3K/Akt growth factor signaling pathway(s). With the growing body of evidence that supports that PI-3K signaling can positively regulate ACL, ACL is a particularly appealing target for the treatment of malignancy. Future experiments will help to evaluate its role.

REFERENCES

1. Melchers, F. and A. Rolink, Ed. By William E. Paul, Lippincott-Raven Publishers, Philadelphia, PA. 1999. *Fundamental Immunology* 4th Ed, CH. 6 B-Lymphocyte Development and Biology. Pp. 183-217.
2. O’Riordan M., and R. Grosschedl. 2000. Transcriptional regulation of early B-lymphocyte differentiation. *Immunol. Rev.* 175:94-103.
3. Benschop, R. J., and J. C. Cambier. 1999. B cell development: signal transduction by antigen receptors and their surrogates. *Curr. Opin. Immunol.* 11:143-151.
4. de Visser, K.E., A. Eichten, and L.M. Coussens. 2006. Paradoxical roles of the immune system during cancer development. *Nature* 6:24-37.
5. Lawrie, C.H., N.J. Saunders, S. Soneji, S. Palazzo, M.N. Dunlop, C.D.O. Cooper, P.J. Brown, X. Troussard, H. Mossafa, T. Enver, F. Pezzella, J. Boulwood, and J.S. Wainscoat, and C.S.R. Hatton. 2008. MicroRNA expression in lymphocyte development and malignancy. *Leukemia* 22:1440-1446.
6. Parham, P., Ed. By Garland Publishing/Elsevier Science Ltd, New York and London. 2000. *The Immune System*, CH 1 Elements of the Immune System and their Roles in Defense. Pp. 1-31.
7. Huang, X., M.D. DiLiberto, A.F. Cunningham, L. Kang, S. Cheng, S. Ely, H.C. Liou, I.C.M MacLennan, and S. Chen-Kiang. 2004. Homeostatic cell-cycle control by BLys: Induction of cell-cycle entry but not G₁/S transition in opposition to p18^{INK4c} and p27^{Kip1}. *PNAS* 101:17789-17794.
8. Piatelli M.J., D. Tanguay, T.L. Rothstein, and T.C. Chiles. 2003. Cell cycle control mechanisms in B-1 and B-2 lymphoid subsets. *Immunol. Res.* 27:31-51.
9. Campbell, K. S., 1999. Signaling transduction from the B cell antigen-receptor. *Curr. Opin. Immunol.* 11:256-264.
10. Morse, L., D. Chen, D. Franklin, Y. Xiong, and S. Chen-Kiang. 1997. Induction of cell cycle arrest and B cell terminal differentiation by CDK inhibitor p18 (INK4c) and IL-6. *Immunity* 6:47-56.
11. Tourigny, M. R., J. Ursini-Siegel, H. Lee, K. M. Toellner, A. F. Cunningham, D. S. Franklin, S. Ely, M. Chen, X. F. Qin, Y. Xiong, I. C. MacLennan, and S. Chen-

- Kiang. 2002. CDK inhibitor p18 (INK4c) is required for the generation of functional plasma cells. *Immunity* 17:179-189.
12. O'Connor, B. P., M. W. Gleeson, R. J. Noelle, and L. D. Erickson. 2003. The rise and fall of long-lived humoral immunity: terminal differentiation of plasma cells in health and disease. *Immunol. Rev.* 194:61-76.
 13. Buttgereit, F., G.R. Vurmester, and M.D. Brand. 2000. Bioenergetics of immune functions: fundamental and therapeutic aspects. *Immunol. Today* 21:192-199.
 14. Frauwirth, K.A., and C.B. Thompson. 2004. Regulation of T lymphocyte metabolism. *J. Immunol.* 172:4661-4665.
 15. Ciofani, M., and J.C. Zuniga-Pflucker. 2005. Notch promotes survival of pre-T cells at the beta-selection checkpoint by regulating cellular metabolism. *Nat. Immunol.* 6:881-888.
 16. Nitschke, L. 2005. The role of CD22 and other inhibitory co-receptors in B-cell activation. *Curr. Opin. Immunol.* 17:290-297.
 17. Schuhmacher, M., M.S. Staeger, A. Pajic, A. Polack, U.H. Weidle, G.W. Bornkamm, D. Eick, and F. Kohlhuber. 1999. Control of cell growth by c-Myc in the absence of cell division. *Curr. Biol.* 9:1255-1258.
 18. Iritani, B.M., and R.N. Eisenman. 1999. c-Myc enhances protein synthesis and cell size during B lymphocyte development. *Proc. Natl. Acad. Sci. USA* 96:13180-13185.
 19. Zhu, X. R. Hart, M.S. Chang, J.W. Kim, S.Y. Lee, Y.A. Cao, D. Mock, E. Ke, B. Saunders, A. Alexander, J. Grosseohme, K.M. Lin, Z. Yan, R. Hsueh, J. Lee, R.H. Scheuermann, D.A. Fruman, W. Seaman, S. Subramaniam, P. Sternweis, M.I. Simon, and S. Choi. 2004. Analysis of the major patterns of B cell gene expression changes in response to short-term stimulation with 33 single ligands. *J. Immunol.* 173:7141-7149.
 20. Hume, D.A., J.L. Radic, E. Ferber, and M.J. Weidemann, 1978. Aerobic glycolysis and lymphocyte transformation. *Biochem. J.* 174:703-709.
 21. Tollefsbol, T.O., and H.J. Cohen. 1985. Culture kinetics of glycolytic enzyme induction, glucose utilization, and thymidine incorporation of extended-exposure phytohemagglutinin-stimulated human lymphocytes. *J. Cell Physiol.* 133:98-104.
 22. Fox, C.J., P.S. Hammerman, and C.B. Thompson. 2005. Fuel feeds function: energy metabolism and the T-cell response. *Nat. Rev. Immunol.* 5:844-852.

23. Frauwirth, K.A., J.L. Riley, M.H. Harris, R.V. Parry, J.C. Rathmell, D.R. Plas, R.L. Elstrom, C.H. June, C.B. Thompson. 2002. The CD28 signaling pathway regulates glucose metabolism. *Immunity* 16:769-777.
24. Doughty, C.A., B.F. Bleiman, D.J. Wagner, J.M. Mataraza, M.F. Roberts, and T.C. Chiles. 2006. Antigen receptor-mediated changes in glucose metabolism in B-lymphocytes: role of phosphatidylinositol 3-kinase signaling in the glycolytic control of growth. *Blood* 107:4458-4465.
25. Deming, P.B., and J.C. Rathmell. 2006. Mitochondria, cell death, and b cell tolerance. *Curr. Dir, Autoimmun.* 9:95-119.
26. Wofford, J.A., H.L. Weiman, S.R. Jacobs, Y. Zhao, and J.C. Rathmell. 2008. IL-7 promotes Glut1 trafficking and glucose uptake via Stat5-mediated activation of Akt to support T-cell survival. *Blood* 111:2101-2111.
27. Dufort, F.J., B.F. Bleiman, M.R. Gumina, D. Blair, D.J. Wagner, M.F. Roberts, Y. Abu-Amer, T.C. Chiles. 2007. Cutting edge: IL-4 mediated protection of primary B lymphocytes from apoptosis via Stat6-dependent regulation of glycolytic metabolism. *J. Immunol.* 179:4953-4957.
28. Buttgereit, F., M.D. Brand, and M. Muller. 1992. ConA induced changes in energy metabolism of rat thymocytes. *Biosci. Rep.* 12:381-386.
29. Jones, R.G., D.R. Plas, S. Kubek, M. Buzzai, J. Mu, Y. Xu, M.J. Birnbaum, and C.B. Thompson. 2005. AMP-activated protein kinase induces a p53-dependent metabolic checkpoint. *Mol. Cell. Biol.* 18:283-293.
30. Zhao, Y., B.J. Altman, J.L. Coloff, C.E. Herman, S.R. Jacobs, H.L. Wieman, J.A. Wofford, L.N. Dimascio, O. Ilkayeva, A. Kelekar, T. Reya, and J.C. Rathmell. 2007. Glycogen synthase kinase 3alpha and 3beta mediates a glucose-sensitive antiapoptotic signaling pathway to stabilize Mcl-1. *Mol. Cell Biol.* 27:4328-4339.
31. Shalom-Barak, T., and U.G. Knaus. 2002. A p21-activated kinase-controlled metabolic switch up-regulates phagocyte NADPH oxidase. *J. Biol. Chem.* 277:40659-40665.
32. Coelho, W.S. K.C. Costa, and M. Sola-Penna. 2007. Serotonin stimulates mouse skeletal muscle 6-phosphofructo-1-kinase through tyrosine-phosphorylation of the enzyme altering its intracellular localization. *Mol. Genet. Metab.* 92:364-370.
33. Rathmell, J.C., M.G. Vander Heiden, M.H. Harris, K.A. Frauwirth, and C.B. Thompson. 2000. In the absence of extrinsic signals, nutrient utilization by

- lymphocytes is insufficient to maintain either cell size or viability. *Mol. Cell.* 6:683-692.
34. Rathmell, J.C., E.A. Farkash, W. Gao, and C.B. Thompson. 2001. IL-7 enhances the survival and maintains the size of naïve T cells. *J. Immunol.* 167:6869-6876.
 35. Plas, D.R., and C.B. Thompson. 2005. Akt-dependent transformation: there is more to growth than just surviving. *Oncogene* 24:7435-7442.
 36. Burgering, B.M., and P.J. Coffey. 1995. Protein kinase B (c-Akt) in phosphatidylinositol-3-OH kinase signal transduction. *Nature* 376:599-602.
 37. Brazil, D.P, Z.Z. Yang, and B.A. Hemmings. 2004. Advances in protein kinase B signaling: AKTion on multiple fronts. *Trends Biochem. Sci.* 29:233-242.
 38. Donahue, A.C., and D.A. Fruman. 2004. PI3K signaling controls cell fate at many points in B lymphocyte development and activation. *Seminars Cell & Dev. Biol.* 15:183-197.
 39. Grumont, R.J. A. Strasser, and S. Gerondakis. 2002. B cell growth is controlled by phosphatidylinositol 3-kinase-dependent induction of Rel/NF-kappaB regulated c-myc transcription. *Mol. Cell. Biol.* 10:1283-1294.
 40. Bone, H. and N.A. Williams. 2001. Antigen-receptor cross-linking and lipopolysaccharide trigger distinct phosphoinositide 3-kinase-dependent pathways to NF-kappa B activation in primary B cells. *Int. Immunol.* 13:807-816.
 41. Glynn, R., G. Ghandour, D.H. Mack, and C.C. Goodnow. 2000. B-lymphocyte quiescence, tolerance, and activation as viewed by global gene expression profiling on microarrays. *Immunol. Rev.* 176:216-246.
 42. Srere P.A. 1972. The citrate enzymes: their structures, mechanisms, and biological functions. *Curr. Top. Cell. Regul.* 5:229-283.
 43. Sullivan, A.C., J. Triscari, J.G. Hamilton, O.N. Miller, and V.R. Wheatley. 1974. Effect of (-)-hydroxycitrate upon the accumulation of lipid in the rat. I. Lipogenesis. *Lipids* 9:121-128.
 44. Towle, H.C., E.N. Kaytor, and H.M. Shih. 1997. Regulation of the expression of lipogenic enzyme genes by carbohydrates. *Ann. Rev. Nutr.* 17:405-433.
 45. Bauer, D.E., G. Hatzivassiliou, F. Zhao, C. Andreadis, and C.B. Thompson. 2005. ATP citrate lyase is an important component of cell growth and transformation. *Oncogene* 24: 6314-6322.

46. Hatzivassiliou, G., F. Zhao, D.E. Bauer, C. Andreadis, A.N. Shaw, D. Dhanak, S.R. Hingorani, D.A. Tuveson, and C.B. Thompson. 2005. ATP citrate lyase inhibition can suppress tumor cell growth. *Cancer Cell* 8:311-321.
47. Potapova, I.A., M.R. El-Maghrabi, S.V. Doronin, and W.B. Benjamin. 2000. Phosphorylation of recombinant human ATP citrate lyase by cAMP-dependent protein kinase abolishes homotropic allosteric regulation of the enzyme by citrate and increases the enzyme activity. Allosteric activation of ATP: citrate lyase by phosphorylated sugars. *Biochemistry* 39:1169-1179.
48. Pierce, M.W., J.L. Palmer, H.T. Keutmann, T.A. Hall, and J. Avruch. 1981. The insulin-directed phosphorylation site on ATP-citrate lyase is identical with the site phosphorylated by the cAMP-dependent protein kinase in vitro. *J. Biol. Chem.* 18:10681-10686.
49. Berwich, D.C., I. Hers, K.J. Heesom, S.K. Moule, J.M. Tavaré. 2002. The identification of ATP-citrate lyase as a protein kinase B (Akt) substrate in primary adipocytes. *J. Biol. Chem.* 277:33895-33900.
50. Gupta, N., and A.L. DeFranco. 2007. Lipid rafts and B cell signaling. *Semin. Cell Dev. Biol.* 18:616-626.
51. Swinnen, J.V., K. Brusselmans, and G. Verhoeven. 2008. Increased lipogenesis in cancer cells: new players, novel targets. *Curr. Opin. Clin. Nutr. Metab. Care* 9:358-365.
52. Pardee, A.B., 1989. G1 events and regulation of cell proliferation. *Science* 246:603-608.
53. Sherr, C.J., and J.M. Roberts. 1999. CDK inhibitors: positive and negative regulators of G₁-phase progression. *Genes Dev.* 13:1501-1512.
54. Weinberg, R.A.. 1995. The retinoblastoma protein and cell cycle control. *Cell* 81:323-330.
55. Alan, H., and S.F. Dowdy. 2002. Regulation of G₁-cell cycle progression by oncogenes and tumor suppressor genes. *Curr. Opin. Gen. Dev.* 12:47-52.
56. Hannon, G. J. and D. Beach. 1994. p15^{INK4B} is a potential effector of TGF-beta-induced cell cycle arrest. *Nature* 371:257-261.
57. Ho, A., and S.F. Dowdy. 2002. Regulation of G₁ cell-cycle progression by oncogenes and tumor suppressor genes. *Curr. Opin. Genet. Dev.* 12:47-52.

58. Moroy, T., and C. Geisen. 2004. Cyclin E. *The International Journal of Biochemistry and Cell Biology* 36:1424-1439.
59. Cheng, M., V. Sexl, C.J. Sherr, and M.F. Roussel. 1998. Assembly of cyclin D-dependent kinase and titration of p27^{Kip1} regulated by mitogen-activated protein kinase kinase (MEK1). *Proc. Natl. Acad. Sci.* 95:1091-1096.
60. Diehl, J.A., M. Cheng, M.F. Roussel, and C.J. Sherr. 1998. Glycogen synthase kinase-3beta regulates cyclin D1 proteolysis and subcellular localization. *Genes Dev.* 12:3499-3511.
61. Morgan, D.O. 1997. Cyclin-dependent kinases: engines, clocks, and microprocessors. *Annu. Rev. Cell Dev. Biol.* 13:261-291.
62. Kato, J.Y., M. Matsuoka, D.K. Strom, and C.J. Sherr. 1994. Regulation of cyclin D-dependent kinase 4 (cdk4) by cdk4-activating kinase. *Mol. Cell Biol.* 14:2713-2721.
63. Tassan, J.P, S.J. Schultz, J. Bartek, and E.A. Nigg. 1994. Cell cycle analysis of the activity of subcellular localization, and subunit composition of human CAK (CDK activating kinase). *J. Cell Biol.* 127:467-478.
64. Bartkova, J., M. Zemanova, and J. Bartek. 1996. Expression of CDK7/CAK in normal and tumor cells of diverse histogenesis, cell-cycle positions and differentiation. *Int. J. Cancer* 66:732-737.
65. Tanguay, D., S. Pavlovic, M.J. Piatelli, J. Bartek, and T.C. Chiles. 1999. B cell antigen receptor-mediated activation of cyclin-dependent retinoblastoma protein kinases and inhibition by co-cross-linking with Fc gamma receptors. *J. Immunol.* 163:3160-3168.
66. Quelle, D.E., R.A. Ashmun, S.A. Shurtleff, J.Y. Kato, D. Bar-Sagi, M.F. Roussel, and C.J. Sherr. 1993. Overexpression of mouse D-type cyclins accelerates G1 phase in rodent fibroblasts. *Genes Dev.* 7:1559-1571.
67. Obaya, A.J., and J.M. Sedivy. 2002. Regulation of cyclin-Cdk activity in mammalian cells. *Cell Mol. Life Sci.* 59:126-142.
68. Honda, R., Y. Ohba, A. Nagata, H. Okayama, and H. Yasuda. 1993. Dephosphorylation of human p34cdc2 kinase on both Thr-14 and Tyr-15 by human cdc25B phosphatase. *FEBS Lett.* 318:331-334.

69. Sebastian, B., A. Kakizuka, and T. Hunter. 1993. Cdc25M2 activation of cyclin-dependent kinases by dephosphorylation of threonine-14 and tyrosine-15. *Proc. Natl. Acad. Sci. USA* 90:3521-3524.
70. Nilsson, I., and I. Hoffmann. 2000. Cell cycle regulation by the Cdc25 phosphatases family. *Prog. Cell Cycle Res.* 4:107-114.
71. Evans, T., E.T. Rosenthal, J. Youngblom, D. Distel, and T. Hunt. 1983. Cyclin: A protein specified by maternal mRNA in sea urchin eggs that is destroyed at each cleavage division. *Cell* 33:389-396.
72. Kozar, K., and P. Sicinski. 2005. Cell cycle progression without cyclin D-cdk4 and cyclin D-cdk6 complexes. *Cell Cycle* 4:388-391.
73. Ho, A., and S.F. Dowdy. 2002. Regulation of G(1) cell-cycle progression by oncogenes and tumor suppressor genes. *Curr. Opin. Genet. Dev.* 12:47-52.
74. Ekholm, S.V., and S.I. Reed. 2000. Regulation of G1 cyclin-dependent kinases in the mammalian cell cycle. *Curr. Opin. Cell Biol.* 12:676-684.
75. Sherr, C.J. 1996. Cancer cell cycles. *Science* 274:1672-1677.
76. Bartkova, J., J. Lukas, M. Strauss, and J. Bartek. 1998. Cyclin D3: requirement for G1/S transition and high abundance in quiescent tissues suggest a dual role in proliferation and differentiation. *Oncogene* 17:1027-1037.
77. Inaba, T., H. Matsushime, M. Valentine, M.F. Roussel, C.J. Sherr, and A.T. Look. 1992. Genomic organization, chromosomal localization, and independent expression of human cyclin D genes. *Genomics* 13:565-574.
78. Xiong, Y., J. Menninger, D. Beach, and D.C. Ward. 1992. Molecular cloning and chromosomal mapping of CCND genes encoding human D-type cyclins. *Genomics* 13:575-584.
79. Baker, G.L., M.W. Landis, P.W. Hinds. 2005. Multiple functions of D-type cyclins can antagonize pRb-mediated suppression of proliferation. *Cell Cycle* 4: 330-338.
80. Tanguay, D.A. and T.C. Chiles. 1996. Regulation of the catalytic subunit (p34^{PSK}-J3/cdk4) for the major D- type cyclin in mature B-lymphocytes. *J. Immuno.* 156:539.

81. Solvason, N., W. Wu, N. Kabra, X. Wu, E. Lees, and M. Howard. 1996. Induction of cell cycle regulatory proteins in anti-immunoglobulin-stimulated mature B-lymphocytes. *J. Exp. Med.* 184:407.
82. Reid, S., and E.C. Snow. 1996. The regulated expression of cell cycle-related proteins as B-lymphocytes enter and progress through the G1 cell cycle stage following delivery of complete versus partial activation stimuli. *Mol. Immunol.* 33:1139-1151.
83. Piatelli, M.J., C. Wardle, J. Blois, C. Doughty, B.R. Schram, T.L. Rothstein, and T.C. Chiles. 2004. Phosphatidylinositol 3-kinase-dependent mitogen-activated protein/extracellular signal-regulated kinase 1/2 and NF- κ B signaling pathways are required for B cell antigen receptor-mediated cyclin D3 induction in mature B cells. *J. Immunol.* 172:2753-2762.
84. Glassford, J. I. Soeiro, S.M. Skarell, L. Banerji, M. Holman, G.G.B. Klaus, T. Kasowaki, S. Koyasu, and E.W.F. Lam. 2003. BCR targets cyclin D2 via Btk and the p85 α subunit of PI-3K to induce cell cycle progression in primary mouse B cells. *Oncogene* 22:2248-2259.
85. Wang, Z., P. Sicinski, R.A. Weinberg, Y. Zhang, and K. Ravid. 1996. Characterization of the mouse cyclin D3 gene: exon/intron organization and promoter activity. *Genomics* 35:156-163.
86. Hsia, C.Y., S. Cheng, A.M. Owyang, S.F. Dowdy, and H.C. Liou. 2002. c-rel regulation of the cell cycle in primary mouse B-lymphocytes. *Int. Immunol.* 14:905-916.
87. Lam, E.W.F., J. Glassford, L. Banerji, N.S.B. Thomas, P. Sicinski, and G.G.B. Klaus. 2000. Cyclin D3 compensates for loss of cyclin D2 in mouse B-lymphocytes activated via the antigen receptor and CD40. *J. Biol. Chem.* 275:3479-3484.
88. Santamaria, D., and S. Ortega. 2006. Cyclins and CDKS in development and cancer; lessons from genetically modified mice. *Frontiers in Bioscience* 11:1164-1188.
89. Ciemerych, M.A., and P. Sicinski. 2005. Cell cycle in mouse development. *Oncogene* 24:2877-2898.
90. Solvason, N., W.W. Wu., D. Parry, D. Mahony, E.W.F. Lam, J. Glassford, G.G.B. Klaus, P. Sicinski, R. Weinberg, Y.J. Liu, M. Howard, and E. Lee. 1999. Cyclin D2 is essential for BCR-mediated proliferation and CD5 B cell development. *International Immunology* 12:631-638.

91. Sanchez-Beato, M., F. I. Camacho, J.C. Martinez-Montero, A.I. Saez, R. Villuendas, L. Sanchez-Verde, J.F. Garcia, and M.A. Piris. 1999. Anomalous high p27/KIP1 expression in a subset of aggressive B-cell lymphomas is associated with cyclin D3 overexpression, p27/KIP1-cyclin D3 colocalization in tumor cells. *Blood* 94:765-772.
92. Wagner, E.F, M. Hleb, N. Hanna, and S. Sharma. 1998. A pivotal role of cyclin D3 and cyclin-dependent kinase inhibitor p27 in the regulation of IL-2-, IL-4-, or IL-10-mediated human B cell proliferation. *J. Immunol.* 161:1123-1131.
93. Alizadeh, A.A., M.B. Eisen, R.E. Davis, C. Ma, I.S. Lossos, A. Rosenwalkd, J.C. Boldrick, H. Sabet, T. Tran, X. Yu, J. I. Powell, L. Yang, G.E. Marti, T. Moore, J. Hudson, L. Lu, D.B. Lewis, R. Tibshirani, G. Sherlock, W.C. Chan, T.C. Greiner, D.D. Weisenburger, J.O. Armitage, R. Warnke, R. Levy, W. Wilson, M.R. Grever, J.C. Byrd, D. Botstein, P.O. Brown, and L.M. Staudt. 2000. Distinct types of diffuse large B-cell lymphoma identified by gene expression profiling. *Nature* 403:503-511.
94. Moller, M.B., P.W. Kania, Y. Ino, A.M. Gerdes, O. Nielsen, D.N. Louis, K. Skjodt, and N.T. Pedersen. 2000. Frequent disruption of the RB1 pathway in diffuse large B cell lymphoma: prognostic significance of E2F-1 and p16^{INK4a}. *Leukemia* 14:898-904.
95. Sicinska, E., I. Aifantis, L.L. Cam, W. Swat, C. Borowski, Q. Yu, A.A. Ferrando, S.D. Levin, Y. Geng, H. von Boehmer, and P. Sicinski. 2003. Requirement for cyclin D3 in lymphocyte development and T cell leukemia's. *Cancer Cell* 4:451-461.
96. Shapiro, G.I. 2006. Cyclin-dependent kinase pathways as targets for cancer treatment. *J. of Clin. Onco.* 24:1770-1783.
97. Ortega, S., M. Malumbres, and M. Barbacid. 2002. Cyclin D-dependent kinases, INK4a inhibitors and cancer. *Biochimica et Biophysica* 1602:73-87.
98. Drexler, H.G. 1998. Review of alterations of the cyclin-dependent kinase inhibitor INK4 family genes p15, p16, p18, and p19 in human leukemia-lymphoma cells. *Leukemia* 12:845-859.
99. Wolfel, T., M. Hauer, J. Schneider, M. Serrano, C. Wolfel, E. Klehmann-Hieb, E. De Plaen, T. Hankeln, K.H. Meyer zum Buschenfelde, and D. Beach. 1995. A p16^{INK4a}-insensitive CDK4 mutant targeted by cytolytic T lymphocytes in a human melanoma. *Science* 269:1281-1284.

100. Reymond, A., and R. Brent. 1995. P16 proteins from melanoma-prone families are deficient in binding to Cdk4. *Oncogene* 11:1173-1178.
101. Fahraeus, R., S. Lain, K.L. Ball, and D.P. Lane. 1998. Characterization of the cyclin-dependent kinase inhibitory domain of the INK4 family as a model for a synthetic tumour suppressor molecule. *Oncogene* 16:587-596.
102. Chen-Kiang, S. 2003. Cell-cycle control of plasma cell differentiation and tumorigenesis. *Immunol. Rev.* 194:39.
103. Besson, A., S.F. Dowdy, and J.M. Roberts. 2008. CDK inhibitors: Cell cycle regulators and beyond. *Dev. Cell* 14:159-169.
104. Cheng, M., P. Olivier, J.A. Diehl, M. Fero, M.F. Roussel, J.M. Roberts, and C.J. Sherr. 1999. The p21(Cip1) and p27(Kip1) CDK 'inhibitors' are essential activators of cyclin D-dependent kinases in murine fibroblasts. *EMBO J.* 18:1571-1583.
105. Sherr, C.J., and J.M. Roberts. 1995. Inhibitors of mammalian G1 cyclin-dependent kinases. *Genes Dev.* 9:1149-1163.
106. Wu, M., R.E. Bellas, J. Shen, W. Yang, and G.E. Sonenshein. 1999. Increased p27^{Kip1} cyclin-dependent kinase inhibitor gene expression following anti-IgM treatment promotes apoptosis of WEHI 231 cells. *J. Immunol.* 163:6530-6535.
107. Chu, I.M., L. Hengst, and J.M. Slinderland. 2008. The cdk inhibitor p27 in human cancer: prognostic potential and relevance to anticancer therapy. *Nature Reviews Cancer* 8:253-267.
108. Tumang, J.R., W.D. Hastings, C. Bai, and T.L. Rothstein. 2004. Peritoneal and splenic B-1a cells are separable by phenotypic, functional, and transcriptomic characteristics. *Eur. J. Immunol.* 34:2158-2167.
109. Kantor, A.B., and L.A. Herzenberg. 1993. Origin of murine B cell lineages. *Annu. Rev. Immunol.* 11:501-538.
110. Hardy, R.R., and K. Hayakawa. 2001. B cell development pathways. *Annu. Rev. Immunol.* 19:595-621.
111. Herzenberg, L.A. 2000. B-1 cells: the lineage question revisited. *Immunol. Rev.* 175:9-22.
112. Wortis, H.H., and R. Berland. 2001. Cutting edge commentary: origins of B-1 cells. *J. Immunol.* 166:2163-2166.

113. Rothstein, T.L. 2002. Cutting edge commentary: two B-1 or not to be one. *J. Immunol.* 168:4257-4261.
114. Kantor, A.B., and L.A Herzenberg. 1993. Origin of murine B cell lineages. *Annu. Rev. Immunol.* 11:501-538.
115. Kroese, F.G., W.A. Ammerlaan, and A.B. Kantor. 1993. Evidence that intestinal IgA plasma cells in mu, kappa transgenic mice are derived from B-1 (Ly-1 B) cells. *Int. Immunol.* 5:1317-1327.
116. Kroese, F.G., E.C. Butcher, A.M. Stall, P.A. Lalor, S. Adams, and L.A. Herzenberg. 1989. Many of the IgA producing plasma cells in murine gut are derived from self-replenishing precursors in the peritoneal cavity. *Int. Immunol.* 1:75-84.
117. Pennell, C.A., L.W. Arnold, G. Haughton, and S.H. Clarke. 1988. Restricted Ig variable region gene expression among Ly-1+ cell lymphomas. *J. Immunol.* 141:2788-2796.
118. Forster, I., H. Gu, and K. Rajewsky. 1988. Germline antibody V regions as determinants of clonal persistence and malignant growth in the B cell compartment. *Embo. J.* 7:3693-3703.
119. Feeney, A.J., 1990. Lack of N regions in fetal and neonatal mouse immunoglobulin V-D-J junctional sequences. *J. Exp. Med.* 172:1377-1390.
120. Gu, H., I. Forster, and K. Rajewsky. 1990. Sequence homologies, N sequence insertion and JH gene utilization in VHDJH joining: implications for the joining mechanism and the ontogenetic timing of LY1 B cell and b-CLL progenitor generation. *Embo. J.* 9:2133-2140.
121. Klinman, D.M., and K.L. Holmes. 1990. Differences in the repertoire expressed by peritoneal and splenic Ly-1 (CD5)+ B cells. *J. Immunol.* 144:4520-4525.
122. Masmoudi, H., T. Mota-Santos, F. Huetz, A. Coutinho, and P.A. Cavenave. 1990. All T15 Id-positive antibodies (but not the majority of VHT15+ antibodies) are produced by peritoneal CD5+ B lymphocytes. *Int. Immunol.* 2:515-520.
123. Su, S.D., M.M. Ward, M.A. Apicella, and R.E. Ward. 1991. The primary B cell response to the O/core region of bacterial lipopolysaccharide is restricted to the Ly-1 lineage. *J. Immunol.* 146:327-331.

124. Mataraza, J.M., J.R. Tumang, M.R. Gumina, S.M. Gurdak, T.L. Rothstein, and T.C. Chiles. 2006. Disruption of cyclin D3 blocks proliferation of normal B-1a cells, but loss of cyclin D3 is compensated by cyclin D2 in cyclin D3-deficient Mice. *J. Immunol.* 177:787-795.
125. Sidman, C.L., L.D. Shultz, R.R. Hardy, K. Hayakawa, and L.A. Herzenberg. 1986. Production of immunoglobulin isotypes by Ly-1+ B cells in viable motheaten and normal mice. *Science* 232:1423-1425.
126. Burastero, S.E., P. Casali, R.L. Wilder, and A.L. Notkins. 1988. Monoreactive high affinity and polyreactive low affinity rheumatoid factors are produced by CD5+ B cells from patients with rheumatoid arthritis. *J. Exp. Med.* 168:1979-1992.
127. Dauphinee, M., Z. Tovar, and N. Talal. 1998. B cells expressing CD5 are increased in Sjogren's syndrome. *Arthritis Rheum.* 31:542-647.
128. Murakami, M., H. Yoshioka, T. Shirai, T. Tsubata, and T. Honjo. 1995. Prevention of autoimmune symptoms in autoimmune-prone mice by elimination of B-1 cells. *Int. Immunol.* 7:87-882.
129. Hayakawa, K., R.R. Hardy, M. Honda, L.A. Herzenberg, and A.D. Steinberg. 1984. Ly-1 B cells: functionally distinct lymphocytes that secrete IgM autoantibodies. *Proc. Natl. Acad. Sci. USA* 81:2494-2498.
130. Stall, A.M., M.C. Farinas, D.M. Tarlinton, P.A. Lalor, L.A. Herzenberg, and S. Strober. 1988. Ly-1 B cell clones similar to human chronic lymphocytic leukemia's routinely develop in older normal mice and young autoimmune animals. *Proc. Natl. Acad. Sci.* 85:7312-7316.
131. van Haelst, C., and T.L. Rothstein. 1988. Cytochalasin stimulates phosphoinositide metabolism in murine B lymphocytes. *J. Immunol.* 140:1256-1258.
132. Rothstein T.L., and D.L. Kolber. 1988. Peritoneal B cells responds to phorbol esters in the absence of co-mitogen. *J. Immunol.* 140:2880-2885.
133. Kantor, A.B., A.M. Stall, S. Adams, K. Watanabe, and L.A. Herzenberg. 1995. De novo development and self-replenishment of B cells. *Int. Immunol.* 7:55-68.
134. Tanguay, D.A., T.P. Colarusso, C. Doughty, S. Pavlovic, T.L. Rothstein, and T.C. Chiles. 2001. Differences in the signaling requirements for activation of assembled cyclin D3-cdk4 complexes in B-1a and B-2 lymphocytes. *J. Immunol.* 166:4273-4277.

135. Sanchez-Beato, M., A. Sanchez-Aguilera, and M.A. Piris. 2003. Cell cycle deregulation in B-cell lymphomas. *Blood* 101:1220-1235.
136. Faber, A.C., and T.C. Chiles. 2007. Inhibition of cyclin-dependent kinase-2 induces apoptosis in human diffuse large B-cell lymphoma. *Cell Cycle* 6: 2982-2989.
137. Donnellan, R., and R. Chetty. 1999. Cyclin E in human cancers. *FASEB J.* 13:773-780.
138. Geng, Y., W. Whoriskey, M.Y. Park, R.T. Bronson, R.H. Medem, T. Li, R.A. Weingerg, and P. Sicinski. 1999. Rescue of cyclin D1 deficiency by knockin cyclin E. *Cell* 97: 767-777.
139. Bowe, D.B., N. J. Kenney, Y. Adereth, and I.G. Maroulakou. 2002. Suppression of *Neu*-induced mammary tumor growth in cyclin D1 deficient mice is compensated for by cyclin E. *Oncogene* 21:291-298.
140. Tetsu, O., and F. McCormick. 2003. Proliferation of cancer cells despite CDK2 inhibition. *Cancer Cell* 3:233-245.
141. Cheson, B.D., and J.P. Leonard. 2008. Monoclonal antibody therapy for B-cell non-Hodgkin's lymphoma. *N. Engl. J. Med.* 359:613-625.
142. Grossbard, M.L., 2002. Malignant Lymphomas. *American Cancer Society* 1-468.
143. Rosenwald, A., G. Wright, W.C. Chan, J.M. Connors, E. Campo, R.I. Fisher, R.D. Gascoyne, H.K. Muller-Hermelink, E.B. Smeland, and L.M. Staudt. 2002. The use of molecular profiling to predict survival after chemotherapy for diffuse large-B-cell lymphoma. *N. Engl. J. Med.* 346:1937-1947.
144. Shaffer, A.L., A. Rosenwald, E.M. Hurt, J.M. Giltneane, L.T. Lam, O.K. Pickeral, and L.M. Staudt. 2001. Signatures of the immune response. *Immunity* 15:375-385.
145. Staudt, L.M. 2003. Molecular diagnosis of the hematologic cancers. *N. Engl. J. Med.* 348:1777-1785.
146. Merup, M., G. Juliusson, X. Wu, M. Jansson, B. Stellan, O. Rasool, E. Roijer, G. Stenman, G. Gahrton, and S. Einhorn. 1997. Amplification of multiple regions of chromosome 12, including 12q13-15, in chronic lymphocytic leukemia. *Eur. J. Haematol.* 20:155-160.

147. Dierlamm, J., I. Wlodarska, L. Michaux, J.R. Vermeesch, P. Meeus, M. Stul, A. Criel, G. Verhoef, and H. Berghe. 1997. FISH identifies different types of duplications with 12q13-15 as the commonly involved segment in B-cell lymphoproliferative malignancies characterized by partial trisomy. *Genes Chrom. Cancer* 20:155-166.
148. Al-Assar, O., K.S. Rees-Unwin, L.P. Menasce, R.E. Hough, J.R. Goepel, D.W. Hammond, and B.W. Hancock. 2006. Transformed diffuse large B-cell lymphomas with gains of the discontinuous 12q12-14 amplicon display concurrent deregulation of *CDK2*, *CDK4*, and *GADD153* genes. *Brit. Journ. of Haem.* 133:612-621.
149. Rao, P.H., J. Houldsworth, K. Dyomina, V.V. Murty, V.E. Reuter, R.J. Motzer, G.J. Bosl, and R.S. Chaganti. 1998. Chromosomal and gene amplification in diffuse large B-cell lymphoma. *Blood* 102:3871-3879.
150. Chang, H., H.A. Messner, X.H. Wang, C. Yess, L. Addy, J. Meharchand, and M.D. Minden. 1992. A human lymphoma cell line with multiple immunoglobulin rearrangements. *J. Clin. Invest.* 89:1014-1020.
151. Hachem, A., and R.B. Gartenhaus. 2005. Oncogenes as molecular targets in lymphoma. *Blood* 106:1911-191923.
152. Flipits, M., U. Jaeger, G. Pohl, T. Stranzl, I. Simonitsch, A. Kaider, C. Skrabs, and R. Pirker. 2002. Cyclin D3 is a predictive and prognostic factor in diffuse large B-cell lymphoma. *Clin Cancer Res.* 8:729-733.
153. Lane, P., T. Brocker, S. Hubele, E. Padovan, A. Lanzavecchia, and F. McConnell. 1993. Soluble CD40 ligand can replace the normal T cell-derived CD40 ligand signal to B cells in T cell-dependent activation. *J. Exp. Med.* 177:1209-1213.
154. Francis, D.A., J.G. Karras, X.Y. Ke, R. Sen, and T.L. Rothstein. 1995. Induction of the transcription factors NF- κ B, AP-1 and NF-AT during B cell stimulation through the CD40 receptor. *Int. Immunol.* 7:151-161.
155. Caligaris-Cappio, F., M. Gobbi, M. Bofill, and G. Janossy. 1982. Infrequent normal B lymphocyte express features of B-chronic lymphocytic leukemia. *J. Exp. Med.* 155:623-628.
156. Fahraeus, R., J. M. Paramio, K. L. Ball, S. Lain, and D.P. Lane. 1996. Inhibition of pRb phosphorylation and cell cycle progression by a 20-residue peptide derived from p16CDKN2/INK4A. *Curr. Biol.* 6:84-91.

157. Guis, D.R., S.A. Ezhevsky, M. Becher-Hapak, H. Nagahara, M.C. Wei, and S.F. Dowdy. 1999. Transduced p16INK4a peptides inhibit hypophosphorylation of the retinoblastoma protein and cell cycle progression prior to activation of Cdk2 complexes in late G₁. *Cancer Res.* 59:2577-2580.
158. Grdisa, M, A. Mikecin, and M. Poznic. 2006. Does transduced p27 induce apoptosis in human tumor cell lines? *Ann. NY Acad. Sci.* 1090:120-129.
159. Nagahara, H., A.M. vocer-Akbani, E.L. Snyder, A. Ho, D.G. Latham, N.A. Lissy, M. Becker-Hapak, S.A. Ezhevsky, and S.F. Dowdy. 1998. Transduction of full length TAT fusion proteins into mammalian cells: TAT-p27^{Kip1} induces cell migration. *Nature Medicine* 12:1449-1452.
160. Seyfried T.N., G.H. Glaser, and R.K. Yu. 1978. Cerebral, cerebellar, and brain stem gangliosides in mice susceptible to audiogenic seizures. *J. Neurochem.* 31:21-27.
161. Denny C.A., J.L. Kasperzyk, K.N. Gorham, R.T. Bronson, and T.N. Seyfried. 2006. Influence of caloric restriction on motor behavior, longevity, and brain lipid composition in Sandhoff disease mice. *J. Neurosci. Res.* 83:1028–1038.
162. Macala L.J., R.K. Yu, and S. Ando. 1983. Analysis of brain lipids by high performance thin-layer chromatography and densitometry. *J. Lipid. Res.* 24:1243–1250.
163. Seyfried T.N., D.J. Bernard, and R.K. Yu. 1984. Cellular distribution of gangliosides in the developing mouse cerebellum: analysis using the staggered mutant. *J. Neurochem.* 43:1152–1162.
164. Kasperzyk J.L., A. d’Azzo, F.M. Platt, J. Alroy, and T.N. Seyfried. 2005. Substrate reduction reduces gangliosides in postnatal cerebrum-brainstem and cerebellum in GM1 gangliosidosis mice. *J. Lipid Res.* 46:744–751.
165. Bligh, E.G., and W.J. Dyer. 1959. A rapid method of total lipid extraction and purification. *Can. J. Biochem. Physiol.* 37:911-917.
166. Seyfried, T.N., A.M. Novikov, R.A. Irvine, and J.V. Brigande. 1994. Ganglioside biosynthesis in mouse embryos: sialyltransferase IV and the asialo pathway. *J. Lipid Res.* 35:993-1001.
167. Srere, P.A. 1959. The citrate cleavage enzyme. *J. Biol. Chem.* 234:2544-2547.

168. Kindt, T.J., R.A. Goldsby, B.A. Osborne. 2007. *Kuby Immunology*. Sixth Edition. 1-574.
169. Zhu, G., S.E. Conner, X. Zhou, C. Shih, T., Li, B.D. Anderson, H.B. Brooks, R.M. Cambell, E. Considine, J.A. Dempsey, M.M. Faul, C. Ogg, B. Patel, R.M. Schultz, C.D. Spencer, B. Teicher, and S.A. Watkins. 2003. Synthesis, structure-activity relationship, and biological studies of indolocarbazoles as potent cyclin D1-cdk4 inhibitors. *J. Med. Chem.* 46:2027-2030.
170. Zhu, G., S.E. Conner, X. Zhou, C. Shih, H.B. Brooks, E. Considine, J.A. Dempsey, C. Ogg, B. Patel, R.M. Schultz, C.D. Spencer, B. Teicher, and S.A. Watkins. 2003. Synthesis of quinolinyl/isoquinolinyl[*a*]pyrrolo [3,4-*c*] carbazoles as cyclin D1/cdk4 inhibitors. *Bioorganic & Med. Chem. Letters* 13:1231-1235.
171. Gu, Y., J. Rosenblatt, and D.O. Morgan. 1992. Cell cycle regulation of Cdk2 activity by phosphorylation of Thr160 and Tyr15. *EMBO J.* 11:3995-4005.
172. Tsutsui, T. B. Hesabi, D.S. Moons, P.P. Pandolfi, K. S. Hansel, A. Koff, and H. Kiyorkawa. 1999. Targeted disruption of cdk4 delays cell cycle entry with enhanced p17^{Kip1} activity. *Mol. Cell. Bio.* 19:7011-7019.
173. Suzuki, H., Y. Terauchi, M. Fujiwara, S. Aizawa, Y. Yazaki, T. Kadowaki, and S. Koyasu. 1999. *Xid*-like immunodeficiency in mice with disruption of the p85 α subunit of phosphoinositide 3-kinase. *Science* 283:390-392.
174. Wymann, M.P., G. Bulgarelli-Leva, M.J. Zvelebil, L. Pirola, B. Vanhaesebroeck, M.D. Waterfield, and G. Panayotou. 1996. Wortmannin inactivates phosphoinositide 3-kinase by covalent modification of Lys-802, a residue involved in the phosphate transfer reaction. *Mol. Cell Biol.* 16:1722-1733.
175. Vlahos, C.J., W.F. Matter, K.Y. Hui, R.F. Brown. 1994. A specific inhibitor of phosphatidylinositol 3-kinase, 2-(4-morpholinyl)-8-phenyl-4H-1-benzopyran-4-one (LY294002). *J. Biol. Chem.* 269:5241-5248.
176. Vasques C.A., S. Rossetto, G. Halmenschlager, R. Linden, E. Heckler, M.S. Fernandez, J.L. Alonso. 2008. Evaluation of the pharmacotherapeutic efficacy fo *Garcinia camboia* plus *Amorphallus konjac* for the treatment of obesity. *Phytother. Res.* 9:1135-1140.
177. Berkhout, T.A., L.M. Havekes, N.J. Pearce, and P.H. Groot. 1990. The effect of (-)-hydroxycitrate on the activity of the low-density-lipoprotein receptor and 3-hydroxy-3-methylglutaryl-CoA reductase levels in the human hepatoma cell line Hep G2. *Biochem. J.* 272:181-186.

178. Parada, Y., L. Banerji, J. Glassford, N.C. Lea, M. Collado, C. Rivas, J.L. Lewis, M.Y. Gordon, N.S.B. Thomas, and E.W.F. Lam. 2001. BCR-ABL and interleukin 3 promote haematopoietic cell proliferation and survival through modulation of cyclin D2 and p27^{Kip1} expression. *J. Bio. Chem.* 276:23572-23580.
179. Bienvenu, F., H. Gascan, and O. Coqueret. 2001. Cyclin D1 represses STAT3 activation through a Cdk4-independent mechanism. *J. Biol. Chem.* 276:16840-16847.
180. Peterson, L.F., A. Boyapat, V. Ranganathan, A. Iwama, D.G. Tenen, S. Tsai, and D.E. Zhang. 2005. The hematopoietic transcription factor AML1 (RUNX1) is negatively regulated by the cell cycle protein cyclin D3. *Molecular and Cellular Biology* 25:10205-10219.
181. Sun, M., Y. Wei, L. Yao, J. Xie, C. Chen, H. Wang, J. Jiang, J. Gu. 2006. Identification of extracellular signal-regulated kinase 3 as a new interaction partner of cyclin D3. *Biochem. And Biophys. Res. Comm.* 340:209-214.
182. Sherr, C.J., and J.M. Roberts. 2004. Living with or without cyclins and cyclin-dependent kinases. *Genes & Dev.* 18:2699-2711.
183. Chiles, T.C. 2004. Regulation and function of cyclin D2 in B lymphocyte subsets. *J. Immunol.* 173:2901-2907.
184. Cai, D., V.M. Latham, X. Zhang, and G.I. Shapiro. 2006. Combined depletion of cell cycle and transcriptional cyclin-dependent kinase activities induce apoptosis in cancer cells. *Cancer Res.* 66:9270-9280.
185. Blagosklonny, M.V. 2004. Flavopiridol, an inhibitor of transcription: Implications, problems, and solutions. *Cell Cycle.* 12:1537-1542.
186. Erlanson, M.C. Portin, B. Linderholm, J. Lindh, G. Roos, and G. Landberg. 1998. Expression of Cyclin E and the Cyclin-Dependent Kinase Inhibitor p27 in Malignant Lymphomas-Prognostic Implications. *Blood* 92:770-777.
187. Gray-Bablin, J., J. Zalvide, M. Fox, C.J. Knickerbocker, J.A. DeCaprio, and K. Keyomarsi. 1996. Cyclin E, a redundant cyclin in breast cancer. *Cell Biology* 93:15215-15220.
188. Malumbres M. R. Sotillo, D. Santamaria, J. Galan, A. Cerezo, S. Ortega, P. Dubus, and M. Barbacid. 2004. Mammalian cells cycle without the D-type cyclin-dependent kinases CDK4 and CDK6. *Cell* 118:493-504.

189. Ewen, M.E., H.K. Sluss, C.J. Sherr, H. Matsushime, J. Kato, and D.M. Livingston. 1993. Functional interactions of the retinoblastoma protein with mammalian D-type cyclins. *Cell* 73:487-497.
190. Fagone, P., R. Sriburi, C. Ward-Chapman, M. Frank, J. Wang, C. Gunter, J.W. Brewer, and S. Jackowski. 2007. Phospholipid biosynthesis program underlying membrane expansion during B-lymphocytes differentiation. *J. Biol. Chem.* 282:7591-7605.
191. Beigneux, A.P, C. Kosinski, B. Gavino, J.D. Horton, W.C. Skarnes, and S.G. Young. 2004. ATP-citrate lyase deficiency in the mouse. *J. Biol. Chem.* 279:9557-9564.
192. Imesch, E., and S. Rous. 1984. Partial purification of rat liver cytoplasmic acetyl-CoA synthetase; characterization of some properties. *Int. j. Biochem.* 16:875-881.
193. Amaravadi, R., and C.B. Thompson. 2005. The survival kinases Akt and Pim as potential pharmacological targets. *J. Clin. Invest.* 115:2618-2624.